

The University of Manitoba

A PROTON MAGNETIC RESONANCE STUDY OF THE
NITROGEN NUCLEAR QUADRUPOLE RELAXATION PROCESS
IN METHYL NITRATE

by

Christine M. Shepperd

A Thesis

Submitted to

The Faculty of Graduate Studies and Research

University of Manitoba

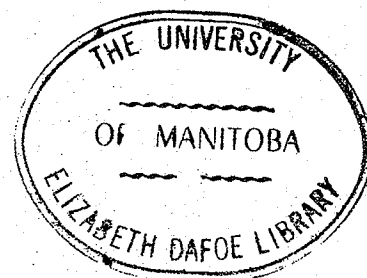
In Partial Fulfillment

Of the Requirements for the Degree

MASTER OF SCIENCE

Winnipeg, Manitoba

October, 1970



ACKNOWLEDGEMENTS

I would like to thank Dr. T. Schaefer for his help and patience throughout the course of this research, but more especially for his genuine concern and understanding of an uncertain student.

It was also my good fortune to be surrounded by willing and able colleagues. Bruce Goodwin's competence at computer programming is once again gratefully acknowledged, as is Jon teRaa for the preparation of methyl nitrate and S.R. Anand for his assistance in viscosity measurements. The friendly interest and helpful comments of Rod Wasylshen merit a special word of thanks.

I am indebted to the Chemistry Department of the University of Manitoba for financial assistance.

ABSTRACT

The temperature dependence of the rate of nitrogen nuclear quadrupole relaxation in methyl nitrate has been studied in two solvents between 30° and 90°C using the steady - state proton magnetic resonance technique. The quadrupolar relaxation times were obtained by matching theoretical and experimental spectra both visually and numerically. The theory of quadrupolar interactions is discussed and a line shape expression developed for the resonance of a proton spin - spin coupled to a quadrupolar nucleus (following the original treatment by Pople). Activation parameters for the reorientation of methyl nitrate in two solvents were determined:

$$E_a = 2.38 \pm 0.06 \text{ kcal. mole}^{-1}; \quad \Delta H^\ddagger = 1.73 \pm 0.07 \text{ kcal. mole}^{-1}$$

(for DMF solution)

$$E_a = 1.36 \pm 0.05 \text{ kcal. mole}^{-1}; \quad \Delta H^\ddagger = 0.70 \pm 0.06 \text{ kcal. mole}^{-1}$$

(for C₆H₁₂ solution)

The current state of theoretical calculations of molecular correlation times is critically reviewed, and examined by the results obtained for the ¹⁴N relaxation rate of methyl nitrate in eleven different solvents. Serious inadequacies are revealed, especially in the more polar solvents where solute - solvent "association" is strongly indicated.

TABLE OF CONTENTS

SECTION		PAGE
	Acknowledgements	
	Abstract	
	Table of Contents	
	List of Tables	
	List of Figures	
[A]	INTRODUCTION	1
[B]	THEORETICAL ASPECTS OF SOME MAGNETIC RESONANCE PHENOMENA	
	(i) Introduction	4
	(ii) The Magnetic Resonance of Quadrupolar Nuclei	5
	(iii) Theoretical Treatment of Quadrupole Interactions.	8
	(iv) The Line Shape of a Spin- $\frac{1}{2}$ Nucleus Coupled to a Quadrupolar Nucleus	12
[C]	NUCLEAR MAGNETIC RESONANCE IN THE STUDY OF LIQUIDS	
	(i) Introduction	20
	(ii) Estimation of Activation Parameters for Molecular Reorientation by NMR Methods	
	<u>a</u> Scope and Limitations.	23
	<u>b</u> Results and Interpretation	24
	(iii) Estimation of Molecular Correlation Times from Physical Properties of the System	
	<u>a</u> Outline of the Theories.	30
	<u>b</u> Assessment of the Three Methods.	34
	<u>c</u> Alternative Treatments	38
[D]	NATURE OF THE PROBLEM	42

[E]	EXPERIMENTAL PROCEDURE	
	(i) Substrates and Samples	45
	(ii) Viscosity Measurements.	46
	(iii) PMR Measurements.	47
	(iv) Analysis of the Resonance Line Shape.	48
[F]	RESULTS	
	(i) Viscosity Measurements	50
	(ii) PMR Measurements	
	<u>a</u> The Determination of $J(^{14}\text{N-H})$	52
	<u>b</u> The Determination of T_2	52
	<u>c</u> Temperature Studies.	55
	<u>d</u> Solvent Studies.	60
[G]	DISCUSSION OF RESULTS	
	(i) Treatment of Data	
	<u>a</u> Determination of Relaxation Rates.	64
	<u>b</u> Determination of Activation Parameters.. . . .	80
	<u>c</u> Evaluation of the Fitting Procedure and Error Estimate	89
	<u>d</u> Dependence of Relaxation Rate on Viscosity	93
	(ii) Interpretation of Data	
	<u>a</u> Thermodynamic Parameters	105
	<u>b</u> Factors Determining Relaxation Rate.	112
	<u>c</u> Chemical Shift Variations.	119
[H]	SUMMARY AND CONCLUSIONS.	127
[I]	SUGGESTIONS FOR FUTURE RESEARCH.	130
[J]	APPENDICES	
	I Contributions to the Spin- Lattice Relaxation of ^{14}N	134
	II Evaluation of the Line Shape Expression.	136
	III Estimation of the Quadrupolar Coupling Constant	139
	BIBLIOGRAPHY	141

LIST OF TABLES

TABLE	PAGE
1 Some Illustrative Activation Energy Results for Molecular Reorientation in pure liquids.	25
2 Comparison of Experimental and Calculated Rotational Correlation Times.	37
3 Results of Viscosity Measurements.	51
4 Spectral Parameters of the Proton Resonance of Methyl Nitrate in DMF solution.	57
5 Spectral Parameters of the Proton Resonance of Methyl Nitrate in Cyclohexane solution.	58
6 Spectral Parameters of the Proton Resonance of Methyl Nitrate in Several Solvents at Ambient Temperature.	62
7 ¹⁴ N Relaxation Times for Methyl Nitrate in Cyclohexane Solution, with T ₂ = 2.0 sec.	73
8 ¹⁴ N Relaxation Times for Methyl Nitrate in Cyclohexane Solution, with T ₂ = 1.68 sec.	74
9 Arrhenius Parameters for the data shown in Tables 7 and 8.	75
10 ¹⁴ N Relaxation Times for Methyl Nitrate in DMF Solution, with T ₂ = 2.0 sec.	76
11 ¹⁴ N Relaxation Times for Methyl Nitrate in DMF Solution, with T ₂ = 1.0 sec.	77
12 ¹⁴ N Relaxation Times for Methyl Nitrate in DMF Solution, with T ₂ = 0.71 sec.	78
13 Arrhenius Parameters for the data shown in Tables 10, 11 and 12.	79
14 Results of a least squares analysis of the data in Tables 7 - 13.	87
15 Activation Parameters for the Reorientation of Methyl Nitrate in Cyclohexane and DMF solutions.	88
16 The Variation of Viscosity with Temperature for 15 mole % solutions of Methyl Nitrate in Cyclohexane and DMF.	94

17	^{14}N Relaxation Rates and Viscosities of 15 mole % Methyl Nitrate in DMF and Cyclohexane solutions, as a Function of Temperature.	96
18	^{14}N Relaxation Rates for Methyl Nitrate in various solvents, at ambient temperature, together with some physical properties of the solvents.	99
19	Reduced Masses and "Molecular Radii" of the Solvents listed in Table 18 together with the parameters used in Figures 16 and 17.	101
20	Activation Energies for Reorientation and Viscous Flow of Methyl Nitrate in DMF and Cyclohexane Solutions.	106
21	Activation Energies for Molecular Reorientation illustrating the dependence on solvent.	109
22	Some Physical Properties of the Solvents.	117
23	Proton Chemical Shift of Methyl Nitrate as a Function of Solvent Dielectric Constant.	122
24	Proton Chemical Shift of Methyl Nitrate as a function of the Dielectric Constant of the Solvent DMF at several different temperatures.	124

LIST OF FIGURES

FIGURE	PAGE
1 The Resonance Line Shape of a Proton spin-spin coupled to a nucleus of spin $I = 1$ which is undergoing varying rates of quadrupolar relaxation.	17
2 The ^1H Spectrum at high power showing the splitting due to ^{15}N -H coupling.	53
3 The PMR Spectra of the Solvents at 100 MHz	54
4 The PMR Spectra of Methyl Nitrate under various conditions. . .	56
5 Diagram to show the Spectral Parameters listed in Table 5.	59
6 The PMR of Methyl Nitrate in various solvents, at ambient temperature.	61
7 The Experimental Spectra for Methyl Nitrate in DMF at 38.5°C and 69.5°C with the Corresponding Calculated Spectra. . .	71
8 The Experimental Spectra for Methyl Nitrate in Cyclohexane at 43°C and 58°C with the Corresponding Calculated Spectra.	72
9 Arrhenius Plot for the Reorientation of Methyl Nitrate in Cyclohexane Solution. $T_2 = 1.68$ sec.	83
10 Arrhenius Plot for the Reorientation of Methyl Nitrate in DMF Solution. $T_2 = 0.71$ sec.	84
11 Eyring Plot for the Reorientation of Methyl Nitrate in Cyclohexane Solution. $T_2 = 1.68$ sec.	85
12 Eyring Plot for the Reorientation of Methyl Nitrate in DMF Solution. $T_2 = 0.71$ sec.	86
13 The Temperature Dependence of the Viscosity of 15 mole % Methyl Nitrate in (a) DMF and (b) Cyclohexane solutions. . . .	95
14 ^{14}N Relaxation Rate as a Function of Viscosity divided by Temperature (a) in DMF and (b) in Cyclohexane solutions. . . .	97
15 ^{14}N Relaxation Rate as a Function of Viscosity in several solvents at ambient temperature.	100
16 ^{14}N Relaxation Rate as a Function of Viscosity divided by the molecular radius of the solvent.	102

17	^{14}N Relaxation Rate as a Function of Viscosity divided by the Reduced Mass of the Solute-Solvent System.	103
18	^{14}N Relaxation Rate as a Function of Viscosity divided by Dielectric Constant, at ambient temperature in several solvents.	104
19	^{14}N Relaxation Rate, at ambient temperature in several solvents, plotted against the Heat of Vaporisation (H_b) of the solvent.	118
20	Chemical Shift of the Methyl Protons in Methyl Nitrate as a function of the "Reaction Field" of the solvent.	123
21	Chemical Shift of the Methyl Protons in Methyl Nitrate as a function of the "Reaction Field" at different temperatures in DMF solution.	125
22	Hypothetical Curves showing the dependence of T_1 on the fraction of complexed solute molecules.	132

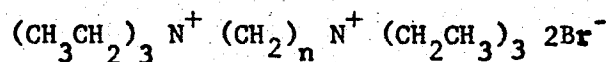
SECTION A

INTRODUCTION TO THE THESIS

The nuclear magnetic resonance of protons bonded directly or indirectly to nitrogen (^{14}N) shows a variety of spectral line shapes. Single sharp lines are obtained with amines and ammonia where proton exchange is rapid⁽¹⁾. Broad lines are observed for many amides and pyrrole⁽²⁾, while sharp triplet absorption has been observed for gaseous and completely anhydrous ammonia⁽²⁾, ammonium ions in acid solution⁽³⁾ symmetrically substituted quaternary ammonium salts^(4,5,6), and certain isocyanides⁽⁷⁾ and nitramines^(8,9). The latter type of absorption (i.e. a 1:1:1 triplet) is that predicted from consideration of the spin-spin interaction between the protons and ^{14}N ($I=1$).

The broad lines associated with N-H absorption of amides and pyrrole could be due to intermediate rates of proton exchange⁽¹⁰⁾. Indeed, significant sharpening of N-H lines by exchange may be achieved by adding small amounts of sodium to pyrrole and concentrated ammonia to formamides⁽²⁾. However, the broad lines in the pure liquids are not the result of intermediate exchange rates because the linewidths in a given molecule are found to increase with increasing temperature - sometimes showing triplet structure at the more elevated temperatures^(11,12,13). This behaviour is opposite to that expected for any exchange process⁽³⁾ having a positive temperature coefficient. A change in the solvent at constant temperature may also modify the proton line shape, increasing viscosity having an effect similar to that of decreasing temperature, viz. a sharpening of the resonance (See Fig. 6, this thesis).

The variation of line shape from one compound to another was systematically investigated by Lehn and Neumann⁽¹²⁾. For a series of the type



(where $n = 2, 3, 4, 5, 6$) they obtained the $-\text{CH}_3$ proton resonance signal.

For $n = 2$ or 3 the resonance indicated coupling only to the CH_2 protons; increasing n broadened the signals until for $n \geq 5$ each component split into a triplet i.e. demonstrating $^{14}\text{N} - \text{C}'\text{H}_3$ coupling. Clearly then, the proton resonance shows a sensitivity to the electronic environment at the ^{14}N nucleus (since increasing n from 2 to 6 merely increases the symmetry of the electric fields about the nitrogen nucleus) in addition to the "external" conditions as manifested by its temperature and solvent dependence.

It is the purpose of this thesis to investigate the effect of "external" conditions on the resonance line shape for the methyl protons in methyl nitrate. A theoretical treatment of the line shape is given in Section B, followed by a consideration of the physical processes involved. (Section C.) The results are discussed and interpreted (Section G) on the basis of established models for molecular motion. Serious deviations from the expected behaviour are reported.

SECTION B

THEORETICAL ASPECTS OF SOME MAGNETIC

RESONANCE PHENOMENA

(i) Introduction

The variations in proton line shape outlined in the Introduction are the result of spin-spin coupling with the nitrogen nucleus. The possession of a quadrupole moment by the latter gives rise to a relaxation process acting on that nucleus, the effect of which is transmitted to the proton resonance. Internal electric field gradients, sample temperature and nature of the solvent all influence the rate of ^{14}N spin relaxation and hence the proton signal. Before a theoretical treatment of such resonance line shapes is attempted the principles of relaxation of quadrupolar nuclei themselves must be understood. This is the content of Part (ii). The mathematical formulation of this, Part (iii), is extended in Part (iv) to derive a line shape expression which successfully reproduces the proton resonance for varying rates of ^{14}N relaxation.

(ii) The Magnetic Resonance of Quadrupolar Nuclei

It is observed and to some extent theoretically justified⁽¹⁴⁾ that nuclei with spin $I \geq 1$ have a charge distribution within the nucleus which is not spherically symmetrical. This gives rise to an electric quadrupole moment, which has an associated positive or negative sign. This implies that the shape of the charge distribution about the spin axis is respectively that of prolate and oblate spheroid. Nuclei do not have electric dipole moments and so the energy of any nucleus is independent of its orientation in a uniform electric field. However, when an electric field gradient exists there is an electrostatic energy of interaction which gives rise to a series of quantised energy levels, even in the absence of a magnetic field. Transitions between these states are observed in the nuclear quadrupole spectroscopy of solids.

In the liquid state rapid molecular reorientation causes a statistical fluctuation of the electric field gradient at the nuclear site, thereby coupling the quadrupolar nucleus to the molecular motion. Pure quadrupole transitions are no longer seen, but a highly efficient "spin relaxation" mechanism now arises. In the presence of a magnetic field there are two opposing influences on a nucleus with a quadrupole moment. The nuclear magnetic dipole moment tends to keep a constant orientation relative to the external field (as the molecule tumbles). On the other hand, the quadrupole moment follows changes in the electric field gradient, which has a fixed direction within the molecule i.e. it tends to keep a constant orientation relative to the molecule during tumbling. (It is important to realize that translational motion does not affect the orientation or magnitude of the molecular electric field gradient, and thus has no effect on quadrupolar phenomena.) In the conflict between an orientation dependence on laboratory or molecule, for ¹⁴N the magnetic

field influence dominates^{*1}. The nuclear Zeeman states are preserved, but the quadrupole interaction causes relaxation between them. Consequently, nuclear resonance can normally be observed (See Reference 15 for example) but the lines are much broader than for spin - $\frac{1}{2}$ nuclei. The breadth reflects the rate of relaxation, which in turn is a measure of the electric field gradient. For other nuclei, such as the halogens, the quadrupole interaction is larger, either because their quadrupole moments are larger (see Footnote) and/or because they commonly occur in a position of higher field gradient. The spectral lines (of ^{35}Cl etc.) are too broad to be detected.

As with other relaxation mechanisms, it is the spectral intensity of the interaction energy at the magnetic resonance frequency which determines the rate of relaxation. Measurement of the relaxation time can thus provide information about reorientation. In molecules where internal rotation is possible there is an additional means of reorienting the field gradient axes, and in principle of affecting the relaxation time⁽¹⁶⁾. Since these rotational processes compete with one another in reorienting the bond direction the internal rotation rate must be at least comparable to that of molecular rotation if its effect on the relaxation time is to be significant. For the system studied in this

*1 The quadrupole moment of ^{14}N is small; $eQ = 2 \times 10^{-26} \text{ cm}^2$. Values for the halogens are:

$$^{35}\text{Cl} = -7.97 \times 10^{-26} \text{ cm}^2$$

$$^{81}\text{Br} = 2.8 \times 10^{-25} \text{ cm}^2$$

$$^{127}\text{I} = -7.5 \times 10^{-25} \text{ cm}^2$$

work, methyl nitrate, overall molecular rotation is the only motion influencing the quadrupole relaxation rate*. Furthermore, it may be shown (Appendix I) that all other relaxation mechanisms are insignificant in comparison to relaxation by the quadrupole interaction i.e. T_1 of the nucleus is in fact equal to T_q , the quadrupole relaxation time. The complication of including several mechanisms for relaxation and accounting for relative translation in an expression for the relaxation time can thus be neatly avoided by the use of quadrupolar nuclei. The next section outlines the derivation of an expression for T_q in terms of nuclear and molecular properties.

* The energy barrier to internal rotation of the CH_3 group is only $2.3 \text{ kcal.mole}^{-1}$ (17) and is therefore comparable to the overall rotation. However, as pointed out by Wallach for internal rotation in dimethylformamide (18), the orientations of the methyl groups should have only a very small effect on the orientation of the field gradient axes at the ^{14}N nucleus. Hence the effect of methyl spinning on the relaxation times will be neglected.

The barrier to rotation about the O-N bond is considerably greater, $(9.1 \text{ kcal.mole}^{-1})$ (17); internal rotation of the $-\text{NO}_2$ group is therefore ineffective in promoting ^{14}N relaxation.

(iii) Theoretical Treatment of Quadrupole Interactions

The interaction energy of a nuclear quadrupole moment with a fluctuating electric field gradient may be written in the form

$$F = \overline{Q} \cdot \overline{\nabla E} = \sum_{p=-2}^{+2} (-1)^p \overline{Q}_p \cdot (\overline{\nabla E})_p \dots\dots\dots(1)$$

The notation is that of Pound⁽¹⁹⁾ where \overline{Q} and $\overline{\nabla E}$ are second rank tensors representing the quadrupole moment and field gradient respectively. The expansion in terms of second order spherical harmonics permits the components of \overline{Q} and $\overline{\nabla E}$ to be written down. For a fuller discussion of this aspect the reader is referred to Pound's original paper⁽¹⁹⁾ or to the review article by Das and Hahn⁽²⁰⁾.

For a nucleus of spin I the matrix elements of F between the different states

$$\text{i.e. } \langle \alpha I m | F | \alpha I m' \rangle \dots\dots\dots(2)$$

are non-vanishing for an allowed transition. Here α represents the external quantum numbers which remain fixed, I is also fixed and m is the component of I along the Z - axis. For a field gradient which is axially symmetric (normally a good approximation), Pound⁽¹⁹⁾ and Pople⁽²¹⁾ show that the non-vanishing matrix components of the electric quadrupole tensor are

$$\langle m | F | m \rangle = \frac{e Q}{2I(2I-1)} \left[3m^2 - I(I+1) \right] (\overline{\nabla E})_0$$

$$\langle m | F | m \pm 1 \rangle = \pm \frac{6\frac{1}{2}}{2} \cdot \frac{e Q}{2I(2I-1)} (2m \pm 1) \left[(I \mp m + 1)(I \mp m) \right]^{\frac{1}{2}} (\overline{\nabla E})_{\pm 1} \dots\dots\dots(3)$$

$$\langle m | F | m \pm 2 \rangle = \frac{6\frac{1}{2}}{2} \cdot \frac{e Q}{2I(2I-1)} \left[(I \mp m)(I \mp m - 1)(I \pm m + 1)(I \pm m + 2) \right]^{\frac{1}{2}} (\overline{\nabla E})_{\pm 2}$$

where $(\overline{\nabla E})_p$ are the components of the tensor $\overline{\nabla E}$, and Q is the scalar

nuclear quadrupole moment. All other matrix elements vanish, so a fluctuating electric field gradient can cause transitions in which $\Delta m = \pm 1$ or ± 2 .

The theory of transitions in random fields (Appendix B of Reference 22) may now be used to obtain the transition probabilities P_1 and P_2 for Δm changing by ± 1 and ± 2 respectively. The theory shows

$$P_{ij} = \hbar^{-2} \left| \langle i | F | j \rangle \right|^2 \frac{2 \tau_c}{1 + 4 \pi^2 \nu_{ij}^2 \tau_c^2} \dots \dots \dots (4)$$

where ν_{ij} is the transition frequency between the initial (i) and final (j) states; τ_c is a correlation time characteristic of the fluctuation of the Hamiltonian, F . Here it is of the order of the time required for molecular reorientation. The mean - square moduli of $(\overline{\nabla E})_p$ required in equation (4) are all equal to $1/20 e^2 q^2$ (23), q being a scalar representing the Z -component of the field gradient (within an axis system determined by the field gradient tensor and fixed in the molecule).

For a nucleus with spin $I = 1$ then, for example, substitution of equation (3) into (4) yields

$$\left. \begin{aligned} P_1 &= \frac{3}{80} e^4 q^2 Q^2 \hbar^{-2} \frac{2 \tau_c}{1 + 4 \pi^2 \nu_{ij}^2 \tau_c^2} \\ P_2 &= \frac{3}{40} e^4 q^2 Q^2 \hbar^{-2} \frac{2 \tau_c}{1 + 16 \pi^2 \nu_{ij}^2 \tau_c^2} \end{aligned} \right\} \dots \dots \dots (5)$$

since the transition frequency for $\Delta m = \pm 2$ is twice that for $\Delta m = \pm 1$.

Equations (5) may be simplified by recognizing the condition of "extreme narrowing" which applies in the present situation. In non-viscous liquids molecular motion occurs at a rate much faster than the Larmor frequency of the nuclei

i.e. $\tau_c \ll \frac{1}{\nu_{ij}}$ or $\tau_c \cdot \nu_{ij} \ll 1$

so that with this approximation Equation(5) may be rewritten

$$P_1 = \frac{3}{40} e^4 q^2 Q^2 \hbar^{-2} \tau_c \dots\dots\dots(6)$$

$$P_2 = \frac{3}{20} e^4 q^2 Q^2 \hbar^{-2} \tau_c$$

The relationship between transition probabilities and spin - lattice relaxation time T_1 for a 3-level system is given on page 214 of Reference 22. There it is shown that

$$\frac{1}{T_1} = P_1 + 2P_2 \dots\dots\dots(7)$$

Substituting (6) into (7) the final result is

$$\frac{1}{T_1} = \frac{1}{T_q} = \frac{3}{8} \left(\frac{e^2 q Q}{\hbar} \right)^2 \tau_q \dots\dots\dots(8)$$

where τ_q is equal to τ_c , the correlation time for molecular rotation - for reasons discussed in part (ii) of Section B. The term $\frac{e^2 q Q}{\hbar}$ is called the quadrupole coupling constant; it is normally quoted in units of MHz. Equation(8) is thus dimensionally correct.

This is the required expression for T_q , the relaxation time of a quadrupole nucleus. The dependence on electric field gradient is expressed by q , and τ_q reflects the dependence on rotational rate which is sensitive to the size and shape of the molecule and to its surroundings.

As the phenomena outlined in the Introduction well illustrate, the spectra of spin $\frac{1}{2}$ nuclei are sensitive to the T_q value of the quadrupolar nucleus to which they are spin - spin coupled. Clearly then, high - resolution proton magnetic resonance is a technique (in addition to spin-

echo or wide - line measurements) for the estimation of relaxation times of nuclei such as ^{14}N , ^2D , ^{17}O etc. The theory for this is given in part (iv).

(iv) The Line Shape of a Spin - $\frac{1}{2}$ Nucleus Coupled to a Quadrupolar Nucleus

If the rate of ^{14}N relaxation is relatively slow it has the effect of broadening the individual components of the multiplet of a spin - coupled proton. The quadrupole relaxation mechanism reduces the lifetime of the spin states of ^{14}N , so that the proton transitions are not associated with a definite nitrogen nuclear spin energy - and thus are broadened. Under these conditions the appearance of the proton signal may be estimated from the ^{14}N transition probabilities, Equations (6).

The total lifetime, τ_m , of state m for a nucleus with spin I is given by the sum of the probabilities of transitions to and from that state. Thus for the $m = +1$ state of ^{14}N ,

$$\frac{1}{\tau_{m=+1}} = P_{1 \rightarrow 0} + P_{1 \rightarrow -1} = P_1 + P_2$$

from (6), therefore

$$\frac{1}{\tau_{m=+1}} = \frac{9}{40} e^4 q^2 Q^2 \hbar^{-2} \tau_c \dots\dots\dots 9(a)$$

Similarly it may be shown that

$$\frac{1}{\tau_{m=0}} = \frac{6}{40} e^4 q^2 Q^2 \hbar^{-2} \tau_c \dots\dots\dots 9(b)$$

and

$$\frac{1}{\tau_{m=-1}} = \frac{9}{40} e^4 q^2 Q^2 \hbar^{-2} \tau_c \dots\dots\dots 9(c)$$

Equations (9) show clearly that the $m = \pm 1$ spin states are relaxing at one and a half times the rate of the $m = 0$ state. The effect on the

proton multiplet is thus to broaden the components in the ratio 3:2:3, or, since the area under each peak is constant, the peak heights will be in the ratio 2:3:2. The proton spectrum of methyl nitrate (Figure 4) shows the extra broadening of the outer components of the triplet very clearly. The experimental ratio (as measured by the heights) is approximately 5:3 (at 90°C); however, the broadening is no longer small compared with the multiplet separation.

For faster rates of relaxation the proton sees only an average of the three ^{14}N spin states and the signal collapses to a singlet. Under these conditions the above treatment breaks down and a more general line shape theory must be used.

The spectral shapes of multiplets of the type mentioned above may be calculated by a stochastic theory based on the work of Anderson⁽²⁴⁾ and Kubo^(25,26). This theory is called stochastic because it assumes that the effective field on a resonating oscillator is fluctuating in time. One case they considered is that of a composite line when the system can absorb radiation in any one of n different "sites" in each of which it would show a sharp absorption line of frequency $\frac{\omega_j}{2\pi}$ ($j = 1, 2, \dots, n$) in the absence of transitions between the sites; the Hamiltonians in the various sites are assumed to commute with each other. Clearly the proton transitions for m_I of the nitrogen nucleus equal to -1, 0 or +1 are of this type, the assumption of commuting Hamiltonians implying that the magnetic field in the different sites may vary in magnitude but not in direction. Thus the effect of spin-coupling is considered equivalent to a magnetic field in the Z - direction (the proton precessing in one of three possible magnetic fields corresponding to the three possible spin - states of the high - spin nucleus) ignoring the x - and y - components

in the scalar product $\vec{I}_1 \cdot \vec{I}_2$. This leads to inaccuracy in the theory, especially at rapid rates of relaxation.

Assuming that the transition between sites is a Markovian process, Sack's alternative treatment⁽²⁷⁾ of the theory outlined in (24) gives the expression

$$I(\omega) = \text{Re} \left(\vec{W} \cdot \vec{A}^{-1} \cdot \vec{1} \right) \dots\dots\dots(10)$$

for the intensity as a function of angular frequency (i.e. line shape) of a proton coupled to a relaxing nucleus. Here Re denotes "real part of"

\vec{W} is a row vector with components equal to the relative probability of the various components of the multiplet (i.e. population probabilities of the ^{14}N spin states at equilibrium) $\vec{W} = (1, 1, 1)$

$$\vec{1} \text{ is the column vector } \begin{pmatrix} 1 \\ 1 \\ 1 \end{pmatrix}$$

and \vec{A}^{-1} is the matrix inverse of the line shape matrix \vec{A} . The general form of \vec{A} is given in (24); for the case of a proton multiplet collapsed by quadrupole relaxation it becomes (P. 504 of Reference 28)

$$A_{mm'} = \left[i(\Delta\omega + 2\pi J_m) - \frac{1}{\tau_m} \right] \delta_{mm'} + P_{mm'} \dots\dots\dots(11)$$

where $\Delta\omega = \omega_0 - \omega$, the shift from the centre of the multiplet, in radians sec^{-1}

J is the ^{14}N - H coupling constant in Hertz,

τ_m is the lifetime of the m^{th} spin - state of the ^{14}N nucleus,

$(m = 0, \pm 1)$,

$\delta_{mm'} = 0$ if $m \neq m'$, otherwise $\delta_{mm'} = 1$

and $P_{mm'}$ is the probability (sec^{-1}) of a transition from state m

to state m' .

Expressions for τ_m and P_{mm} , have already been developed (Equations 6 and 9) so that the diagonal elements of A are recognized to be

$$\begin{aligned} A_{11} &= i(\Delta\omega + 2\pi J) - \frac{9}{40} \left[\frac{e^2 q Q}{\hbar} \right]^2 \tau_q \\ A_{00} &= i\Delta\omega - \frac{6}{40} \left[\frac{e^2 q Q}{\hbar} \right]^2 \tau_q \dots\dots\dots(12) \\ A_{-1-1} &= i(\Delta\omega - 2\pi J) - \frac{9}{40} \left[\frac{e^2 q Q}{\hbar} \right]^2 \tau_q \end{aligned}$$

and the off-diagonal elements are

$$\begin{aligned} A_{m,m+1} &= P_{1,0} = P_{0,1} = P_{0,-1} = P_{-1,0} = \frac{3}{40} \left[\frac{e^2 q Q}{\hbar} \right]^2 \tau_q \\ A_{m,m+2} &= P_{1,-1} = P_{-1,1} = \frac{3}{20} \left[\frac{e^2 q Q}{\hbar} \right]^2 \tau_q \dots\dots\dots(13) \end{aligned}$$

The definition of quadrupole relaxation time, T_q , from Equation (8) allows simplification of Equations (12) and (13) so that the matrix A may be written

$$\vec{A} = \begin{bmatrix} i(\Delta\omega + 2\pi J) - \frac{3}{5T_q} & \frac{1}{5T_q} & \frac{2}{5T_q} \\ \frac{1}{5T_q} & i\Delta\omega - \frac{2}{5T_q} & \frac{1}{5T_q} \\ \frac{2}{5T_q} & \frac{1}{5T_q} & i(\Delta\omega - 2\pi J) - \frac{3}{5T_q} \end{bmatrix} \dots\dots(14)$$

Up to this point the effect of a non-zero linewidth for the proton resonance in the absence of ^{14}N relaxation has not been considered.

Clearly, however, this is important if accurate line shape analyses are to be performed. It may be incorporated into expression (14) by defining the natural linewidth of the proton signal, $W_{\frac{1}{2}} = (\pi T_2)^{-1}$. The complete

equation for the line shape $I(\omega)$ is then⁽²⁹⁾(15)

$$I(\omega) = \text{Re} \left\{ (1,1,1) \begin{bmatrix} i(\Delta\omega + 2\pi J) - \frac{3}{5T_q} - \frac{1}{T_2} & \frac{1}{5T_q} & \frac{2}{5T_q} \\ \frac{1}{5T_q} & i\Delta\omega - \frac{2}{5T_q} - \frac{1}{T_2} & \frac{1}{5T_q} \\ \frac{2}{5T_q} & \frac{1}{5T_q} & i(\Delta\omega - 2\pi J) - \frac{3}{5T_q} - \frac{1}{T_2} \end{bmatrix} \begin{pmatrix} -1 \\ 1 \\ 1 \end{pmatrix} \right\}$$

The inversion of matrix A and expansion of Equation (15) is straightforward if tedious (Appendix II). The final expression from which line shapes are computed is

$$I(\nu) = \frac{C_3 + \Delta\nu^2 (C_2 + \Delta\nu^2 C_1)}{C_6 + \Delta\nu^2 [C_5 + \Delta\nu^2 (C_4 + \Delta\nu^2)]} \dots\dots\dots(16)$$

where $C_1 - C_6$ are constants involving J , T_q and T_2 ; $\Delta\nu$ is the shift in Hz from the centre of the multiplet.

The form of the absorption spectrum depends on J , T_q and T_2 ; changes in one or more of these parameters result in an alteration of the line shape. In the present work J and T_2 were measured directly and kept constant; the dependence of the resonance on T_q is shown for a series of values in Figure 1. For large T_q (slow quadrupole relaxation) the spectrum consists of individual lines (Figure 1a) broadened as discussed at the beginning of this section. Gradually the maxima of the outer peaks move inwards as the lines broaden further, (Figure 1b), until eventually all three coalesce into one wide signal (Figure 1c). Further increase in relaxation rate merely sharpens this single resonance. (Figure 1d).

FIGURE 1

The resonance line shape of a proton spin-spin coupled to a nucleus of spin $I=1$ which is undergoing varying rates of quadrupolar relaxation.

(a) $T_q = 1.000$ sec

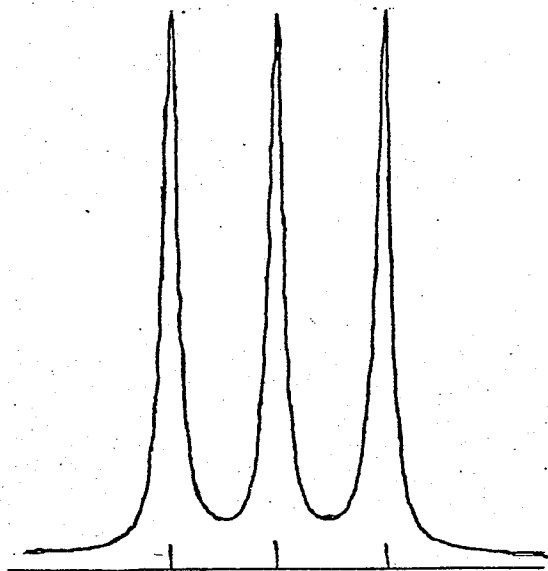
(b) $T_q = 0.130$ sec

(c) $T_q = 0.055$ sec

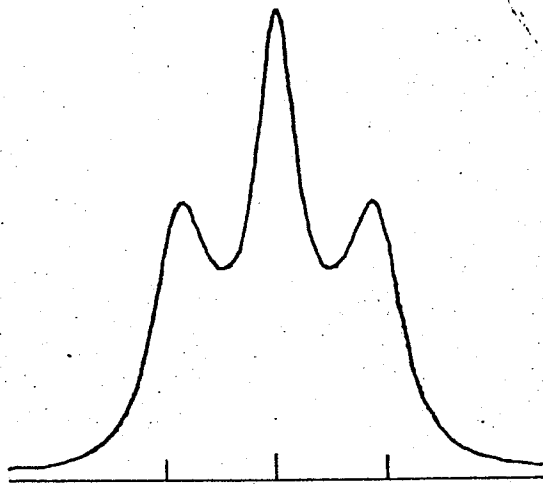
(d) $T_q = 0.010$ sec

($T_2=1.0$ sec $J=2.75$ Hz)

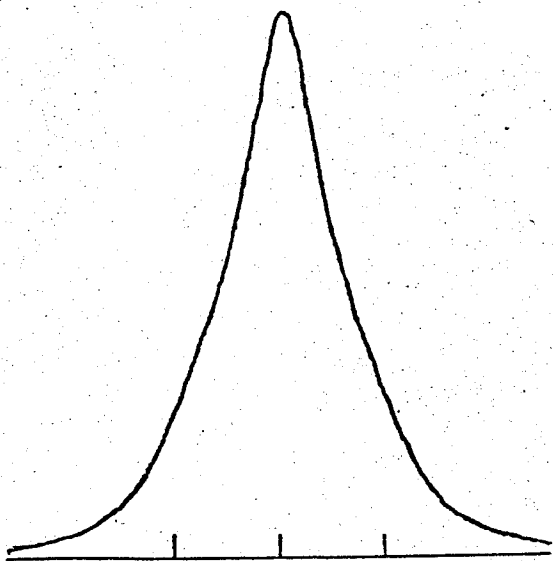
The vertical lines indicate the position of the triplet in the absence of quadrupolar relaxation.



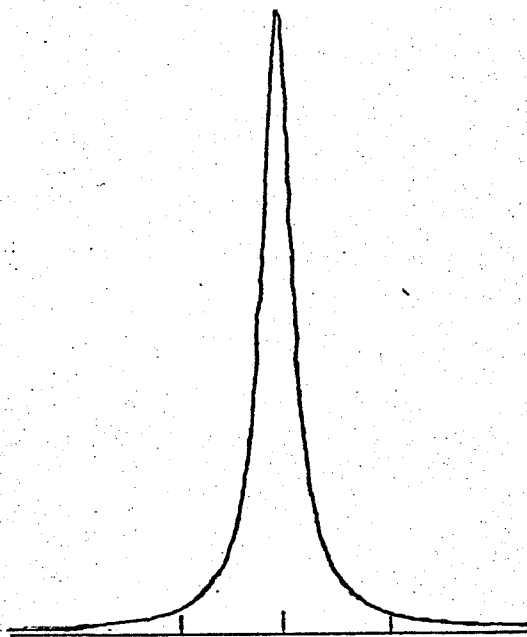
(a)



(b)



(c)



(d)

NOTE: The above theory is applicable to a quadrupolar nucleus coupled to one or one group of equivalent spin - $\frac{1}{2}$ nuclei. The situation where there is more than one type of spin - $\frac{1}{2}$ nucleus in the molecule, and where coupling between the different types exists, requires an extension of the theory. See Reference 30.

SECTION C

NUCLEAR MAGNETIC RESONANCE IN THE STUDY

OF LIQUIDS

(1) Introduction

The effect of structure and behaviour of the surrounding medium on nuclear magnetic resonance experiments is most directly reflected in the spin - lattice relaxation time, T_1 (the time constant characterising the approach to thermal equilibrium of a spin system when placed in a magnetic field). The magnitude of the spin - lattice relaxation time varies considerably with the type of nucleus and the environment. For protons and other nuclei of spin $1/2$, the only way in which the nuclear spin can be coupled with other degrees of freedom is by means of local fluctuating magnetic fields. Nuclei with higher spin, however, have electric quadrupole moments which can interact with fluctuating electric fields, so that such nuclei usually have smaller values of T_1 . Whatever the mechanism of spin - lattice coupling it is the random molecular motions in the liquid which provide the oscillating field. Transitions between spin states are induced by these fields.

The frequency of fluctuation is determined by the type of molecular motion. For instance, rotation of a molecule causes changes in the electric field gradient at nuclei (due to other nuclei and electrons in the molecule) and changes in the local magnetic field at one nucleus due to another in the same molecule. Thus intramolecular relaxation processes such as anisotropic electronic shielding, electric quadrupole and magnetic dipole - dipole interactions are related to the reorientation rate of molecules, i.e. characterized by a rotational correlation time, τ_c . Analogously, the relative diffusion of molecules determines intermolecular relaxation (since the local fields at the nuclei of one molecule due to those of another are caused to fluctuate by this motion). The relevant

time characteristic is then τ_d , the diffusional correlation time*. For any random motion there is the whole spectrum of frequencies and the variation of the intensity of the fluctuations with frequency must depend on the type of motion concerned. Thus the composite motions within a liquid will cause relaxation of the spins by a number of mechanisms, the overall effect of which is reflected in the experimental T_1 value

$$\text{i.e. } \frac{1}{T_1}_{\text{exp}} = \left(\frac{1}{T_{d-d}}\right)_{\text{inter}} + \left(\frac{1}{T_{d-d}}\right)_{\text{intra}} + \frac{1}{T_{\text{sr}}} + \frac{1}{T_{\text{as}}} + \frac{1}{T_{\text{q}}} + \dots \dots \dots (17)$$

where

$\left(\frac{1}{T_{d-d}}\right)_{\text{inter}}$ represents the contribution to the overall relaxation rate by intermolecular dipole - dipole relaxation.

and $\left(\frac{1}{T_{d-d}}\right)_{\text{intra}}$, $\frac{1}{T_{\text{sr}}}$, $\frac{1}{T_{\text{as}}}$ and $\frac{1}{T_{\text{q}}}$ are the corresponding terms for intramolecular dipole-dipole, spin - rotational, anisotropic electronic shielding and quadrupolar relaxation, respectively.

Changes in τ_c and τ_d will be reflected in the T_1 value and thus measurements of the latter may be used to monitor changes in the former. Assuming molecular reorientation is a thermally activated process, the dependence of τ on temperature is characterized by an activation energy, E_a , which may in principle, therefore, be determined from measurements of T_1

* Some workers feel that it is unrealistic to separate τ_c and τ_d in this way. For instance, if a molecule "jumped" by a distance of the order of one molecular diameter it might well at the same time reorient by a substantial angle and in this case both the inter and intra - interactions would be modulated in much the same way, i.e. their correlation times would be similar. However, this is not to deny the validity of the analysis presented here.

at various temperatures. However, the contributions to T_1 (Equation 17) arise from a variety of interactions which exhibit different dependencies on temperature. The interpretation of E_a is thus ambiguous unless the rotational and translational terms can be separated. A brief survey of the ways in which "pure" E_a values have been obtained from T_1 measurements is given in the next section, C(ii).

The direct calculation of correlation times from spin - lattice relaxation measurements is not possible unless the form of the correlation function for molecular motion, $g(\tau)$ is known. It is common to use an exponential function, which is physically reasonable for some types of motion, and in this case τ may be estimated. Using the results of the theory of Brownian motion, Bloembergen, Purcell and Pound (hereafter referred to as B.P.P.) attempted to estimate τ from physical constants of the medium ⁽³¹⁾. Numerous modifications of the B.P.P. original equation have been proposed; comparison with correlation times from T_1 measurements commonly being used as a test of such models. Section C(iii) describes the principles involved in the various treatments and assesses their value in the light of current experimental data.

(ii) Estimation of Activation Parameters for Molecular Reorientation By NMR Methods

(a) Scope and Limitations of the Method

Conventional line shape analysis of nuclear magnetic resonance spectra has been extensively used to study inter - and intra-molecular rate processes lying in the $1 - 10^4 \text{ sec}^{-1}$ frequency range^(32,33). Without recourse to other instruments (as for example, microwave techniques which measure rates of the order of $10^6 - 10^9 \text{ sec}^{-1}$) the range of NMR spectroscopy can be extended to processes in the $10^8 - 10^{12} \text{ sec}^{-1}$ range by the determination of nuclear relaxation times⁽³⁴⁻³⁶⁾. This is the frequency of molecular motions in a liquid, and activation energies of this order of magnitude (a few kcal.mole⁻¹) may be conveniently estimated from the temperature dependence of the spin - lattice relaxation time, provided the translational and rotational contributions can be separated (Equation 17).

For nuclei of spin $I = \frac{1}{2}$ there is no quadrupolar term; by measuring T_1 for mixtures of the molecule with an inert magnetic solvent (preferably the perdeuterated analogue) and extrapolation to zero proton concentration, the intramolecular dipole - dipole term can be separated from the inter-molecular. (See, for instance, the T_1 measurements on benzene performed by Bonera and Rigamonti⁽³⁷⁾ where separating $(T_1)_{\text{inter}}$ and $(T_1)_{\text{intra}}$ in this way shows that the two behave quite differently in their temperature dependencies.) In addition, $(T_1)_{\text{intra}}$ contains a spin - rotational contribution^(38,39) which is especially important at high temperatures. By using the method of Hubbard⁽⁴⁰⁾, Powles and coworkers^(41,42) extracted the T_{sr} term and showed that it behaves in the opposite manner to $(T_{\text{dd}})_{\text{intra}}$. Having separated the dependencies of τ_c and τ_d on temperature, the individual activation energies for rotation and translation can be estimated

with confidence^(41,42).

The use of quadrupolar nuclei (spin $I \geq 1$) is finding increasing popularity in studies of this sort. Not only does the T_q^{-1} term invariably dominate all others (Appendix I) and so avoids messy corrections, but the molecular process involved is pure rotation so that temperature studies yield an E_a which can be unambiguously assigned to molecular reorientation.

Table I lists some results for translational and rotational activation energies obtained by a variety of techniques.

(b) Results and Interpretation

Reference to the literature shows that the spin - echo technique is most commonly used to measure T_1 ; however, in certain cases (as, for instance, where the number of nuclei per cc. is low) wide-line or high-resolution methods are preferable. The results for H_2O/D_2O , CH_3COCH_3/CD_3COCD_3 and in particular BF_3 confirm that E_a is independent of the method used to obtain $(T_1)_{intra}$. Powles et al⁽⁴³⁾ demonstrated (for water, ammonia and benzene) that the results from T_q measurements coincided with those from $(T_{dd})_{intra}$. This is only to be expected since both depend on the same correlation function, but with different numerical factors.

Before considering any implications of the results in Table I the physical meaning of E_a must be understood. Moniz and Gutowsky⁽⁴⁸⁾ defined E_a simply from the dependence of the quadrupolar correlation time on temperature:

TABLE 1

Some Illustrative Activation Energy Results

MOLECULE ^(a)	E_a (kcal.mole ⁻¹)	COMMENT ^(b)	REFERENCE
H ₂ O	~ 5 at 0°C 3.5 from 40°-100°	(T ₁) _{inter} was calculated at each temperature and subtracted from (T ₁) _{exp} to yield (T ₁) _{intra} .	44
D ₂ O	3.5 from 40°-100°	T _q values of ² D confirm the separation of ¹ H T ₁ in H ₂ O.	43 45
CH ₃ COCH ₃	1.5 ± 0.2	(T ₁) _{intra} obtained by dilution (CD ₃ COCD ₃) and extrapolation.	37
CD ₃ COCD ₃	1.7 ± 0.2	Again ² D T _q measurements confirm the ¹ H (T ₁) _{intra} values.	46
CCl ₄ CHCl ₃ C ₆ H ₅ Cl	1.3 1.4 1.6	³⁵ Cl linewidth measurements (T ₂ = T _q)	47
C ₂ H ₅ NO ₂ n-C ₃ H ₇ NO ₂ i-C ₃ H ₇ NO ₂	1.8 2.2 2.4	from ¹⁴ N T _q values	48

$^{11}\text{BF}_3$	1.4	Estimated from T_q of ^{11}B - as found from ^{19}F line shape.	49
	1.43	From T_q of ^{11}B found from ^{11}B line shape.	
$^{10}\text{BF}_3$	1.36	From T_q of ^{10}B - found from ^{19}F line shape.	50
<hr/>			
ND_3	1.88 ± 0.05	From ^{14}N T_q values	51
	$1.62 \pm .06$	From ^2D T_q	
<hr/>			
CH_3CN	1.9	From ^{14}N T_q	48
	1.4	From ^1H T_1	
CD_3CN	1.7 ± 0.1	From ^{14}N T_q	52
	1.2 ± 0.1	From ^2D T_q	53
<hr/>			
CH_3CCl_3	1.8	From ^1H T_1	54
	1.7	From ^{35}Cl T_1	
<hr/>			
C_6H_6	3.0	From ^1H T_1 (inter)	41
	1.2	From ^1H T_1 (intra)	
		Terms separated by dilution (C_6D_6) and extrapolation.	
<hr/>			

(a) Pure liquids.

(b) T_1 values obtained by the spin - echo technique unless otherwise stated.

$$\tau_q = \tau_q^0 \exp\left(\frac{E_a}{RT}\right)$$

and E_a was extracted from a plot of $\log T_1$ vs $\frac{1}{T}$. This "activation energy" appears to be more of an empirical quantity than one with any physical significance. Hertz⁽³⁴⁾ attempts a loose definition. He attributes E_a to "the change in potential energy of the molecule associated with the dynamical processes which cause the decay of the time correlation of the property under consideration", i.e. merely a potential energy associated with molecular reorientation. He further considers that this change in potential energy occurs somewhere on the rotational path of the molecule and may take place several times during reorientation, i.e. not necessarily a difference in potential energy between initial and final states. For a process like rotation, envisaged as occurring in a series of jumps, this is an entirely reasonable interpretation. An extreme view taken by Powles and Gough⁽⁵⁵⁾ questions the significance of activation parameters obtained in this way, considering that the physical parameters of the theory cannot be deduced from experimental results. However, the vast majority of literature results are discussed with the concept that E_a represents the facility with which a solute molecule can reorient in its surroundings, and such a "meaning" of E_a will be assumed here.

In this context the values for E_a , and the differences among the compounds, appear to be generally compatible with the relative size and shapes of the molecules. The series of nitro compounds⁽⁴⁸⁾ shows this well. The errors in E_a are usually less than 10%, so that an usually large or small E_a may confidently be attributed to a specific effect in that system. For instance, the relatively small value for benzene (1.2

kcal.mole⁻¹) is doubtless a reflection of the facile rotation about the hexad axis which requires far less disturbance of neighbouring molecules than end-over-end rotation. Translation of the molecule necessitates even greater interaction, so that the E_a value of 3.0 kcal.mole⁻¹, derived from $(T_1)_{\text{inter}}$ measurements for benzene, is reasonable and consistent with the inequality $\tau_c < \tau_d$. (i.e. that a benzene molecule takes longer to translate a molecular diameter than to reorient by an angle of order one radian). The surprisingly large E_a value for water may be explained in terms of hydrogen - bonding, a strong, temperature dependent type of molecular interaction which inhibits rotation.

The results for acetonitrile (both the protonated and deuterated species) reveal the complex nature of reorientation in that molecule. The activation energy derived from T_q measurements of ^{14}N is substantially higher than that from either ^1H or ^2D studies, i.e. the correlation time governing ^{14}N relaxation shows a stronger temperature dependence than that for the methyl group. In acetonitrile the axially symmetric field gradient at ^{14}N is along the C-N bond axis, so that reorientations of the molecule about this axis are ineffective in producing ^{14}N relaxation via the quadrupole mechanism, though they would contribute to proton dipole - dipole interaction or deuteron quadrupole relaxation. Motions perpendicular to the C-N axis do affect the field gradient. If all such rotations were equally probable (i.e. if the reorientation were isotropic) then the E_a values from both ^{14}N and ^1H would be identical. The fact that they are not demonstrates that the motion in pure CH_3CN is anisotropic, and specifically that rotation about the symmetry axis is faster than about axes perpendicular to the symmetry axis. These early observations of Moniz and Gutowsky⁽⁴⁸⁾ lead to investigations of anisotropy in molecular

motion by observing the relaxation of several nuclei in the same molecule. Woessner⁽⁵⁶⁾ and Buntress⁽⁵⁷⁾ developed expressions for the relaxation time of a nuclear spin in a molecule undergoing anisotropic rotation; applied to N, N - dimethylformamide⁽⁵⁸⁾ and chloroform⁽⁵⁹⁾, for example, they demonstrated anisotropic reorientation for both molecules. It is surprising therefore, that the work of O'Reilly et al⁽⁵⁴⁾ shows rotation in methyl chloroform to be essentially isotropic. A comprehensive review of this area of research is given in a recent article by Woessner⁽⁶⁰⁾.

(iii) Estimation of Molecular Correlation Times from Physical Properties of the System(a) An outline of the theories

There have been numerous theories proposed to calculate correlation times for molecular motion from bulk properties of the liquid, all of which use the "hard sphere" model for the rotating (or translating) molecule. A single correlation time is estimated for the molecule which means that all such theories are incapable of treating anisotropy in the rotational motion (since this requires the calculation of more than one correlation time for the same molecule). As the results of Section (ii) have shown this is often an important aspect of rotation. However, there are deficiencies in the theories more significant than this; the basic principles and assumptions of the various models are outlined below, considering only rotational motions, although calculation of translational correlation times is also possible. The relative successes of the three models are assessed; in view of certain ambiguities and inadequacies inherent in them, two entirely different approaches to correlation times are outlined and shown to give promising results.

B.P.P. Model: In their treatment of magnetic relaxation in liquids B.P.P.⁽³¹⁾ developed an expression for T_1 which included a correlation time τ_c ; for intramolecular relaxation this refers to rotational motions. In order to estimate τ_c B.P.P. recognised the similarity to the Debye theory of dielectric relaxation in polar liquids (61); there also it is necessary to estimate the time, τ , during which molecular orientation persists⁽⁶¹⁾. Debye assumed that in the first approximation the molecule could be treated as a sphere of radius a imbedded in a continuous medium of viscosity η . He obtained

$$\tau_{\text{Debye}} = \frac{\beta}{2kT} = \frac{4\pi\eta a^3}{kT} \dots\dots\dots(18)$$

where β is the damping constant for rotation of a sphere and given by the Stokes' expression as

$$\beta = 8 \pi \eta a^3 \dots\dots\dots(19)$$

The rotational correlation time, τ_c , characterizing nuclear spin relaxation is smaller by a factor of 3 than that given in Equation (18). This is because in the theory of dielectric relaxation spherical harmonics of $l=1$ occur, but, for nuclear - spin relaxation, spherical harmonics of $l=2$ occur in the corresponding expressions. Thus B.P.P. obtained

$$\tau_c \text{ (B.P.P.)} = \frac{4 \pi \eta a^3}{3kT} \dots\dots\dots(20)$$

The use of Stokes' expression in the derivation of Equation (20) assumes that the reorientation rate of a molecule is determined only by frictional forces. Thus it might be predicted to give better results for highly polar, nonspherical molecules than for relatively nonpolar, spherical ones where rotation can occur on the lattice site without having to push adjacent molecules out of the way. This is borne out by comparison with experimental results. In addition, Stokes' formula for β is valid only if the radius of the sphere is much greater than that of the particles of the surrounding medium. In most liquids this approximation of a continuous fluid cannot be justified; in an attempt to overcome the unsatisfactory basis of Equation (20) Gierer et al. proposed

The Theory of Microviscosity.^(62,63)

They accounted for the discontinuous nature of the liquid by calculating the friction exerted upon a spherical solute molecule, radius a , by successive spherical shells of solvent molecules of thickness $2b$. In the limiting case when $a \gg b$ the sum of these contributions can be expressed

as an integral which gives Stokes' law; more generally, a "microviscosity factor", f , was obtained where

$$f = \left\{ 6 \frac{b}{a} + \left(1 + \frac{b}{a} \right)^{-3} \right\}^{-1} \dots\dots\dots(21)$$

The microviscosity factors are calculated using molecular radii obtained from molecular weights and densities. Neglecting the last term in Equation (21) the expression for τ_c on a microviscosity model is

$$\tau_c \text{ (micro)} = \frac{4 \pi \eta a^3}{3kT} \frac{a}{6b} \dots\dots\dots(22)$$

thus predicting a relaxation time some six times smaller than that of B.P.P.

The Hill Theory of Mutual Viscosity

An alternative approach was given by Hill⁽⁶⁴⁾ using Andrade's theory of viscosity⁽⁶⁵⁾ which supposes that friction in a liquid is due to temporary solute - solvent association. The viscosity of a mixture, η_s , for a polar solute in a non-polar solvent is given by

$$\eta_s = \frac{f_A^2 \eta_A \sigma_A}{\sigma_m} + \frac{f_B^2 \eta_B \sigma_B}{\sigma_m} + \frac{2 f_A f_B \eta_{AB} \sigma_{AB}}{\sigma_m} \dots\dots\dots(23)$$

where f_A and f_B are the mole fractions of A (solvent) and B (solute) respectively, σ_A and σ_B is the average distance between A molecules in pure A, and likewise for B, σ_{AB} is the average distance between an A and a B molecule in solution, σ_m is the average distance between molecules (of both types) in solution and η_{AB} is a novel term, called the "mutual viscosity" and defined by Equation (23). By considerations of momentum transfer, (the basis of Andrade's theory) and conservation thereof, the correlation time for dielectric relaxation of solute B is given by Equation

(24)

$$\tau = \frac{1}{2kT} \left(6f_A \eta_{AB} \sigma_{AB} K_A^2 + 3f_B (3-\sqrt{2}) K_B^2 \eta_B \sigma_B \right) \dots\dots\dots(24)$$

where $K_A^2 = \frac{I_{AB} \cdot I_B}{I_{AB} + I_B} \cdot \frac{M_A + M_B}{M_A M_B}$ - a momentum transfer term.

Here M_A, M_B is the mass of A and B respectively, I_B is the moment of inertia of B, and I_{AB} is the moment of inertia of A about the centre of B during a collision. Hill is assuming that the resistive force on a rotating polar molecule in a non-polar solvent depends on the mutual viscosity, η_{AB} (c.f. Stokes' assumption of a dependence on the macroscopic viscosity).

For a dilute solution of B in solvent A, $f_B \approx 0$ and $f_A \approx 1$ so that (dividing by 3 to yield the appropriate expression for nuclear - spin relaxation)

$$\tau_{\text{(Hill)}} = \frac{\eta_{AB} \sigma_{AB}}{k T} \cdot \frac{I_{AB} I_B}{I_{AB} + I_B} \cdot \frac{M_A + M_B}{M_A M_B} \dots\dots\dots(25)$$

Hill stresses that the main point of Equation (25) is the use of mutual viscosity between solute and solvent which arises from picturing viscosity as an intermolecular interaction.

The calculation of correlation times from Equation (25) requires additional data to estimate η_{AB} and this is often unavailable. However, Mitchell and Eisner⁽⁶⁶⁾ from the results of some T_1 measurements have proposed an approximate form of Hill's theory which facilitates calculation of τ_c . They measured $(T_1)_{\text{intra}}$ for a series of molecules and estimated τ_c , comparing it with τ_{Hill} found from Equation (25). Reasonable agreement was found; more interestingly, however, they observed that

$$\eta_{AB} \sigma_{AB} \approx 2 \eta a$$

and since $\sigma_{AB} \approx 2a$ (ie. the average distance between solvent and solute molecules is roughly twice the radius of the solute molecule) then

$$\eta_{AB} \approx \eta$$

They therefore concluded that the success of the Hill model was not due to the mutual viscosity term (as Hill had claimed) but rather to the momentum transfer term. This term, K_A^2 , is of the form of a "reduced moment of inertia" divided by the reduced mass of the solvent - solute system. Since the term I_{AB} is usually large compared with I_B , little error is introduced by replacing the reduced moment of inertia by I_B .

$$\text{ie. } \frac{I_{AB} I_B}{I_{AB} + I_B} \approx I_B$$

So that an approximate expression for the Hill correlation time is

$$\tau_{\text{Hill (approx.)}} = \frac{2I\eta a}{\mu kT} \dots\dots\dots(26)$$

where I is the average of the principal moments of inertia of the molecule,*1
 a is the average of the semiaxes of the molecule, η is the solvent viscosity
 and μ is the reduced mass of the solvent - solute system.

(b) An Assessment of the Three Methods

Substitution of Equations (20), (22) and (26) into (8) gives the relationships

*1. Mitchell and Eisner note that there appears to be a significant way of "choosing" an average I , depending upon which axis has the greater rotational probability (ie the effects of anisotropy are apparent). Thus, for benzene a greater weighting of the moment of inertia about the hexad axis gives better results than if all three are considered equally.

$$\frac{1}{T_q} = A \frac{\eta}{T} \dots\dots\dots \text{B.P.P.} \dots\dots\dots (27a)$$

$$\frac{1}{T_q} = A \frac{\eta}{bT} \dots\dots\dots \text{micro} \dots\dots\dots (27b)$$

$$\frac{1}{T_q} = A \frac{\eta}{\mu T} \dots\dots\dots \text{Hill (approx)} \dots\dots\dots (27c)$$

where A is a constant for a given solute molecule; it includes the quadrupole coupling constant, $\frac{e^2 qQ}{h}$, and the remaining terms are dependent on the particular model used. Thus a linear dependence of T_q^{-1} on $\frac{\eta}{T}$, $\frac{\eta}{bT}$ and $\frac{\eta}{\mu T}$ is predicted by Equations (27a), (27b) and (27c), respectively.

There is much experimental evidence to confirm this. B.P.P. in their original paper showed that the spin - lattice relaxation time for liquid ethyl alcohol was proportional to η/T ⁽³¹⁾ even though they did not separate $(T_1)_{\text{intra}}$ and $(T_1)_{\text{inter}}$. Both contributions to the overall spin - lattice relaxation time are predicted to depend on η/T , but with different constants of proportionality. The observed linearity is thus surprising; Powles and Figgins⁽⁴¹⁾ however found that the overall T_1 of benzene did not follow η/T linearly, but resolved into $(T_1)_{\text{intra}}$ and $(T_1)_{\text{inter}}$, the individual components did conform to Equation (27). Whitesides and Mitchell⁽⁶⁷⁾ for toluene solutions of π -tropyivanadium (-I) tricarbonyl found a T_1 vs η/T linearity, as did Richards et al^(68,69) in numerous studies of quadrupolar relaxation in electrolyte solutions; proton spin - lattice relaxation times in water also conform to this theory⁽⁷⁰⁾. Constant temperature measurements for nitriles⁽⁷¹⁾ and 2-fluoropyridine⁽⁷²⁾ in a range of solvents, and for some ²³Na and ⁸¹Br salts in aquo⁽⁷³⁾ add to the vast quantity of data supporting Equation (27).

However, under more rigorous examination neither the micro - nor mutual viscosity modifications of the B.P.P. theory are satisfactory. Petrakis⁽⁷⁴⁾ studied the ²⁷Al relaxation time in some aluminium alkyls

over a very wide temperature range and found distinct curvature in the T_q^{-1} vs η/T plots; he predicted that other systems might well show this behaviour if the temperature range were sufficiently extended. Also disturbing are the results obtained from T_1 measurements where viscosity changes are brought about by variation in pressure. In all the liquids examined^(55,75-77) T_1^{-1} was found to increase with increasing pressure but the viscosity rises more rapidly, so that the product $T_1\eta$ actually increases with pressure, rather than maintaining a constant value. Bull and Jonas⁽⁷⁸⁾ separated the $(T_1)_{inter}$ and $(T_1)_{intra}$ terms for acetone over a considerable pressure range and showed that (contrary to B.P.P. theory which predicts comparable pressure dependencies) $(T_1)_{inter}$ changed markedly with pressure, parallel to viscosity changes, whereas $(T_1)_{intra}$ varied far less. Similar results have been reported for benzene⁽⁷⁹⁾ and confirm the inadequacy of B.P.P. theory in describing rotation i.e. $(T_1)_{intra}$. The effect of pressure on translational correlation times would be predicted to be greater than that on rotational motion, since a decrease in free volume affects the freedom to migrate far more than to rotate. As a result the intramolecular contribution to T_1 will not fall off as rapidly with increasing pressure as the B.P.P. theory predicts.

As mentioned in the Introduction, the most severe test of a model is to compare absolute values of calculated and experimental correlation times. Some results (from Reference 80) are shown in Table 2. B.P.P.-Debye model invariably predicts τ_c 's which are an order of magnitude too large, that is, it overestimates the rate of relaxation^(28,66,71,74,81,etc.). The correlation times calculated with the aid of the microviscosity factors (line (3)) are much closer to those observed experimentally; marginal improvement is given by the Hill theory, either in its approximate or

complete form (lines (4) and (5)). Free rotation of the methyl groups attached to an aromatic skeleton should reduce the correlation time of these protons compared to the rest of the molecule, and this is observed to be so experimentally, though allowance can be made for this only in the Hill theory.

Clearly then, molecular correlation times can be calculated to within a factor of three or less using a mutual or microviscosity modification of the B.P.P. theory. However, they all suffer from an ultimate dependence on the Stokes hydrodynamic equation with the assumption that reorientational rates are completely controlled by frictional forces. This is certainly an oversimplification (See Part C). Furthermore, the type of

TABLE 2

Rotational Correlation Times \neq Experimental and Calculated

	Benzene	Toluene		p - Xylene	
		ring	methyl	ring	methyl
(1) Exp.	1.18	1.70	1.27	2.38	1.77
(2) B.P.P.	13.1 (4.67)	15.71 (6.24)	15.71 (6.24)	17.66 (7.30)	17.66 (7.30)
(3) Micro	2.63 (1.07)	3.34 (1.55)	3.34 (1.55)	3.85 (1.89)	3.85 (1.89)
(4) Hill	1.47	2.60	2.37	4.23	4.00
(5) Hill (approx)	1.62 (1.15)	2.60 (1.91)	2.20 (1.62)	3.66 (2.72)	3.27 (2.44)

\neq of protons at infinite dilutions in CS_2 at $25^\circ C$ in $sec \times 10^{-12}$ (80)
 Values in brackets have been calculated from covalent radii; otherwise van der Waals radii have been used. In both cases the relaxation theory of B.P.P. (31) was used to estimate τ_c from observed T_1 values.

radii used in the calculations is critical; τ_c computed from covalent atomic radii is always considerably less (and closer to the experimental value) than if van der Waals radii are used (see the values in brackets, Table 2). This improvement, however, is difficult to justify, since use of covalent radii implies that during collisions the interatomic distances for the colliding molecules become of the order of magnitude of chemical bonds!

In view of these unsatisfactory aspects of the theories outlined above, it is perhaps worthwhile to consider briefly two alternative treatments which appear to give promising results in the few systems to which they have been applied.

(c) Alternative Treatments.

Steele^(82,83) has questioned the entire basis of B.P.P.'s model. From his work it not only appears that the Stokes equation for rotational friction is inapplicable in the case of molecular rotations but also that the correlation functions of spheroidal molecules may be primarily dependent upon inertial parameters rather than friction constants. Thus there would be no direct relationship between macroscopic viscosity and molecular rotation. He treats rotation in terms of classical equations of motion for a rigid rotator; the torque on the rotator is decomposed into a frictional term proportional to the angular velocity and a randomly fluctuating term. Calculations then show that the rotational friction tensor is zero for a spherical molecule (entirely reasonable on physical grounds since no torques can act on a rotating object unless its potential energy depends upon the angles of orientation of the body) and that rotational relaxation of such molecules is almost completely dominated by inertial

effects. Some experimental results substantiate this analysis. Moniz, Steel and Dixon⁽⁸⁴⁾ measured proton T_1 's for certain spheroidal molecules known to have a large moment of inertia and small rotational friction constant. They evaluated $(T_1)_{\text{rot}}$ by applying the Gaussian approximation to the autocorrelation function for molecular reorientation and obtained

$$\left(\frac{1}{T_1}\right)_{\text{rot}} = \frac{3\gamma^4 \hbar^2}{4b^6} \cdot \left(\frac{\pi I}{3kT}\right)^{\frac{1}{2}} \dots\dots\dots(28)$$

where γ is the magnetogyric ratio of the nucleus, b the distance between spins (they used van der Waals radii) and I the moment of inertia of the molecule. It was assumed that the B.P.P. model was adequate to give the translational contribution to T_1 - so that an experimental rotational relaxation time $(T_1)_{\text{rot}}^{\text{exp}}$ was estimated from the observed T_1 . Comparison of Equation (28) with $(T_1)_{\text{rot}}^{\text{exp}}$ over a considerable temperature range gave excellent agreement - for benzene, toluene and decalin; for more polar molecules the results were less encouraging. The authors therefore concluded that for nonpolar spheroidal molecules rotational relaxation is adequately described by a Gaussian decay of the angular autocorrelation functions. In general, Gaussian decays are characteristic of processes in which dynamical coherence is the predominant factor; thus the reorientational motion of these molecules must be essentially that of a freely rotating molecule for times long enough to permit roughly one complete rotation of the molecule. For larger values of the friction constant, the viscosity dependent result is recovered, and $(T_1)_{\text{rot}}^{-1}$ is indeed proportional to the friction constant. Thus, in principle, Steele's theory permits the computation of rotational relaxation in liquids from molecular interaction potential functions.

The "quasilattice" theory of liquids^(85,86) is readily extended to derive an expression for the rotational correlation time. In this model molecules of the liquid are considered to occupy a face-centred cubic lattice, transport properties such as viscosity and diffusion occurring because of vacant lattice sites in the liquid. Furthermore,⁽⁴⁷⁾ it is presumed that when a molecule is at a lattice site it does not reorient, or does so relatively slowly; molecular reorientation occurs when the molecule "jumps" to the top of the energy barrier at the cell boundary (a requisite for changing sites). A criticism of the quasilattice model is based on the fact that the correlation function is derived from the rotational diffusion equation⁽⁸⁴⁾ which implies that molecular reorientation occurs in small steps -- hardly consistent with a model which assumes reorientation during a molecular jump to the cell boundary! However, O'Reilly has overcome the problem and his calculations for τ_c on this model agree very closely with the experimental values⁽⁸⁷⁾, except where rotational coherence occurs.

Neither of these two theories, however, has been as widely examined as the B.P.P. model and modifications thereof. The results so far appear highly promising but must be vastly extended before either could be regarded as a reliable method for estimating correlation times.

SECTION D

NATURE OF THE PROBLEM

The proton magnetic resonance spectrum of methyl nitrate in cyclohexane solution at 10°C is a broadened singlet (half-height linewidth, $\Delta\nu_{\frac{1}{2}} = 4.6$ Hz); at 90°C it is a well resolved triplet but with the intensity of the outer components approximately two-thirds that of the central peak. A similar dependence of line shape on temperature is observed for methyl nitrate as a pure liquid and in solution in other solvents. In addition, at ambient temperature there is a considerable variation in line shape from one solvent to another. In dimethylsulphoxide the solute resonance is a relatively sharp singlet ($\Delta\nu_{\frac{1}{2}} = 2.1$ Hz); in carbon disulphide it is a partially resolved triplet. Other solvents show line shapes intermediate between these two extremes.

These observations indicate the presence of a rate process which is both temperature and solvent dependent - it is the reorientation of the molecule itself in solution. The changes in the proton line shape are brought about by the variation in spin-lattice relaxation time, T_1 , of the nitrogen nucleus to which the protons are spin-spin coupled, which in turn is a function of the reorientation rate. The possession of a quadrupole moment by the ^{14}N nucleus means that contributions to T_1 other than quadrupole interactions are negligible, thus $T_1 = T_q$, the quadrupolar relaxation time. A method of obtaining T_q from the proton signal has recently been developed and one of the aims of this project was to investigate the feasibility of such an approach.

The quadrupolar relaxation rate, T_q^{-1} , of ^{14}N in methyl nitrate was measured at a series of different temperatures and in various solvents. The temperature studies yielded ΔH^\ddagger and ΔS^\ddagger for molecular reorientation and these were found to be solvent dependent. Comparison with viscosity activation parameters suggests the possibility of solute - solvent

complex formation (not improbable for methyl nitrate in polar solvents) and this was further investigated by the solvent studies at constant temperature. The data was also used to test the predictions of models employed in the calculation of correlation times for molecular rotation.

SECTION E

EXPERIMENTAL PROCEDURE

(i) Substrates and Samples

Methyl nitrate (CH_3NO_3) was prepared by the esterification of methanol by nitric acid⁽⁸⁸⁾ and purified by vacuum distillation. It is a volatile liquid, explosive at the boiling point (65°C) and so for the temperature studies 15 mole % solutions were used. The solvents, dimethylformamide (DMF) and cyclohexane (C_6H_{12}), were obtained from NMR specialities and Chemical Samples Company, respectively. The other nine solvents (for constant temperature measurements) were obtained from the following companies,

- (a) Fisher Scientific Co. (carbon disulphide and acetone)
- (b) Matheson, Coleman and Bell (carbon tetrachloride)
- (c) Aldrich Chemical Co. Inc. (cyclooctane)
- (d) NMR Specialities (acetonitrile, dimethylsulphoxide, and toluene)
- (e) Merck Sharp and Dohme (benzene - d_6 and chloroform - d)

In each case the solvents were used without further purification.

Viscosity and density measurements were also carried out on 15 mole % solutions.

For the proton magnetic resonance measurements approximately 10 mole % tetramethylsilane (TMS) was added as internal reference. The samples were enclosed in glass tubes and degassed by the normal freeze-pump-thaw technique.

(ii) Viscosity Measurements

The viscosities of 15 mole % methyl nitrate/DMF and methyl nitrate/ C_6H_{12} solutions were measured at three different temperatures, using an Ostwald viscometer calibrated with distilled water. The temperature of the water bath was constant to within $0.01^\circ C$.

Density determinations at the same temperatures were carried out with a pycnometer, also calibrated with distilled water.

(iii) Proton Magnetic Resonance Measurements

All proton magnetic resonance (PMR) spectra were measured on a Varian HA - 100 D spectrometer operated in the frequency sweep mode and locked to internal TMS. The spectrum of each sample was measured and calibrated (by a period averaging technique) at least six times, with a sweep rate of 0.02 Hz sec^{-1} .

For neat methyl nitrate and for methyl nitrate in eleven different solvents spectra were recorded at ambient temperature (29.5°C). For the DMF and C_6H_{12} solutions PMR spectra were recorded every 10°C and 5°C , respectively. The spectrometer was equipped with a V - 4341/V - 6057 variable temperature controller. Approximately twenty minutes were allowed for equilibration of the system at each temperature and the spectrometer resolution was optimised immediately before each spectrum was run. The temperature was determined from a previously prepared calibration graph^{*1} of dial setting against actual temperature, as recorded by a thermocouple. This was checked periodically by comparison with the internal chemical shift in glycol using the calibration graph prepared by Varian. Over the period of time during which this study was carried out, no serious discrepancy developed.

*1 To the credit of James Peeling, graduate student.

(iv) Analysis of the Resonance Line Shape

Spectral analysis of the proton magnetic resonance signal of methyl nitrate is trivial. It is an A_3X system, the single resonance of the three methyl protons being split into a triplet by the X nucleus, ^{14}N , which has a spin $I = 1$. The chemical shift of the central component was measured directly from the spectrum, and $J(^{14}\text{N-H})$ was also obtained experimentally (albeit by an indirect method. See Section G(i)).

T_2 was measured from the linewidth of the solvent resonance and hence, Equation (16), the only unknown parameter in the line shape expression is T_q (^{14}N spin-lattice relaxation time.).

Using an IBM 360/65 computer equipped with a Calcomp 562 graph plotter, a series of line shapes were generated from Equation (16) with varying T_q . The step size between T_q 's in this programme (which will hereafter be referred to as QUAD) was made as small as possible whilst remaining consistent with the variation in line shape from one temperature to the next. i.e. large enough that there was a measurable difference in successive spectra, and yet small enough to permit an accurate fit. In this way visual comparison of experimental and theoretical spectra was possible.

A fitting subroutine developed by B. Goodwin⁽⁸⁹⁾ was applied to the line shape expression in QUAD, and the resultant programme, QUADFIT, then gave the location and heights of extrema (maxima and minima) and line-widths at half-height of the maxima, for the resonance line shape at various T_q values. Hence numerical comparison of experimental and calculated spectra was also possible. Both these programmes, QUAD and QUADFIT, were used with the experimental data in the estimation of ^{14}N quadrupolar relaxation rates.

SECTION F

RESULTS

(i) Viscosity Measurements

The results of flow-time and density measurements for the two solutions are given in Table 3. The viscosity of one liquid relative to that of another is given by ⁽⁹⁰⁾

$$\frac{\eta_1}{\eta_2} = \frac{t_1 d_1}{t_2 d_2}$$

where t_1 is the time of flow and d_1 the density of liquid 1 and similarly for t_2 and d_2 . A convenient reference liquid is water, whose viscosity and density are known accurately over a large temperature range. Hence by measuring t_1, d_1, t_2 and d_2 the ratio (η_1/η_2) was calculated. The viscosities of pure water (η_2) at the three temperatures chosen are ⁽⁹¹⁾

0.8937	cP	at 25°C
0.7225	cP	at 35°C
0.5494	cP	at 50°C

The last column in Table 3 shows the viscosities of the solutions calculated using these values for η_2 .

TABLE 3

Results of Viscosity Measurements(a) For MeNO₃/DMF solution

Temp (°C)	t ₂ (sec)	t ₁ (sec)	d ₁ (gm.cc ⁻¹)	$\frac{\eta_1}{\eta_2}$	η_1 (cP)
25	394.0	333.6	1.0094	0.8572	0.7661
*35	385.2	363.4	0.9653	0.9161	0.6619
*50	295.1	326.7	0.9497	1.0641	0.5846

*A different viscometer was used at these temperatures.

(b) For MeNO₃/C₆H₁₂ solution

Temp (°C)	t ₂ (sec)	t ₁ (sec)	d ₁ (gm.cc ⁻¹)	$\frac{\eta_1}{\eta_2}$	η_1 (cP)
25	394.0	390.3	0.8054	0.8002	0.7151
35	320.2	362.6	0.7809	0.8896	0.6427
50	245.3	333.6	0.7578	1.0430	0.5730

Note: Subscript 1 refers to the solution in each case, and subscript 2 to water.

(ii) PMR Measurementsa The determination of $J(^{14}\text{N-H})$

The ^{15}N - H coupling constant was determined from the satellite bands of the main signal recorded at high power. Figure 2 shows some typical spectra obtained in this way. The satellite bands are clearly visible on top of the main resonance in toluene and chloroform-d solutions, but are not as well resolved in neat methyl nitrate. The magnitude of the splitting, however, was the same in all three cases.

Direct measurement gave $J(^{15}\text{N-H}) = 3.90 \pm .05$ Hz

and hence $J(^{14}\text{N-H}) = 2.78 \pm .04$ Hz (See Section G(i))

b The determination of T_2

The value of T_2 was found from measurement of the half-height linewidths of the solvent peak.

The resonance of cyclohexane is a single sharp line (Fig. 3a) from which the linewidth at half-height was found to be $0.19 \pm .01$ Hz

From the relationship $\Delta\nu_{\frac{1}{2}} = \frac{1}{\pi T_2}$

T_2 was calculated to be $1.68 \pm .08$ sec

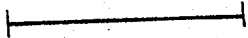
The resonance of D.M.F. is more complicated (Fig. 3b). The aldehydic proton signal could not be used to measure T_2 since it showed extensive broadening by coupling to the nitrogen quadrupole. The higher field methyl protons gave two separate signals approximately 16 Hz apart (at 100 MHz and 28.5°C) due to their being rendered non-equivalent by hindered rotation about the C-N bond. Coupling to the aldehydic proton is apparent, but did not preclude measurement of the half-height linewidth.

FIGURE 2

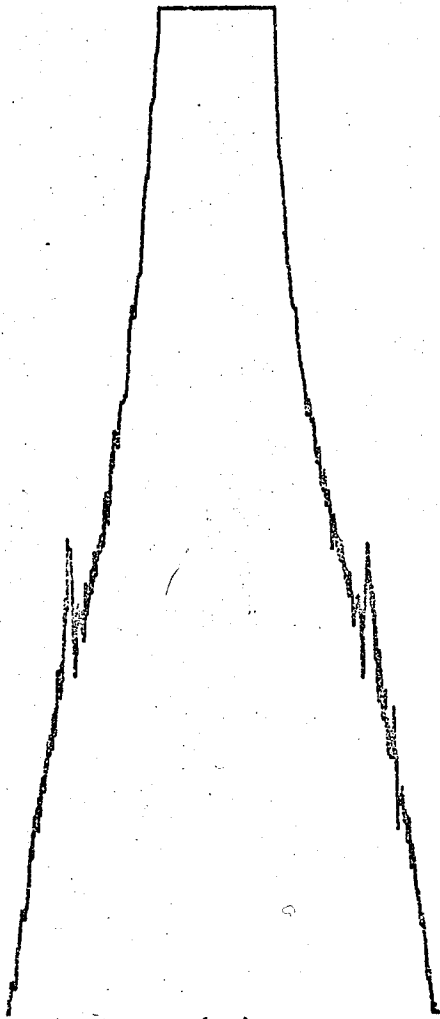
The ^1H spectrum at high power showing the splitting due to ^{15}N -H coupling.

- (a) Neat methyl nitrate.
- (b) 50 mole % toluene.
- (c) 50 mole % chloroform-d.

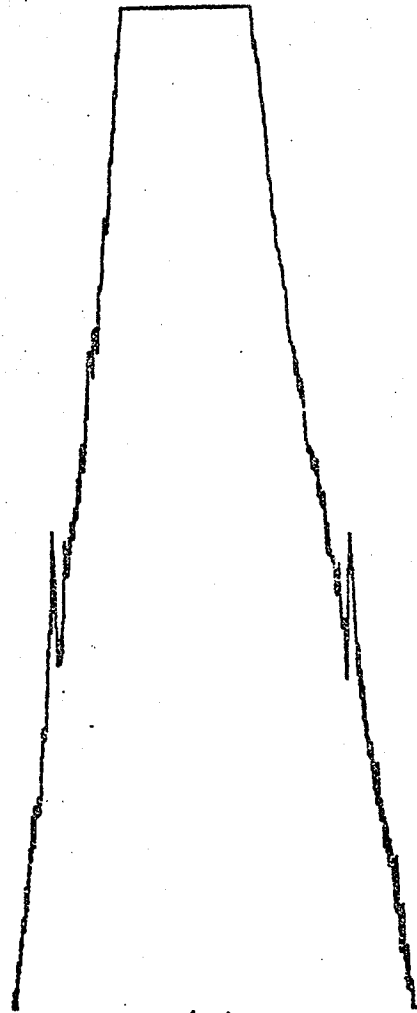
3 Hz.



(a)



(b)



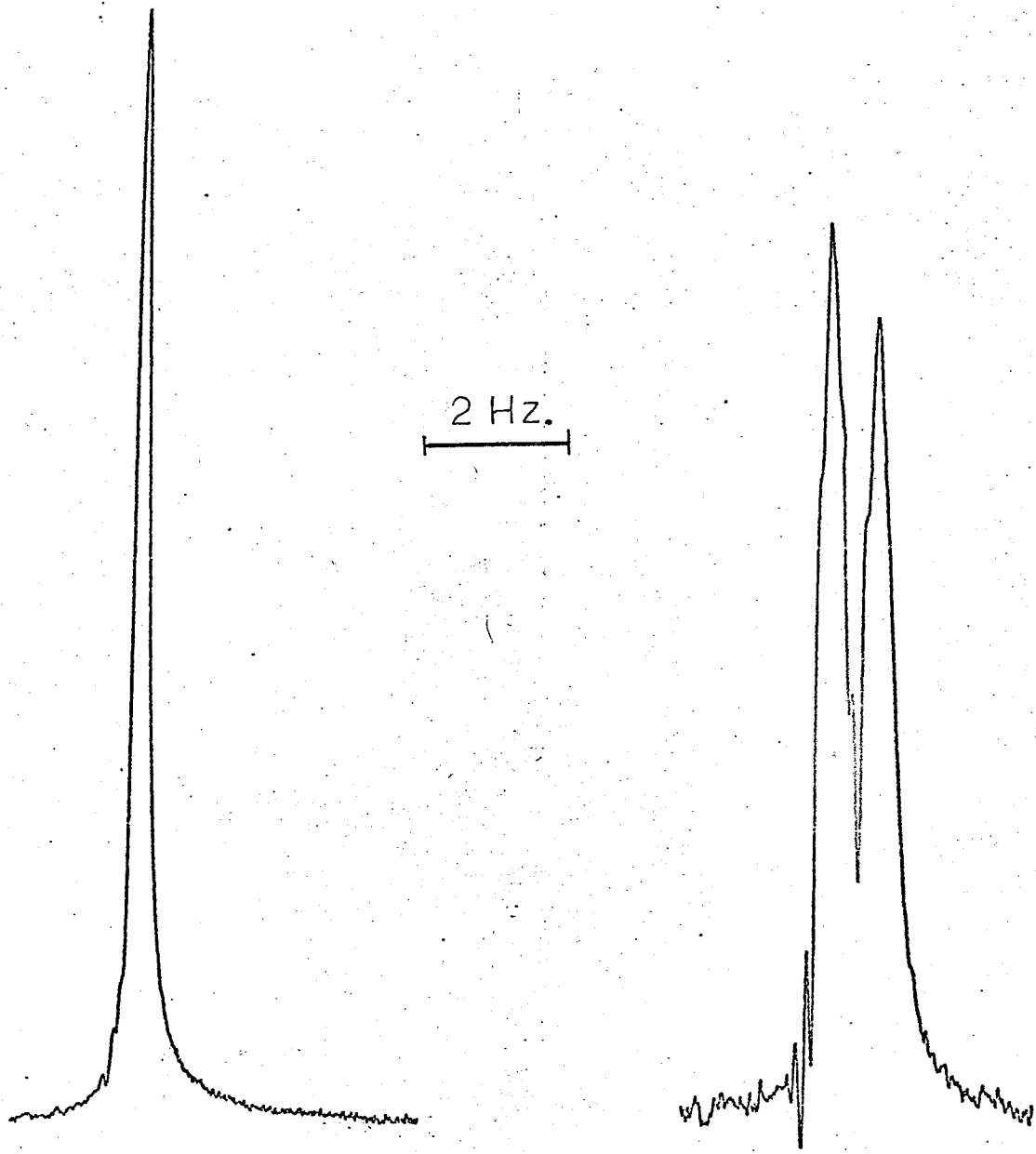
(c)

FIGURE 3

The PMR spectra of the solvents at 100 MHz.

(a) C_6H_{12}

(b) DMF (high field methyl group)



(a)

(b)

The barrier to rotation is sufficiently high ($\Delta G^\ddagger = 21.0 \text{ kcal.mole}^{-1(92)}$) that exchange broadening of the methyl signal at 303°K is negligible.

Using the Eyring Equation

$$\frac{1}{\tau} = K = \frac{kT}{h} e^{-\frac{\Delta G^\ddagger}{RT}}$$

the lifetime, τ , is estimated as 2.2×10^{-2} sec. at 303°K . Under conditions of slow exchange the linewidth is given by

$$\Delta\nu_{\frac{1}{2}} = \frac{1}{\pi T_2} + \frac{1}{\pi \tau}$$

Measurement of the methyl resonance gave $\Delta\nu_{\frac{1}{2}} = 0.45 \pm 0.01 \text{ Hz}$

Hence $T_2 = 0.71 \pm .02$ sec. The $\frac{1}{\pi \tau}$ term is negligibly small, as stated above.

c Temperature Studies

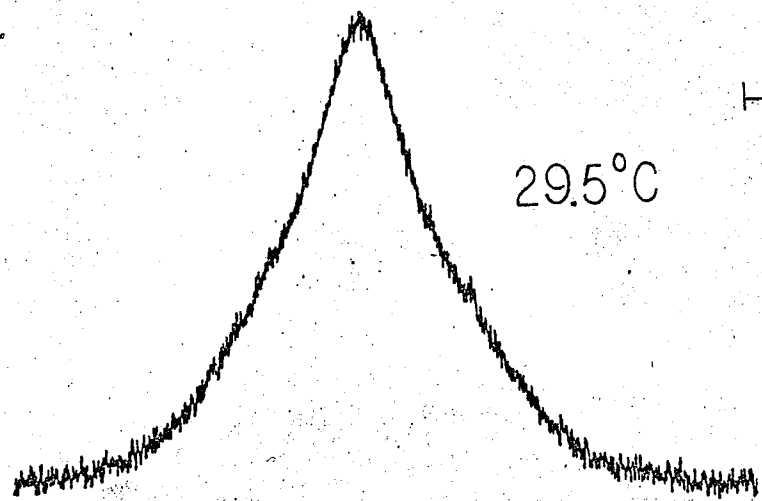
Some typical spectra of methyl nitrate in the two solvents at different temperatures are given in Fig. 4. These show the methyl resonance in DMF solution, Fig. 4a, to be a broadened singlet at all but the highest temperatures, whereas in C_6H_{12} solution, Fig. 4b, triplet structure is apparent even at 28.5°C . In the former case simply the position of the centre of resonance and the linewidths at half-height were measured. These parameters are summarised in Table 4. Table 5 for C_6H_{12} solution includes more parameters, associated with the greater degree of triplet structure shown in the spectra. For convenience these parameters are defined in Fig. 5 below.

FIGURE 4

The PMR spectra of methyl nitrate under various conditions.

(a) 15 mole % in DMF solution at 29.5 and 90°C.

(b) 15 mole % in C₆H₁₂ solution at 28.5 and 90°C.



5 Hz.

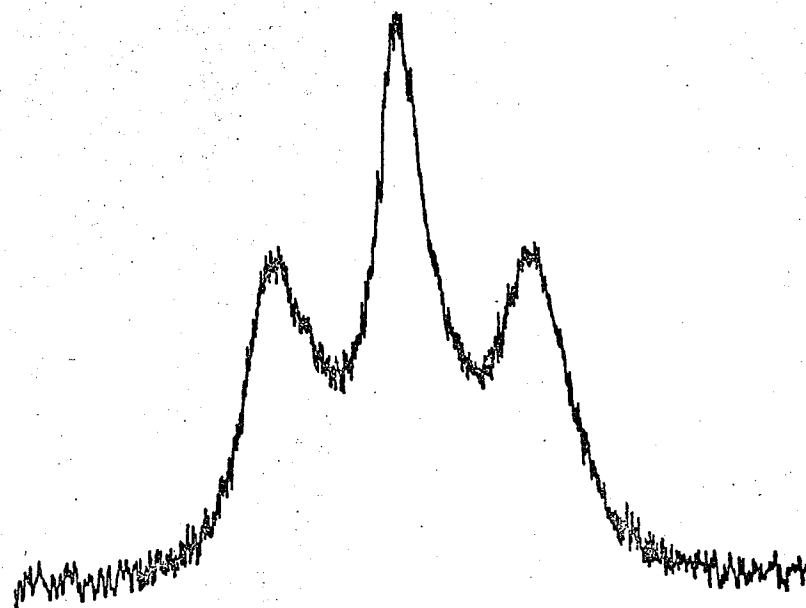
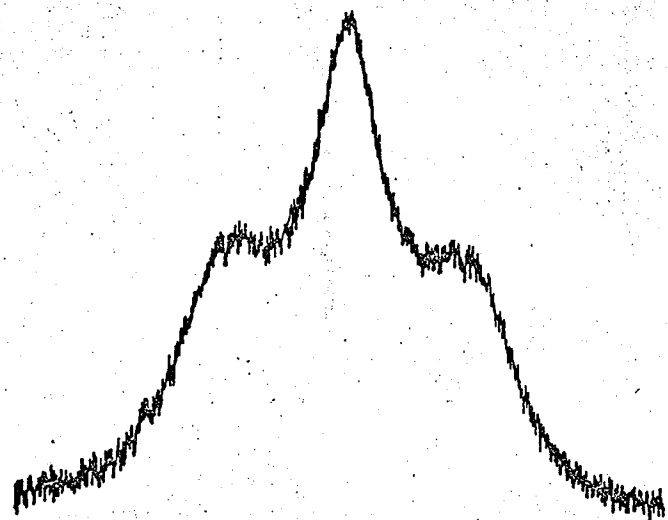
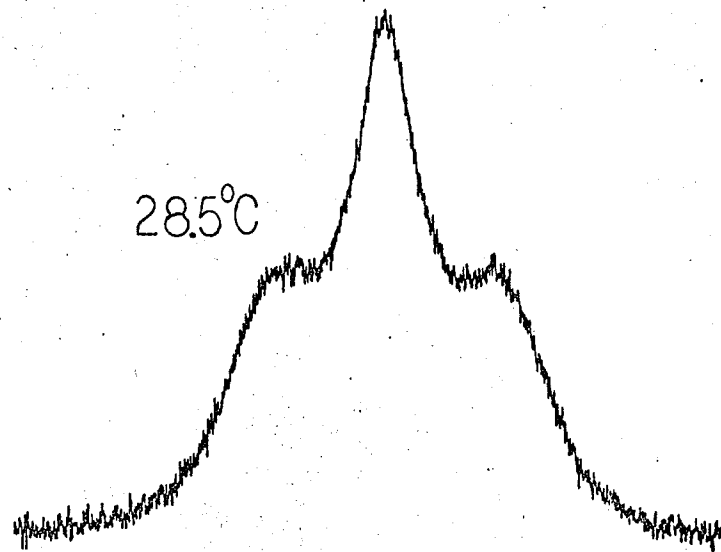


TABLE 4

Spectral Parameters of the Proton Resonance in Methyl Nitrate
(15 mole % in DMF)

Temperature (°C)	Shift (Hz)	$\Delta\nu_{\frac{1}{2}}$ (Hz)
29.5	419.49 ± .09	3.21 ± .05
38.5	419.17 ± .08	3.32 ± .06
49	418.62 ± .08	3.68 ± .05
59	418.28 ± .06	4.28 ± .08
69.5	417.91 ± .06	4.53 ± .07
80	417.57 ± .09	4.68 ± .05
90	417.19 ± .06	5.18

TABLE 5

Spectral Parameters of the Proton Resonance of
Methyl Nitrate in Cyclohexane Solution.

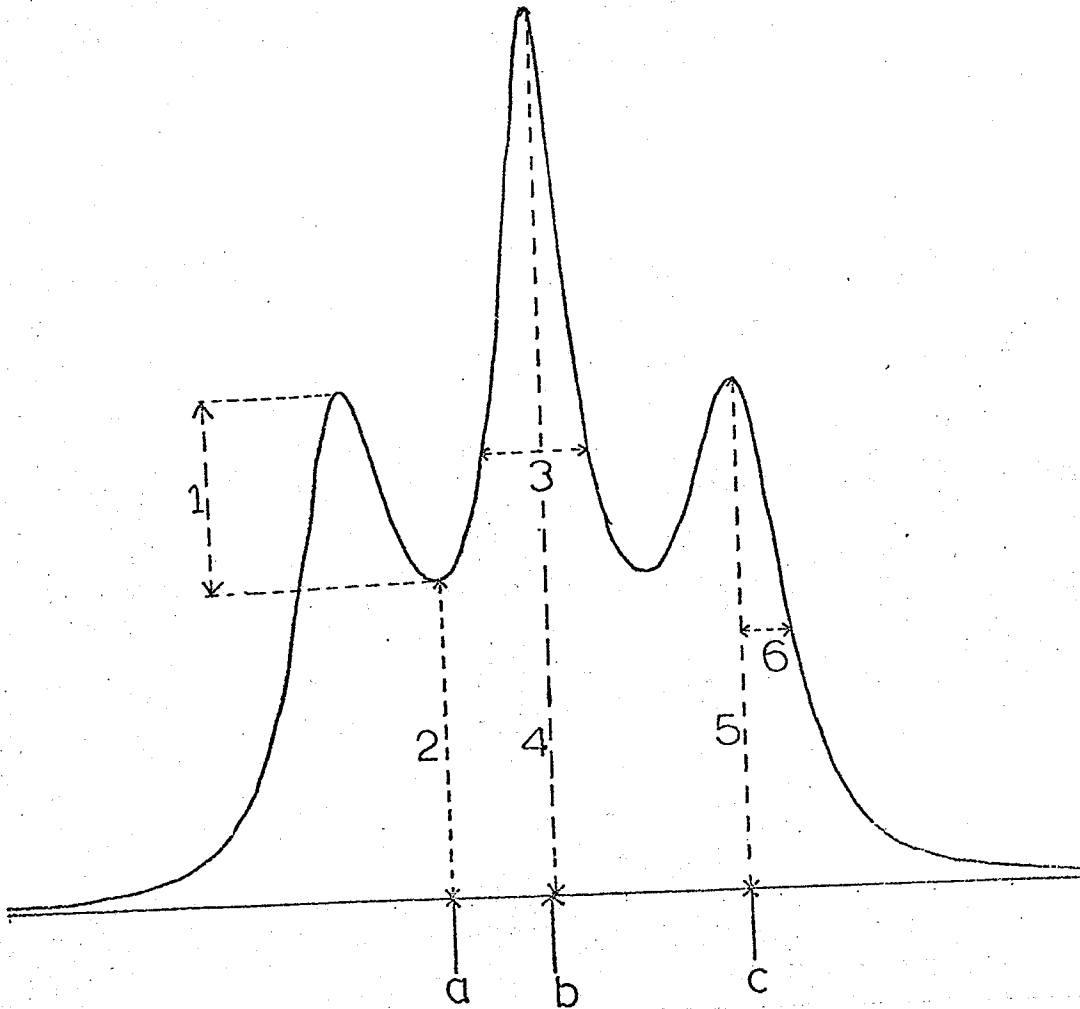
TEMP. °C	CENTRAL MAX. ν_{\max_c} Hz	MAX. $\Delta\nu_{\frac{1}{2}c}$ Hz	OUTER MAXIMA ν_{\max_o} Hz	MAXIMA $\neq\Delta\nu_{\frac{1}{2}o}$ Hz	MINIMA ν_{\min} Hz	* $\Delta_{\min}^{\max_o}$ cm
28.5	395.56	2.77	397.52 393.57	2.67	397.13 394.03	0.25
38	395.50	2.62	397.63 393.33	2.22	396.99 394.01	0.32
43	395.52	2.27	397.72 393.32	2.18	396.99 394.03	0.52
48	395.55	2.21	397.78 393.29	2.22	397.05 394.10	0.64
53	395.64	2.10	397.94 393.40	2.11	397.04 394.16	0.76
58	395.42	1.93	397.81 393.01	1.85	396.83 394.00	1.02
63	395.52	1.82	397.97 393.05	1.74	396.91 394.06	1.15
68	395.54	1.72	397.96 393.07	1.72	396.96 394.16	1.24
80	395.57	1.72	398.07 393.10	1.62	397.01 394.24	1.66
90	395.64	1.45	398.19 393.09	1.48	397.06 394.29	2.04

\neq averaged over the high and low field wings.

* This parameter obviously depends on the maximum peak height. These values are taken from a central peak height of 10.15 cm and represent an average over the two outer maxima.

FIGURE 5

Diagram to show the spectral parameters listed
in Table 5.



KEY:

- a v_{\min}
- b v_{\max_c}
- c v_{\max_o}
- 1 Δ_{\min}^{\max}
- 2 min
- 3 $\Delta v_{\frac{1}{2}}$
- 4 \max_c
- 5 \max_o
- 6 $\frac{1}{2} \Delta v_{\frac{1}{2}}$

d Solvent Studies

The proton resonance of methyl nitrate was recorded in several solvents of different viscosity and dielectric constant, at ambient temperature. All solutions were 15 mole % unless stated otherwise. Considerable variation in line shape was found, as shown in Fig. 6. The spectral parameters are displayed in Table 6.

T_2 was determined from the solvent peak unless marked * in which case it was estimated from other values in the second column.

The half-height linewidths were used to determine the relaxation rate, as described in the next section. The effect of solvent on the chemical shift of the methyl resonance is noteworthy; See Section G(ii) c.

FIGURE 6

The PMR of methyl nitrate in various solvents at ambient temperature.

- (a) Pure methyl nitrate.
- (b) 15 mole % in CS_2 .
- (c) 15 mole % in DMSO.
- (d) 15 mole % in toluene.

5 Hz

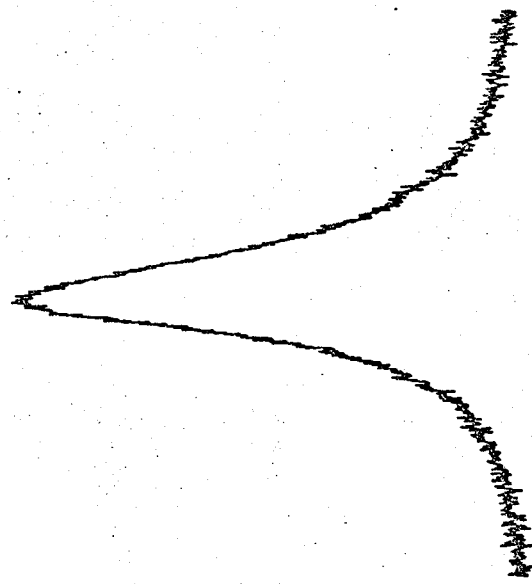
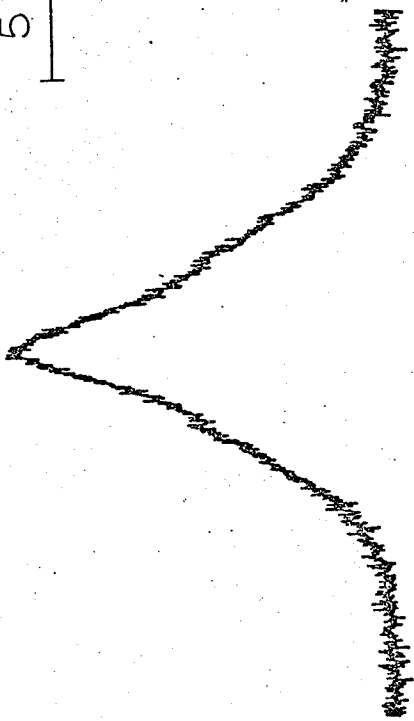
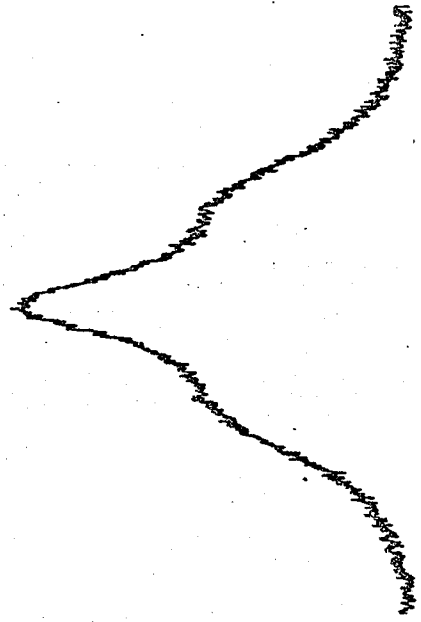
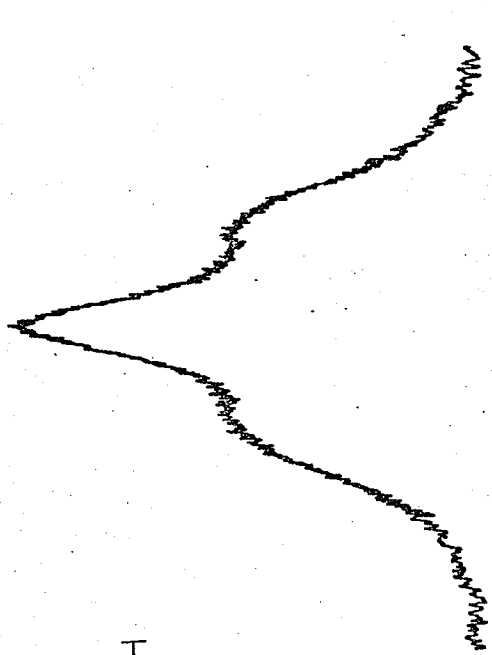


TABLE 6

Lineshape parameters for the methyl resonance in methyl nitrate in several solvents at ambient temperature.

Solvent	T_2 (sec)	$\nu_{\max c}$ (Hz)	$\Delta\nu_{\frac{1}{2}c}$ (Hz)
DMF	0.71	419.49 \pm .09	3.21 \pm .05
C ₆ H ₁₂	1.68	395.56 \pm .06	2.77 \pm .03
neat	*0.71	413.68 \pm .08	3.76 \pm .03
CS ₂	*1.35	403.62 \pm .05	4.78 \pm .07
CH ₃ COCH ₃	1.45	415.31 \pm .03	4.47 \pm .09
CH ₃ CN	1.27	410.90 \pm .03	4.16 \pm .03
DMSO	1.07	415.33 \pm .02	2.11 \pm .02
CCl ₄	*1.20	408.55 \pm .04	3.93 \pm .05
C ₇ H ₈	1.27	322.29 \pm .08	4.07 \pm .07
(1) CDCl ₃	1.45	410.63 \pm .04	3.69 \pm .03
(2) C ₈ H ₁₆	1.18	393.19 \pm .05	4.52 \pm .06
(1) C ₆ D ₆	1.27	361.97 \pm .09	3.85 \pm .04

(1) 50 mole % MeNO₃

See text.

(2) 4 mole % MeNO₃

SECTION G

DISCUSSION OF RESULTS

(i) Treatment of Data(a) Determination of Relaxation Rates

Two computer programs, QUAD and QUADFIT, were used to assign ^{14}N spin-lattice relaxation times to the data in Table 4, 5 and 6.*1 The input parameters were J (the ^{14}N -H coupling constant), T_2 (natural linewidth of the proton resonance in the absence of relaxation) and a "guessed" value for T_q . Additional measurements were required to obtain J and T_2 and these are outlined below.

The Determination of J

If there was no relaxation of the ^{14}N nucleus the proton signal of the methyl group would be a 1:1:1 triplet with $J(^{14}\text{N-H})$ given by the separation between components. However, even in cyclohexane solution at 90°C , where the relaxation rate is lowest, considerable broadening of the proton signal is apparent and the outer components are still moving apart. (Fig. 4). Thus the coupling constant cannot be measured directly from the observed splitting in any of the recorded spectra.*2

Fortunately, however, there is an alternative method of obtaining $J(^{14}\text{N-H})$ where quadrupolar relaxation does significantly broaden and collapse the proton resonance⁽⁹³⁾. The naturally occurring isotope of ^{14}N is ^{15}N and this has a spin $I=\frac{1}{2}$ so that its coupling to the methyl protons will give a doublet of separation equal to $J(^{15}\text{N-H})$. This coupling is related to $J(^{14}\text{N-H})$ by the magnetogyric ratios of the two nuclei.

*1 Both programs are documented and readily available.

*2 In certain instances where the electric field gradient at the quadrupolar nucleus is very small, relaxation may be so slow that there is no effect on the resonance of the coupled nucleus. Thus in the isonitriles (7) and nitramines^(8,9), for example, J is obtainable by direct measurement.

$$\text{ie. } \frac{J(^{15}\text{N-H})}{J(^{14}\text{N-H})} = \frac{\gamma^{15}\text{N}}{\gamma^{14}\text{N}} = -1.403$$

Thus in principle the ^{14}N coupling constant may be estimated from direct measurement of $J(^{15}\text{N-H})^{*1}$. However, observation of the satellite lines is invariably difficult, for in addition to their low intensity (^{15}N is present only to the extent of 0.36%), coupling constants between nitrogen and hydrogen are often small so that the lines lie close to the main resonances and are obscured by them. The most favourable situation for observing the ^{15}N lines is when the band due to molecules containing ^{14}N nuclei is very broad; under such circumstances the isotopic coupling appears as a sharp pair of lines superimposed on the main resonance.

Fig. (2) shows this for methyl nitrate, both neat and as a solution in toluene and chloroform. In all three cases the splitting is the same and yields $J(^{14}\text{N-H}) = 2.78 \pm 0.04 \text{ Hz}$. The N-H coupling constants measured by Bullock et al. ⁽⁴⁾ showed a similar independence of the medium. Confirmation of the magnitude of $J(^{14}\text{N-H})$ may be taken from the work of Lehn ⁽²⁹⁾ who derived a value of 2.75 Hz for MeNO_3 in pyridine and tetrachloroethylene solutions by complete line shape fitting of the experimental spectrum.

The value of $J(^{14}\text{N-H})$ was assumed to be temperature independent, for although this may not be absolutely true, any change that there is will be negligibly small.

The determination of T_2

The signal from methyl nitrate is broadened by the ^{14}N quadrupole at all

*¹ The presence of a negative sign merely implies that the two couplings are of opposite sign; it is of no consequence in the present work.

temperatures and hence a value for T_2 can never be found from this resonance. However, since the limiting factor determining the natural linewidth is the inhomogeneity of the magnet, it is possible to deduce an approximate value for T_2 from other peaks which are not broadened by relaxation or exchange processes. In most cases the solvent was found suitable for this purpose (Fig. 3), but for both CS_2 and CCl_4 (where there are no protons) and for neat methyl nitrate, there is no direct method of obtaining T_2 . For these solutions, therefore, a T_2 value was estimated from the variation of T_2^{-1} with viscosity for the solvents in Table 6. In view of the approximate methods used to obtain T_2 , the further assumption of a constant value for T_2 as the temperature was changed should be of little significance.

The fitting method is quite sensitive to the T_2 parameter, especially in the region of near-complete collapse of the triplet structure, so an accurate value is important. Further discussion of this point may be found in the section on errors. It should be emphasized that fitting done with T_2 values of 1.0 and 2.0 sec. is merely for illustrative purposes; they have no experimental justification. Values of $T_2 = 1.68$ and 0.71 sec were used for the C_6H_{12} and DMF solutions, respectively (as shown in the results section, from measurement of the solvent resonance).

The line shape fit was attempted in two ways, using the program QUAD alone and in conjunction with a subroutine developed for similar rate studies. Details and limitations of the procedure are discussed below.

QUAD

This was the basic program written to calculate $I(\nu)$ as given by Equation (16). The density of points (number of points in the plot) was variable; for most spectra 500 were found to be sufficient, but in

the region of near-complete collapse of the triplet it was necessary to use 5,000 points over the 5 Hz span of the spectrum. The output was obtained on a Calcomp plotter as a series of theoretical spectra on the same scale (1 Hz per cm.) as the experimental ones. A "reasonable" T_q value was specified in each case and a search made around this central figure. The number and magnitude of the step sizes used in the search were optional variables. When iteration was almost complete spectra were calculated at 0.0025 sec intervals, five on either side of the most probable T_q value.

The experimental and calculated spectra were compared visually by superimposing one on the other for different T_q values until optimum agreement was found. For each temperature and solvent all six experimentally recorded spectra were matched with the Calcomp plots; invariably this lead to a "best" T_q value, with upper and lower limits estimated from the extreme T_q 's which gave reasonable agreement. The experimental spectra were not corrected for non-linearity in the recorder.

The use of QUAD in this way is a rapid method for obtaining relaxation rates and also a reliable one since the entire line shape is fitted at the same time. However, at relaxation rates greater than the coupling constant, ($J^{14}\text{N-H}$), where the resonance is a broadened singlet, the fit is less sensitive to changes in T_q and the error limits are correspondingly larger. In addition, the contribution to the half-height linewidth of the experimental spectrum from the non-linearity in the recorder is now similar to the difference in $\Delta\nu_{1/2}$ in going from one temperature to another, 10° higher. For example, in DMF solution at 60° the measured half-height linewidth is 4.50 Hz corrected to 4.28 Hz after calibration. These widths correspond to T_q values of 0.080 sec

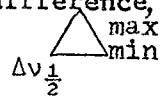
and 0.075 sec respectively; the difference of 0.005 sec is significant in this region. However by careful fitting, concentrating on the shape of the partially resolved shoulder (rather than the entire resonance signal), the uncertainty in the relaxation rate can be substantially reduced.

QUADFIT:

By applying the subroutine FIT⁽⁸⁹⁾ to the output, i.e. $I(\nu)$ of the main program QUAD certain characteristics of the resonance line shape sensitive to the rate of relaxation (e.g. positions of maxima and minima and their height) were generated. Comparison of these with the corresponding experimental parameters (as measured from the recorded spectra) permitted an exact determination of T_q values.

The experimental spectra were measured as shown in Figure 5 taking an average over the six recorded at each temperature. The half-height linewidths and positions of maxima and minima were corrected for non-linearity. For small T_q values (≤ 0.090 sec), the proton resonance shows no measurable triplet structure, so that only the half-height linewidth was useful. This is a poor method, however, since it is relatively insensitive to changes in T_q (c.f. the problems encountered with QUAD) and difficult to measure to the degree of precision required for a meaningful fit. For larger T_q values there are numerous parameters which change more rapidly with the rate of ^{14}N relaxation; those examined were

- (a) the position of minima and outer maxima,
- (b) the height of minima and outer maxima and their difference,
- (c) the half-height linewidth of the central maximum $\Delta\nu_{\frac{1}{2}}$
- and (d) the half-height linewidth of the outer maxima.



In addition, several workers^(94,95) have used combinations of (a) - (d) (eg. the ratio of central peak height to height of minimum) for fitting experimental spectra. This proved unsatisfactory for the present case

of methyl nitrate, there being only a small variation in such quantities over the entire temperature range. For instance, the ratio $\frac{\max_c}{\min}$ varies from 2.01 to 2.74 and $\frac{\max_c}{\max_o}$ goes from 1.90 to 1.72 in a 60° temperature interval. (\max_c , \max_o and \min refer to the height of the central maximum, outer maxima and minima respectively.) For the cyclohexane solution fits were thus attempted using all the parameters in Table 5.

The positions of the outer maxima and minima relative to the central peak hardly change at all and cannot therefore be used for fitting. The same applies to the half-height linewidth of the outer maxima where, although the variation is somewhat greater, considerable error is involved in its determination. The linewidth can only be measured (and calculated) on one side of the peak (see Figure 5) and is therefore highly dependent on the exact location of the centre of the outer maximum - an ambiguous parameter with such spectra. (See Figure 4b for example.) Whilst the half-height linewidth of the central maximum shows a similar sensitivity to T_q , its determination is more accurate as the entire peak is resolved. However, in regions where the half-height occurs close to the minima, the measurement of $\Delta\nu_{\frac{1}{2}}$ is nearly impossible and QUADFIT cannot calculate it. Unlike the half-height linewidth measurements which require an accurate location of the baseline, the $\frac{\max}{\min}$ parameter does not have this dependence so that its determination has less uncertainty. In addition, it shows a considerable variation with temperature, making it a suitable fit parameter in regions where the triplet structure is apparent.

From these observations, the most satisfactory method therefore appeared to be the use of $\frac{\max}{\min}$ in conjunction with $\Delta\nu_{\frac{1}{2}}$. For example, in C_6H_{12} at 70°C, from Table 5

$$\Delta\nu_{\frac{1}{2}} = 1.72 \text{ Hz}$$

$$\frac{\max}{\min} = 1.34$$

In this region QUADFIT yields -

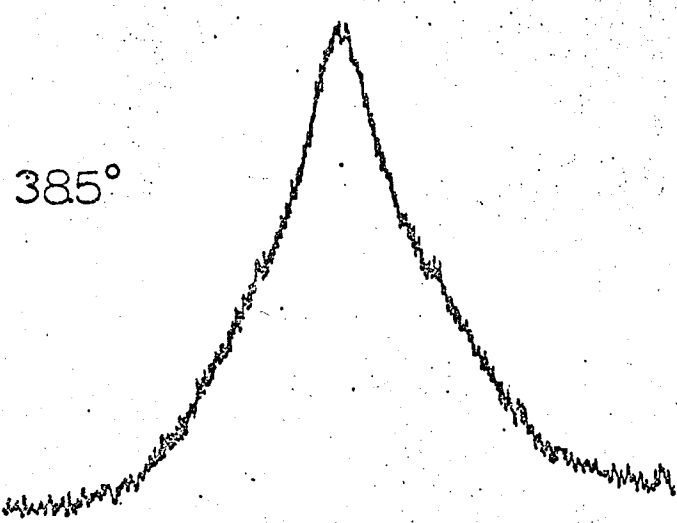
$\Delta v_{\frac{1}{2}}$ (Hz)	\triangle_{\min}^{\max} (cm)	
1.83	1.17	for $T_q = 0.1150$ sec
1.77	1.30	for $T_q = 0.1175$ sec
1.71	1.43	for $T_q = 0.1200$ sec
1.66	1.55	for $T_q = 0.1225$ sec

from which T_q is seen to lie between 0.1175 and 0.120 sec. In most cases the $\Delta v_{\frac{1}{2}}$ and \triangle_{\min}^{\max} parameters implied the same T_q values, but where there was a discrepancy, the value from \triangle_{\min}^{\max} was weighted more heavily, and checked against the T_q obtained from the use of QUAD.

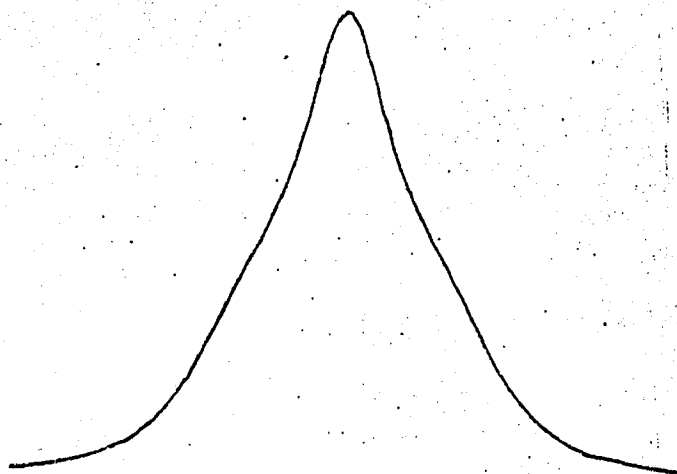
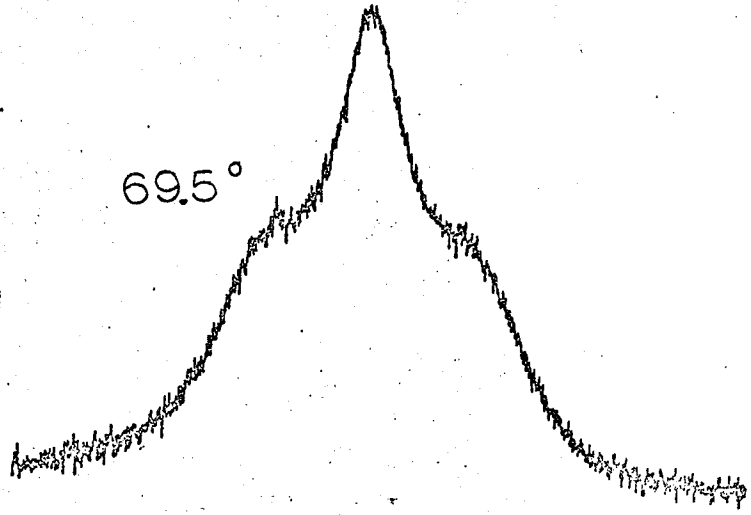
Examples of experimental and computer simulated spectra are given in Figures 7 and 8. Using QUAD in this way and QUADFIT with the data in Table 4 - 6, T_q values were assigned to each spectrum. Tables 7, 8, 10, 11, 12 and 18 list the results.

FIGURE 7

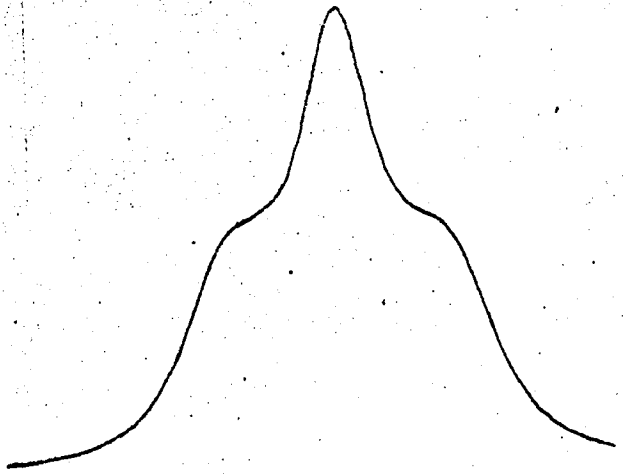
The experimental spectra for methyl nitrate in DMF at 38.5°C and 69.5°C with the corresponding calculated spectra.



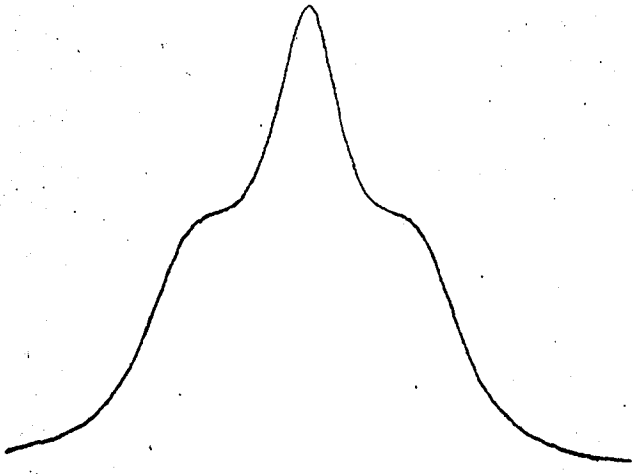
5 Hz.



$T_q = 0.0625$



0.0875



0.090 SEC

FIGURE 8

The experimental spectra for methyl nitrate
in C_6H_{12} at $43^\circ C$ and $58^\circ C$ with the corres-
ponding calculated spectra.

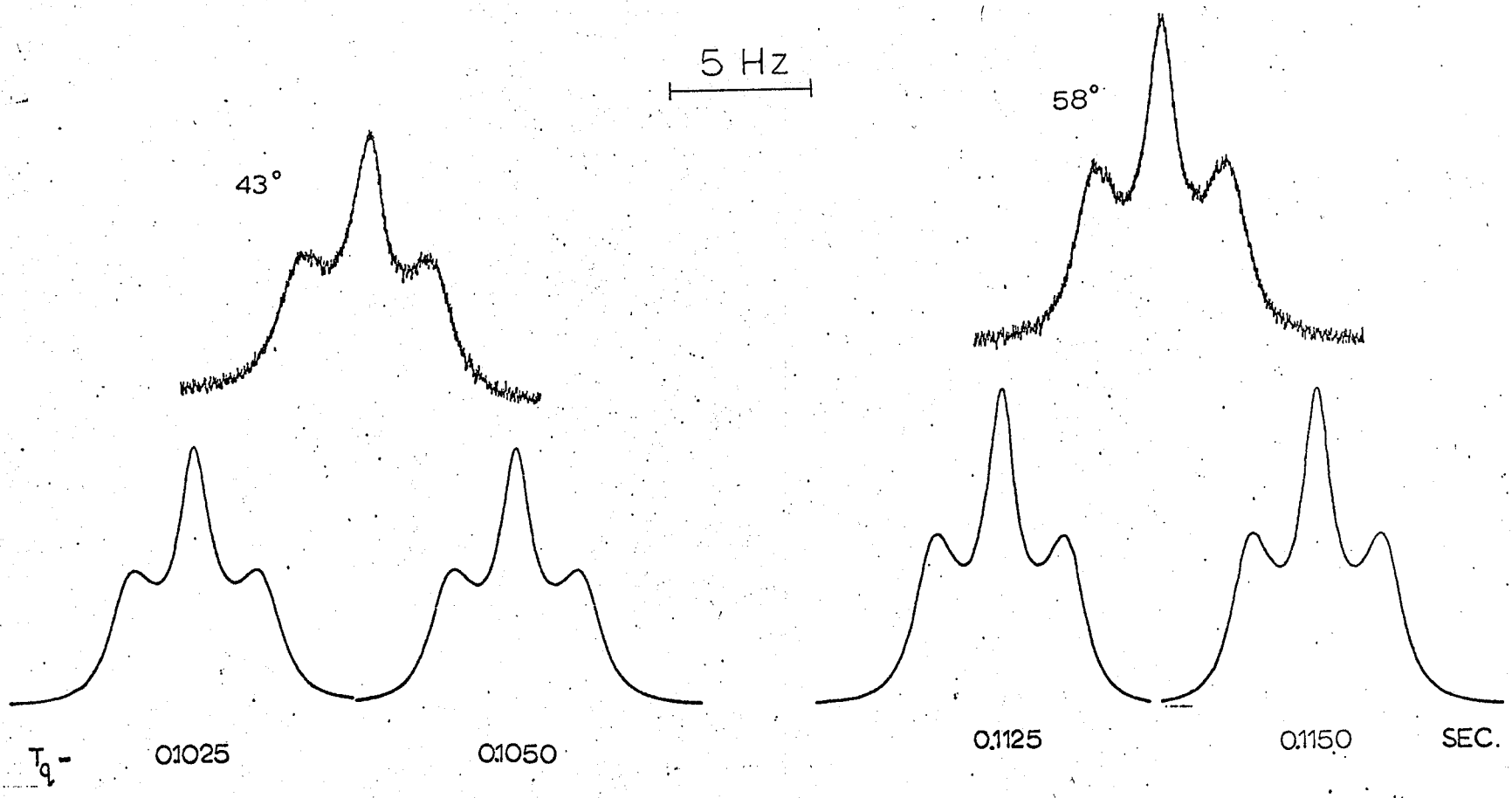


TABLE 7

¹⁴N Relaxation Times for methyl nitrate in C₆H₁₂ solution.T₂ = 2.0 sec

Temp. (°C)	$\frac{1}{T} \cdot 10^3$ (°K ⁻¹)	T _q (sec.)	log $\frac{T_q}{T}$	* Error Estimate.			
				T _q (sec)		log $\frac{T_q}{T}$	
28.5	3.315	0.0925	-3.5134	.0950	.0900	-3.5012	-3.5252
38	3.213	0.1000	-3.4931	.1025	.0975	-3.4824	-3.5041
43	3.163	0.1025	-3.4892	.1050	.1000	-3.4788	-3.4999
48	3.113	0.1050	-3.4856	.1075	.1025	-3.4755	-3.4961
53	3.066	0.1100	-3.4720	.1125	.1075	-3.4623	-3.4820
58	3.019	0.1125	-3.4689	.1150	.1100	-3.4594	-3.4788
63	2.974	0.1175	-3.4567	.1200	.1150	-3.4475	-3.4660
68	2.931	0.1200	-3.4538	.1225	.1175	-3.4449	-3.4629
80	2.831	0.1275	-3.4425	.1300	.1250	-3.4340	-3.4511
90	2.753	0.1350	-3.4299	.1375	.1325	-3.4219	-3.4380

* An estimate of the upper and lower values of T_q as determined from Calcomp fitting (QUAD) and matching of spectral parameters using QUADFIT.

TABLE 8

^{14}N Relaxation Times for methyl nitrate in C_6H_{12} solution.

$$T_2 = 1.68\text{sec}$$

Temp. ($^{\circ}\text{C}$)	$\frac{1}{T} \cdot 10^3$ ($^{\circ}\text{K}^{-1}$)	T_q (sec)		$\log \frac{T}{T_q}$	
28.5	3.315	(1) 0.0925 0.0950	0.0900	-3.5134 -3.5012	-3.5252
38	3.213	(2) 0.1000	0.0975	-3.4931	-3.5041
43	3.163	0.1050	0.1025	-3.4788	-3.4892
48	3.113	0.1075	0.1050	-3.4755	-3.4856
53	3.066	0.1100	0.1075	-3.4720	-3.4820
58	3.019	0.1150	0.1125	-3.4594	-3.4689
63	2.974	0.1175	0.1150	-3.4567	-3.4660
68	2.931	0.1200	0.1175	-3.4538	-3.4629
80	2.831	0.1300	0.1275	-3.4340	-3.4425
90	2.753	0.1375		-3.4219	

(1) See footnote * at the bottom of Table 7

(2) Both values weighted equally.

TABLE 9

Arrhenius Parameters for the data shown in Tables 7 and 8.

$\frac{1}{T} \cdot 10^3$ ($^{\circ}\text{K}^{-1}$)	$T_2 = 1.68 \text{ sec}$			$T_2 = 2.00 \text{ sec}$		
	log T_q	Extrema		log T_q	Extrema	
3.315	-1.0339	-1.0223	-1.0458	-1.0339	-1.0223	-1.0458
3.213	(1) -1.000	-1.0110		-1.0000	-0.9893	-1.0110
3.163		-0.9788	-0.9893	-0.9893	-0.9788	-1.0000
3.113		-0.9685	-0.9788	-0.9788	-0.9685	-0.9893
3.066		-0.9586	-0.9685	-0.9586	-0.9489	-0.9685
3.019		-0.9393	-0.9489	-0.9489	-0.9393	-0.9586
2.974		-0.9299	-0.9393	-0.9299	-0.9208	-0.9393
2.931		-0.9208	-0.9299	-0.9208	-0.9119	-0.9299
2.831		-0.8861	-0.8945	-0.8945	-0.8861	-0.9031
2.753	-0.8617	-	-	-0.8697	-0.8617	-0.8788

(1) See footnote (2) at the bottom of Table 8

TABLE 10

 ^{14}N Relaxation Times for methyl nitrate in DMF solution. $T_2 = 2.0$ sec

Temp. ($^{\circ}\text{C}$)	$\frac{1}{T}$ ($^{\circ}\text{K}^{-1}$)	T_q (sec)	$\log \frac{T_q}{T}$	Error Estimate.			
				T_q (sec)	$\log \frac{T_q}{T}$		
29.5	3.304	0.0575	-3.7214	0.0600	0.0550	-3.7029	-3.7407
38.5	3.208	0.0625	-3.6979	0.0650	0.0600	-3.6808	-3.7156
49	3.104	0.0700	-3.6629	* 0.0725	0.0675	-3.6478	-3.6788
59	3.010	0.0750	-3.6463	* 0.0775	0.0725	-3.6320	-3.6611
69.5	2.918	0.0800	-3.6319	* 0.0825	‡ -	-3.6186	-
80	2.831	0.0900	-3.5938	* -	-	-	-
90	2.753	0.0975	-3.5712	* 0.0950	-	-3.5823	-

* Fit done with QUAD only. (QUADFIT unreliable here.)

‡ Blanks indicate an unambiguous fit (uncertainty in T_q is less than 0.0025 sec.)

TABLE 11

 ^{14}N Relaxation Times for methyl nitrate in DMF solution. $T_2 = 1.0$ sec

Temp. ($^{\circ}\text{C}$)	$\frac{1}{T}$ $(^{\circ}\text{K}^{-1})$	T_q (sec)	$\log \frac{T}{T_q}$	Error Estimate.			
				T_q (sec)		$\log \frac{T}{T_q}$	
29.5	3.304	0.0550	-3.7407	0.0575	0.0525	-3.7214	-3.7610
38.5	3.208	0.0600	-3.7156	0.0625	0.0575	-3.6979	-3.7340
49	3.104	0.0700	-3.6629	0.0725	0.0675	-3.6478	-3.6788
59	3.010	0.0800	-3.6184	0.0825	0.0775	-3.6050	-3.6320
69.5	2.918	0.0850	-3.6055	*	-	-	-
80	2.831	0.0925	-3.5819	0.0900	-	-3.5938	-
90	2.753	0.1025	-3.5495	0.1000	-	-3.5602	-

* See note \neq Table 10.

TABLE 12

¹⁴N Relaxation Times for methyl nitrate in DMF solution.T₂ = 0.71 sec

Temp. (°C)	$\frac{1}{T} \cdot 10^3$ (°K ⁻¹)	T _q (sec)	log $\frac{T}{T_q}$	Error Estimate.			
				T _q (sec)		log $\frac{T}{T_q}$	
29.5	3.304	0.0550	-3.7407	0.0575	0.0525	-3.7214	-3.7610
38.5	3.208	0.0625	-3.6979	0.0650	0.0600	-3.6808	-3.7156
49	3.104	0.0725	-3.6478	0.0750	0.0700	-3.6330	-3.6629
59	3.010	0.0800	-3.6184	0.0825	0.0775	-3.6050	-3.6320
69.5	2.918	* 0.0875	-3.5930	* 0.0900		-3.5807	
80	2.831	0.0975	-3.5591	0.1100	0.0950	-3.5480	-3.5704
90	2.753	0.1075	-3.5289	0.1050	-	-3.5389	-

* weighted equally.

TABLE 13

Arrhenius Parameters for the data shown in Tables 10, 11 and 12.

$\frac{1}{T}$ ($^{\circ}\text{K}^{-1}$)	$T_2 = 2.00\text{sec}$		$T_2 = 1.00\text{ sec}$		$T_2 = 0.71\text{ sec}$	
	log T_q	Extrema	log T_q	Extrema	log T_q	Extrema
3.304	-1.2403	-1.2596 -1.2218	-1.2596	-1.2798 -1.2403	-1.2596	-1.2798 -1.2403
3.208	-1.2041	-1.2218 -1.1871	-1.2218	-1.2403 -1.2041	-1.2041	-1.2218 -1.1871
3.104	-1.1549	-1.1707 -1.1397	-1.1549	-1.1397 -1.1707	-1.1397	-1.1549 -1.1249
3.010	-1.1249	-1.1397 -1.1107	-1.0969	-1.1107 -1.0835	-1.0968	-1.1107 -1.0835
2.918	-1.0969	-1.0835	-1.0706	-	-1.0580 -1.0458	
2.831	-1.0458	-	-1.0339	-1.0458	-1.0110	-1.0223 -1.0000
2.753	-1.0110	-1.0223	-0.9893	-1.0000	-0.9685	-0.9788

(b) Determination of Activation Parameters

As discussed in Section B(ii), τ_q depends only on the molecular reorientational rate; its temperature dependence therefore should yield an activation energy for a purely rotational motion. If this process is thermally activated then it will be described by the usual rate equation (48)

$$\tau_q = \tau_q^0 \exp\left(\frac{E_a}{RT}\right) \dots\dots\dots(29)$$

where τ_q is the correlation time for the process causing quadrupolar relaxation, τ_q^0 is an inverse frequency factor and E_a is defined by the relationship between τ_q and $1/T$.

Substituting equation (29) for τ_q into equation (8) and rearranging, the logarithmic form is

$$\log_{10} \tau_q = \log_{10} \left[\tau_q^0 \frac{3}{8} \left(\frac{e^2 q Q}{h} \right)^2 \right]^{-1} - \frac{E_a}{2.303 RT} \dots\dots\dots(30)$$

A plot of $\log_{10} \tau_q$ vs. $\frac{1}{T}$ therefore gives

- (a) E_a from the slope
and (b) τ_q^0 from the intercept, providing the quadrupolar coupling constant, $\frac{e^2 q Q}{h}$, is known. (See Appendix III)

Table 14 gives a least squares analysis of the $\log_{10} \tau_q$ vs $\frac{1}{T}$ data; Figures 9 and 10 display graphically Arrhenius plots for the C_6H_{12} and DMF solutions respectively.

The entropies and enthalpies for the rotational process may also be calculated if it is assumed that such motions can be described by the Eyring Equation

$$k = \frac{1}{\tau_q} = \left(\frac{k_B f}{h} \right) T \exp\left(-\frac{\Delta G^\ddagger}{RT}\right) \dots\dots\dots(31)$$

where

k_B is the Boltzmann constant,
 f is the transmission coefficient (taken as equal to unity),
 h is Planck's constant
 and ΔG^\ddagger is the free energy of activation for molecular reorientation.

Taking logarithms of Equation (31), substituting $K = \frac{k_B f}{h}$ and expanding ΔG^\ddagger

$$\log_{10} \tau_q^{-1} - \log_{10} T = \log_{10} K + \frac{\Delta S^\ddagger}{4.577} - \frac{\Delta H^\ddagger}{4.577 T} \dots\dots\dots (32)$$

Again substituting into Equation (8)

$$\log_{10} \left(\frac{\tau_q}{T} \right) = \log_{10} K - \log_{10} \left\{ \frac{3}{8} \left(\frac{e^2 q Q}{h} \right)^2 \right\} + \frac{\Delta S^\ddagger}{4.577} - \frac{\Delta H^\ddagger}{4.577 T} \dots\dots\dots (33)$$

Hence, ΔH^\ddagger may be obtained from the slope of a plot of $\log_{10} \frac{\tau_q}{T}$ vs. $\frac{1}{T}$ and ΔS^\ddagger may also be determined from the intercept, again provided the quadrupolar coupling constant is known. Figures 11 and 12 are Eyring plots of the data for the C_6H_{12} and DMF solutions respectively. See also Table 14.

A complete list of all activation parameters for both solvents, with errors derived from the least mean-squares fit, is given in Table 15.

FIGURE 9

Arrhenius plot for the reorientation of methyl
nitrate in C_6H_{12} solution.

$$T_2 = 1.68 \text{ sec}$$

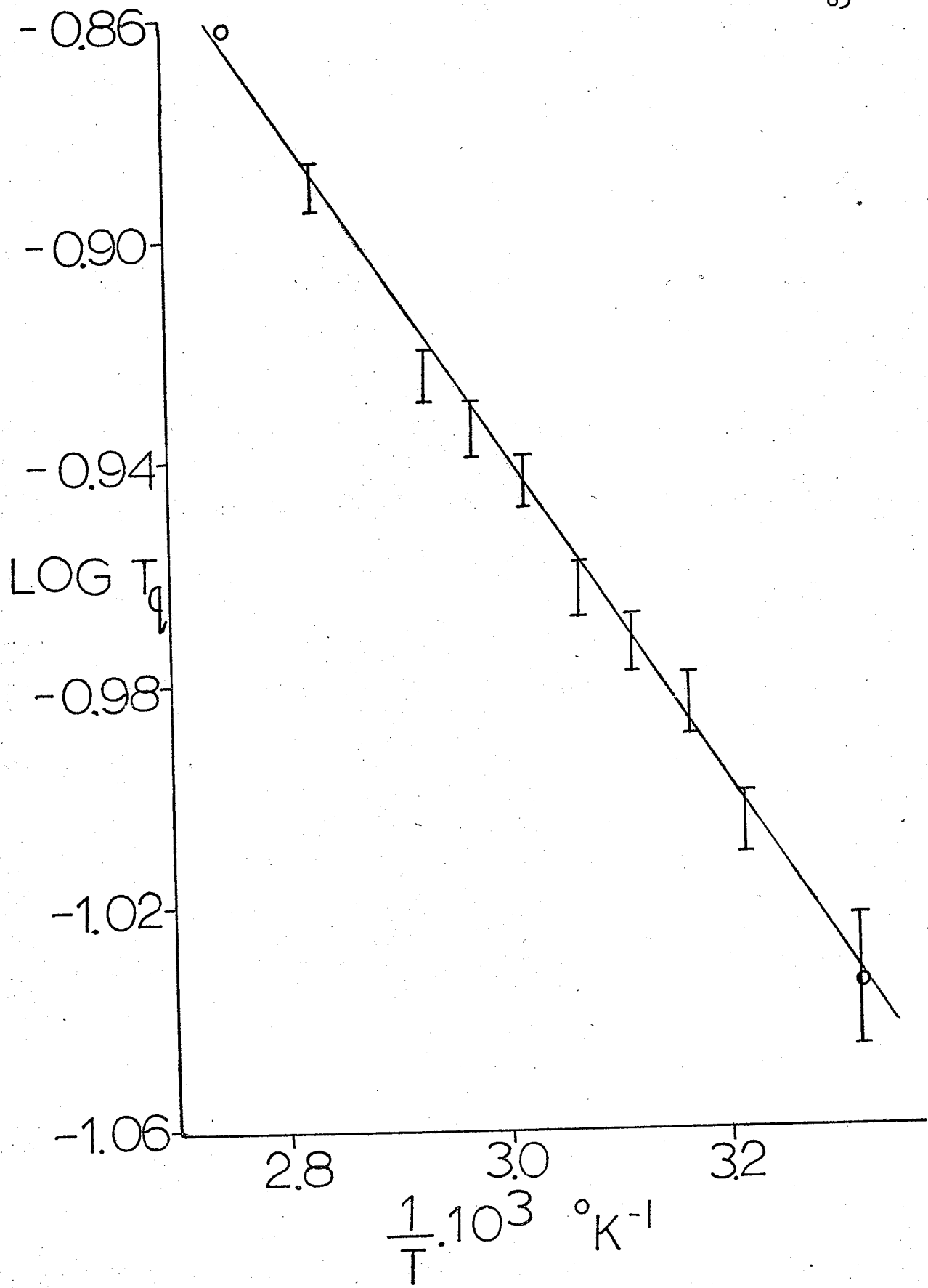


FIGURE 10

Arrhenius plot for the reorientation of methyl
nitrate in DMF solution.

$$T_2 = 0.71 \text{ sec}$$

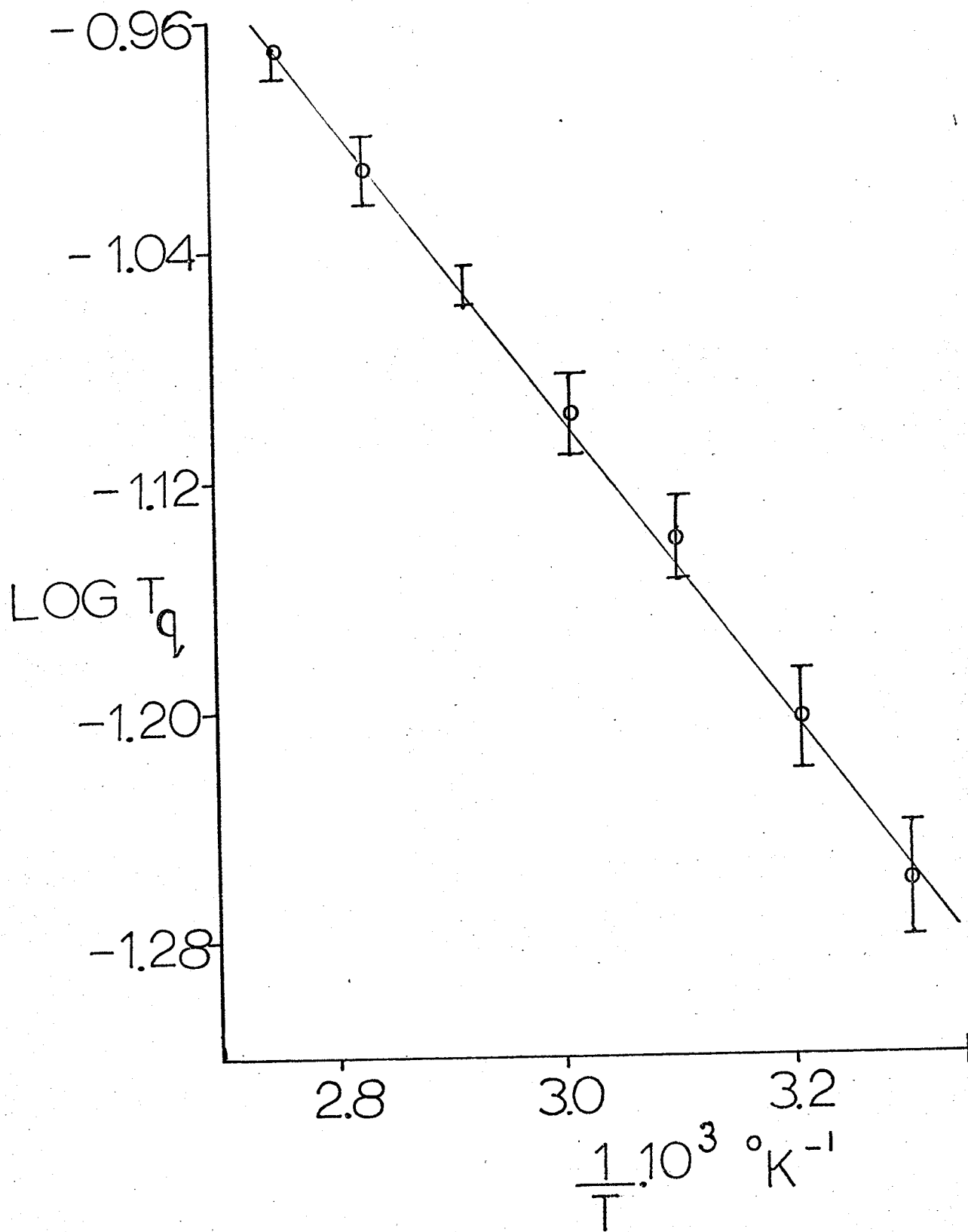


FIGURE 11

Eyring plot for the reorientation of methyl
nitrate in C_6H_{12} solution.

$$T_2 = 1.68 \text{ sec}$$

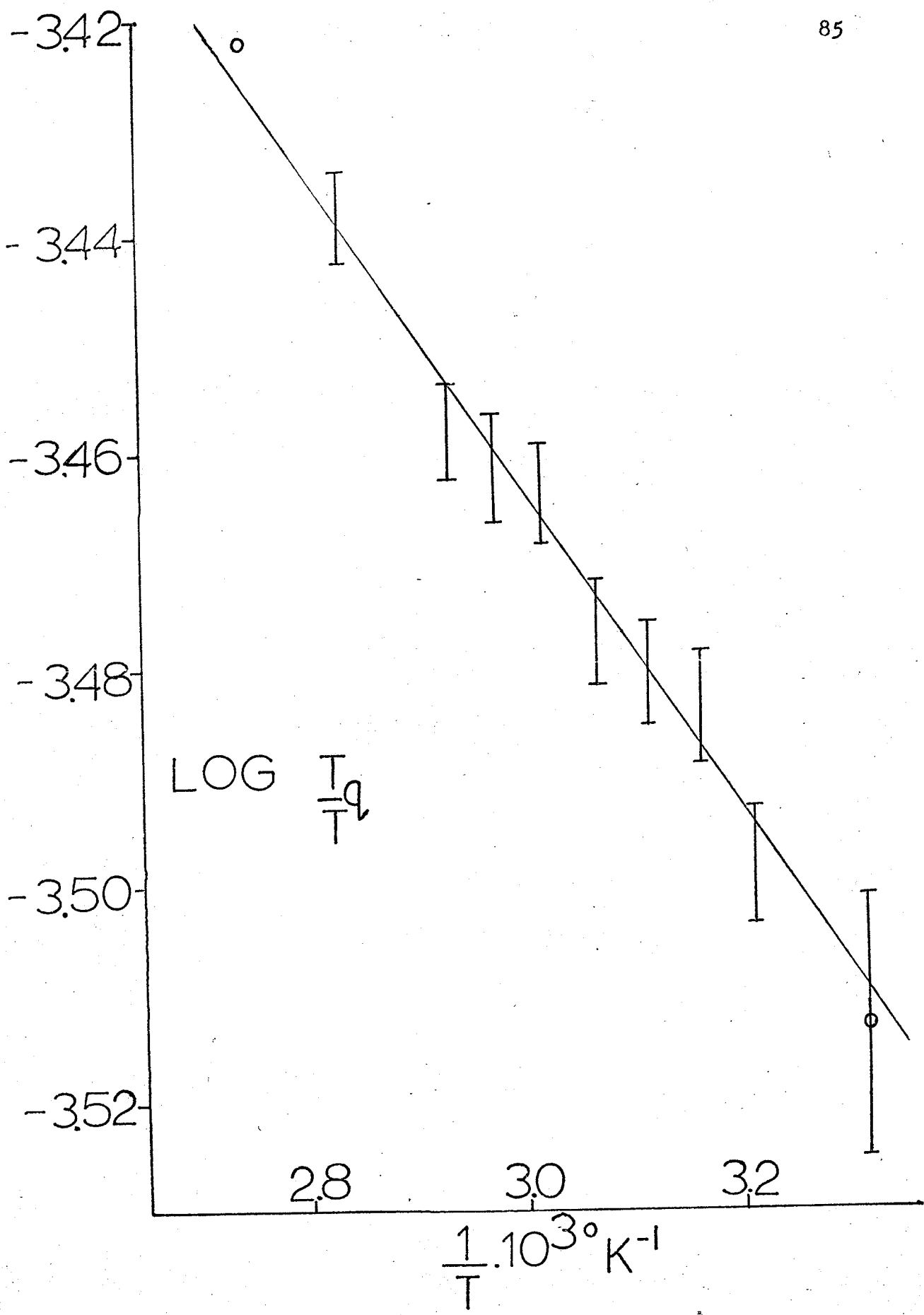


FIGURE 12

Eyring plot for the reorientation of methyl
nitrate in DMF solution.

$$T_2 = 0.71 \text{ sec}$$

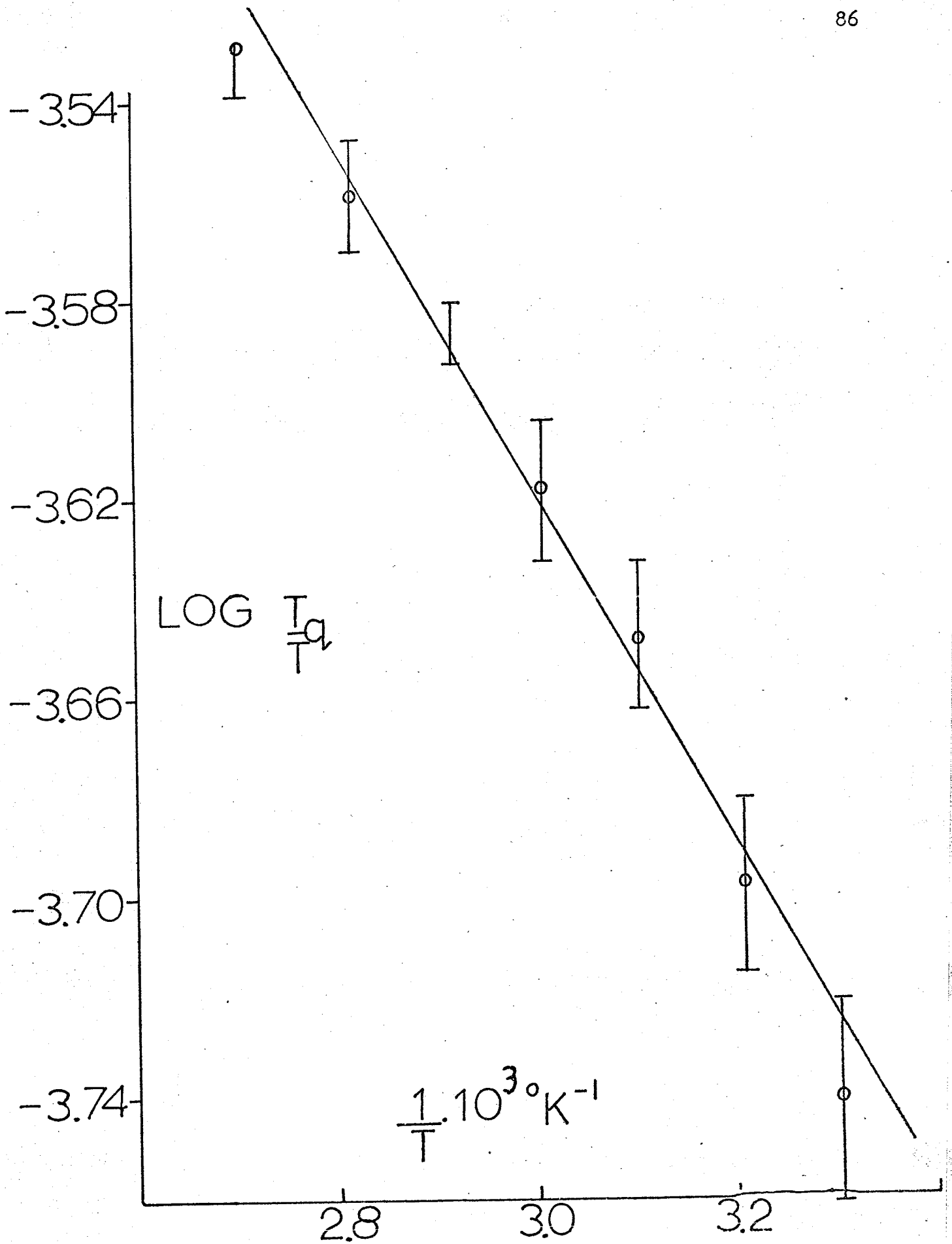


TABLE 14

Results of a least squares analysis of the data in
Tables 7-13.

δ_m , δ_b and δ_y represent the standard errors in
slope, intercept and $\log \frac{T_q}{T}$ (or $\log T_q$), respectively.

Table	T_2 (sec)	Slope ($^{\circ}\text{K} \cdot 10^3$)	$^* \delta_m \cdot 10^3$	Intercept	$^* \delta_b$	$^* \delta_y$	Corr. Coeff
7	2.00	-0.1468	0.0110	-3.0244	0.0334	0.0026	0.9773
8	1.68	-0.1538	0.0131	-3.0027	0.0400	0.0054	0.9491
9	2.00	-0.2898	0.0064	-0.0719	0.0194	0.0025	0.9980
9	1.68	-0.2961	0.0100	-0.0524	0.0305	0.0054	0.9909
10	2.00	-0.2655	0.0123	-2.8445	0.0373	0.0057	0.9933
11	1.00	-0.3477	0.0205	-2.5894	0.0618	0.0088	0.9944
12	0.71	-0.3772	0.0160	-2.4871	0.0434	0.0064	0.9969
13	2.00	-0.4089	0.0143	0.1090	0.0434	0.0060	0.9969
13	1.00	-0.4909	0.0209	0.3635	0.0632	0.0085	0.9955
13	0.71	0.5203	0.0139	0.4659	0.0419	0.0054	0.9981

TABLE 15

Activation parameters for the reorientation of methyl nitrate in
cyclohexane and dimethylformamide solutions.

Activation Parameter	DMF Solution			C ₆ H ₁₂ Solution	
	T ₂ = 2.0	T ₂ = 1.0	T ₂ = 0.71	T ₂ = 2.0	T ₂ = 1.68
ΔH^\ddagger kcal.mole ⁻¹ (Eq.33)	1.22 ± 0.06	1.59 ± 0.09	1.73 ± 0.07	0.67 ± 0.05	0.70 ± 0.06
ΔH^\ddagger at 298°K kcal.mole ⁻¹ (Eq.34)	1.28 ± 0.07	1.65 ± 0.09	1.79 ± 0.06	0.73 ± 0.03	0.77 ± 0.05
ΔS^\ddagger e.u. (Eq.33)	-1.35 ± 0.17	-0.18 ± 0.28	0.28 ± 0.22	-2.18 ± 0.15	-2.08 ± 0.18
ΔS^\ddagger e.u. at 298°K (Eq.36)	-1.18 ± 0.18	0.02 ± 0.29	0.45 ± 0.17	-1.98 ± 0.11	-1.91 ± 0.14
E _a kcal.mole ⁻¹ (Eq.30)	1.87 ± 0.07	2.25 ± 0.09	2.38 ± 0.06	1.33 ± 0.03	1.36 ± 0.05
$\tau_q \cdot 10^{14}$ sec (Eq.30)	10.73 ± 1.02	5.97 ± 0.81	4.72 ± 0.44	16.3 ± 0.7	15.5 ± 1.1
ΔG^\ddagger at 353°K kcal.mole ⁻¹	1.70 ± 0.12	1.65 ± 0.18	1.64 ± 0.15	1.44 ± 0.11	1.43 ± 0.12

Errors: Quoted values are standard errors derived from the least squares analysis.

T₂ values are in seconds.

(c) Evaluation of the fitting procedure and error estimate

The statistical errors in the activation parameters are doubtless overly optimistic. Uncertainties in temperature ($\pm 1^\circ\text{C}$) and T_2 (see below) are significant and will increase the errors quoted by a factor of at least 3-4. In addition, the small size of the energy barrier being measured (of the order of 1-2 kcal.mole⁻¹) gives rise to further problems. Labhart⁽⁹⁷⁾ has suggested that when the activation energy is of the order of RT (circa 0.6 kcal.mole⁻¹ at 298°K) the measured value is an "apparent" activation energy, smaller than the real one. However, largely because of the difficulty in estimating the magnitude of such an effect for methyl nitrate, but also because it is the relative rather than absolute magnitudes which are of interest, the problem was not considered further.

Hence, for a reliable result, it would appear desirable to employ a large temperature range and to have a line shape which is highly sensitive to T_q . Unfortunately, ~~neither~~ is available in the case of methyl nitrate. It is explosive above 65°C and below about 10°C, in any solvent, the resonance is a broadened singlet which changes only slowly with temperature. An example of a more suitable system is trifluoronitromethane, CF_3NO_2 , which shows the whole range of spectral shapes over a 90° temperature interval⁽⁹⁵⁾, and should therefore yield a more accurate value for the reorientational activation energy. The availability of an accurate and sensitive method of fitting the experimental spectra of methyl nitrate is thus clearly of paramount importance.

Both Packer⁽⁹⁴⁾ and Lee⁽⁹⁵⁾ in their analyses of spin - $\frac{1}{2}$ nuclei (^{19}F) spin - spin coupled to a quadrupolar nucleus which is undergoing varying rates of relaxation, used an indirect method to estimate T_q . They generated a large number of theoretical spectra covering a range of T_q

values and measured these to give parameters similar to those used in QUADFIT (and combinations thereof). Plots of $\frac{\max_c}{\min}$, say, versus the function $2\pi JT_q$ were found to be smoothly varying so that calculation of a sufficient number of values made linear interpolation between points acceptable. These graphs were then used to obtain the value of $2\pi JT_q$ (and hence T_q) corresponding to a particular observed spectrum. This is a satisfactory method for a line shape which changes rapidly with T_q (as here for fluorine nuclei, since J is large) but, as mentioned previously, is too insensitive for methyl nitrate where the changes are smaller. It was found preferable to use QUAD and QUADFIT with sufficiently small increments in T_q that interpolation was unnecessary. Whilst the use of only the half-height linewidth in matching spectra is not rigorously correct, since in principle it might be possible to fit this accurately while the overall line shape was not, in practice it was found to be quite sufficient, especially when used in conjunction with visual matching of the experimental and computed line shapes.

By far the greatest limitation on fitting by this method is an accurate determination of the J and T_2 values. Both Pople⁽²¹⁾ and Suzuki and Kubo⁽⁹⁸⁾ ignored T_2 in their line shape theories; since then several instances have been reported of a sensitivity of T_q to T_2 . Harris⁽⁹³⁾ with 3,4,5-trichloro-2,6-difluoropyridine and Luz⁽⁹⁹⁾ in relaxation studies on the permanganate ion found that T_2 was important. This is also apparent in the present results. A smaller T_2 value tends to decrease T_q at low temperatures and to increase it at the higher ones, thereby increasing both the slope and intercept of the T_q vs temperature plots. See Table 14. As a result, ΔH^\ddagger , E_a and ΔS^\ddagger are all sensitive to the T_2 used in fitting; for the DMF solution E_a varies from 1.87 to 2.38

kcal.mole⁻¹ for a T_2 of 2.00 and 0.71 sec, respectively, Obviously this is significant for energy barriers of a few kcal.mole⁻¹, particularly as statistical errors in E_a are less than 0.1 kcal.mole⁻¹ and therefore give an unrealistic uncertainty estimate. The fitting method itself provides a test for the T_2 value; when it is either too large or too small the QUAD and QUADFIT T_q 's do not converge, and furthermore the overall line shape fit with QUAD is invariably poor. A correct T_2 resolves these problems. Thus the possible error introduced by T_2 can be minimised and is not as significant as it might appear initially.

In view of these and other error possibilities, it has been suggested^(100,101) that any discussion of barrier magnitudes should centre on ΔG^\ddagger values rather than ΔH^\ddagger or ΔS^\ddagger since this parameter is less prone to systematic errors. The calculated ΔG^\ddagger values at 353°K (Table 15) confirm this view, showing far less variation with T_2 than either of its components ΔH^\ddagger or ΔS^\ddagger .

A complete line shape analysis, such as that of Gutowsky et al.⁽¹⁰²⁾, where the spectra are matched directly by the computer, appears to be the best method. The intensity of the experimental spectrum at given frequency intervals is stored in the computer memory and a theoretical spectrum calculated which is the least squares fit to these values. Lehn⁽²⁹⁾ used a modified version in his treatment of methyl nitrate, as did Bacon⁽⁵⁰⁾ for BF_3 ; best values for J , T_2 and T_q are obtained for the smallest value of the sum of the differences between experimental and computed points. The output consists of experimental and theoretical spectra plotted on the same graph, intensity difference at each point and the values of J , T_2 and T_q which give this agreement. Gutowsky claims that the method is far superior to visual matching and that computer time

and capacity required are quite modest; it also overcomes the problems associated with an independent determination of J and T_2 .

The results of this thesis show that even for the rather unsuitable instance of ^{14}N relaxation in methyl nitrate, line shape analysis of the signals of protons coupled to the nitrogen nucleus by scalar spin-spin interaction represents an accurate method for determining T_q and for studying the relevant molecular properties. The estimated error in T_q is certainly no more than $\pm 5\%$ (probably nearer $\pm 3\%$) in contrast to the ^{14}N T_1 measurements of Moniz and Gutowsky⁽⁴⁵⁾ where the error quoted is $\pm 50\%$! The low resonance frequency (giving poor signal-to-noise ratio) and small concentration of ^{14}N nuclei per unit volume makes spin-echo methods unsuitable for most nitrogen relaxation studies; where applicable, the use of high-resolution PMR measurements is superior. Moniz and Gutowsky give no estimate of error in their activation energy results; from this work it is felt that $E_a = 2.4 \pm 0.2 \text{ kcal.mole}^{-1}$ for DMF solution and $E_a = 1.4 \pm 0.2 \text{ kcal.mole}^{-1}$ for C_6H_{12} solution are realistic error limits.

(d) Dependence of Relaxation Rate on ViscosityAt different temperatures

As described in the Experimental Section, the viscosities of 15 mole % methyl nitrate in cyclohexane and dimethylformamide were measured at three different temperatures. Assuming viscosity to be a thermally activated process of the type

$$\eta = A \exp \frac{B}{RT} \dots\dots\dots(34)$$

the activation energy, B, may be found from the slope of a plot of $\log_{10} \eta$ versus $\frac{1}{T}$. The data in Table 16 confirms the validity of Equation (34); straight lines of correlation coefficient > 0.99 were obtained (Figure 13). Viscosities at other temperatures were then calculated by extrapolation and interpolation from Table 16.

The form of Equation (27) shows that relaxation rate will be directly proportional to the term $\frac{\eta}{T}$, other factors being constant. Table 17 lists these values (from Tables 8, 12 and 16) and they are shown graphically in Figure 14. A discussion of this plot is given in Section G(ii)b.

In different solvents

Equation (27) may also be investigated by the use of different solvents thereby encompassing a wider viscosity range than is possible by temperature variation alone. Using twelve different solutions (including neat methyl nitrate) relaxation rates were determined at ambient temperature (29.5°C); these are listed in Table 18 together with the viscosity of the solvent. Strictly speaking, solution viscosity should be used, but at a concentration of 15 mole % solute (plus TMS) the difference is negligible in the present case.

TABLE 16

The variation of viscosity with temperature for 15 mole % solutions of methyl nitrate in DMF and C₆H₁₂.

Temperature (°C)	$\frac{1 \cdot 10^3}{T}$ (°K ⁻¹)	DMF Solution		C ₆ H ₁₂ Solution	
		η (cP)	log ₁₀ η	η (cP)	log ₁₀ η
25	3.356	0.766	-0.1157	0.715	-0.1456
35	3.247	0.662	-0.1792	0.643	-0.1920
50	3.096	0.585	-0.2332	0.573	-0.2418

A least squares analysis of the data yields

For C₆H₁₂:

$$\log_{10} A = -1.38 \pm 0.05$$

$$B = 1.68 \pm 0.07 \text{ kcal.mole}^{-1}$$

For DMF:

$$\log_{10} A = -1.62 \pm 0.11$$

$$B = 2.04 \pm 0.16 \text{ kcal.mole}^{-1}$$

FIGURE 13

The temperature dependence of the viscosity of
15 mole % methyl nitrate in

(a) DMF solution o

(b) C₆H₁₂ solution †

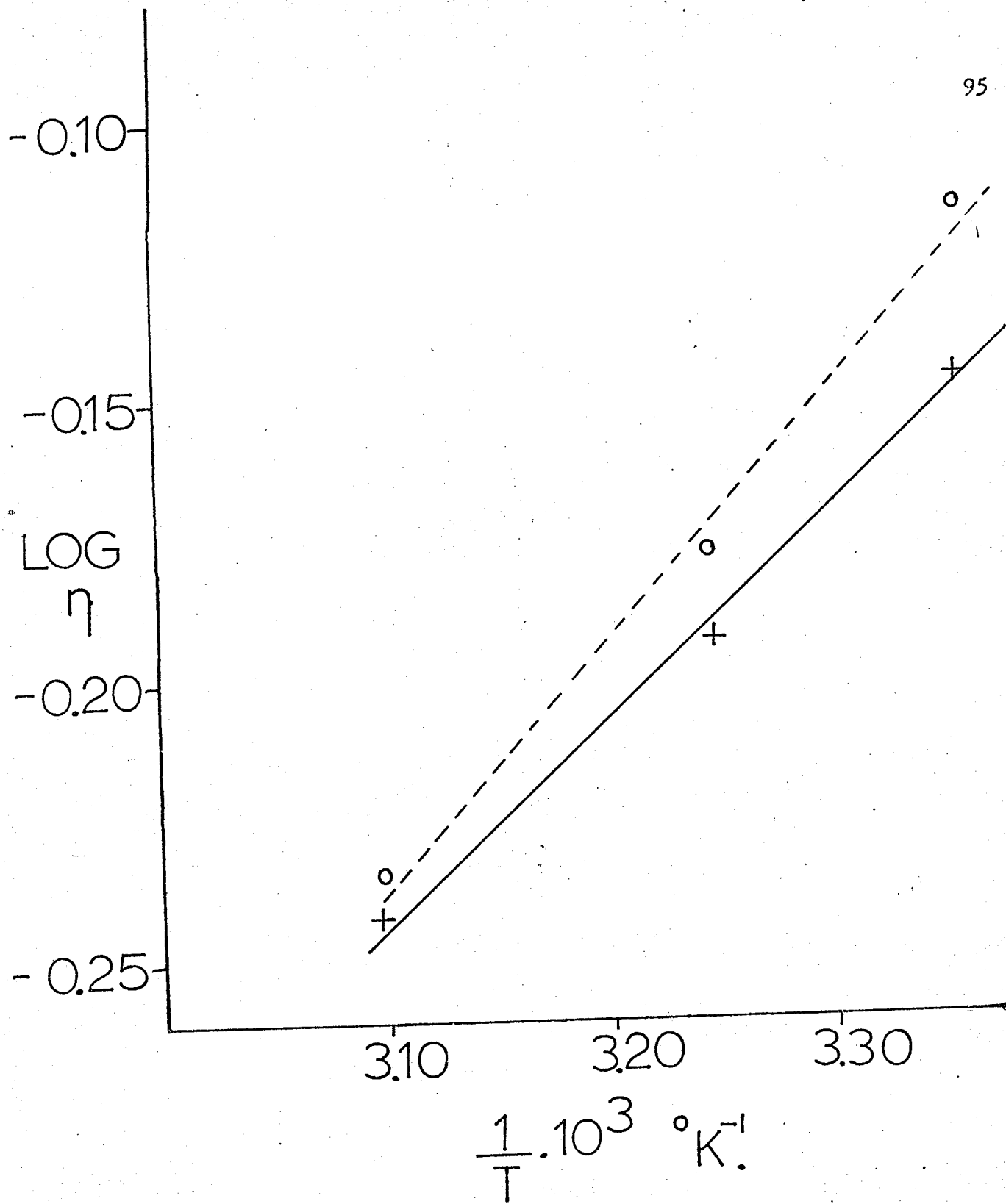


TABLE 17

^{14}N Relaxation rates and viscosities of 15 mole % methyl nitrate in DMF and C_6H_{12} solutions, as a function of temperature.

(a) C_6H_{12} solution:

T (°C)	$\frac{1}{T} \cdot 10^3$ (°K ⁻¹)	T_q^{-1} (sec ⁻¹)	η (cP)	$\frac{\eta}{T} \cdot 10^3$ (cP deg. ⁻¹)
28.5	3.315	10.81	0.6869	2.277
38	3.213	10.13	0.6301	2.025
43	3.163	9.64	0.6040	1.910
48	3.113	9.41	0.5790	1.802
53	3.066	9.20	0.5564	1.706
58	3.019	8.79	0.5348	1.615
63	2.974	8.60	0.5147	1.531
68	2.931	8.42	0.4964	1.455
80	2.831	7.77	0.4561	1.291
90	2.753	7.27	0.4270	1.176

(b) DMF solution:

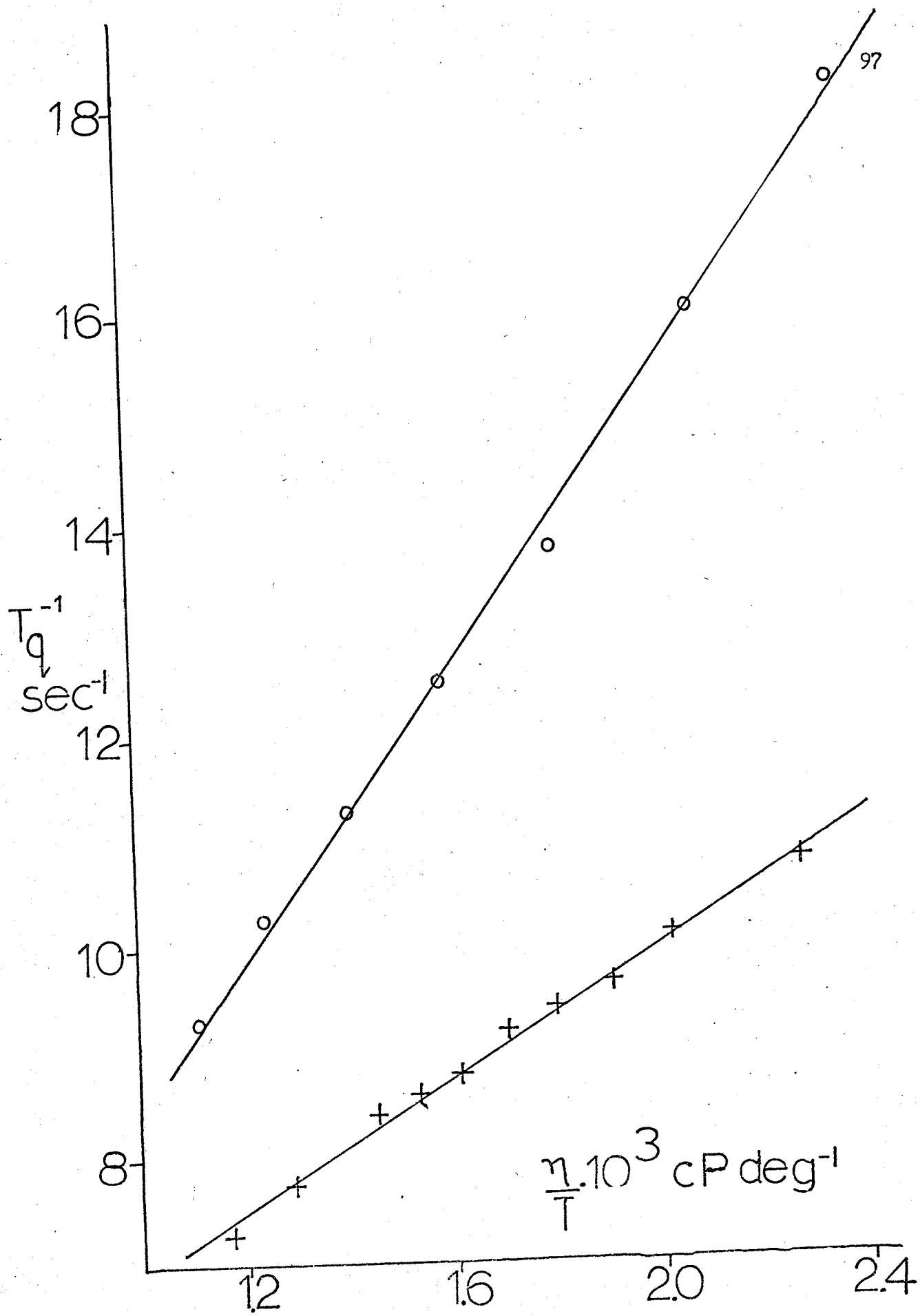
T (°C)	$\frac{1}{T} \cdot 10^3$ (°K ⁻¹)	T_q^{-1} (sec ⁻¹)	η (cP)	$\frac{\eta}{T} \cdot 10^3$ (cP deg. ⁻¹)
29.5	3.304	18.18	0.7174	2.370
38.5	3.208	16.00	0.6501	2.086
49	3.104	13.79	0.5842	1.813
59	3.010	12.50	0.5306	1.597
69.5	2.918	11.27	0.4826	1.408
80	2.831	10.26	0.4414	1.250
90	2.753	9.30	0.4074	1.122

FIGURE 14

^{14}N relaxation rate as a function of viscosity
divided by temperature

(a) in DMF solution ○

(b) in C_6H_{12} solution +



Plotting T_q^{-1} against viscosity, Figure 15, gives a scatter of points, although a general trend of increasing relaxation rate with viscosity is apparent in accordance with Equation (27a); the agreement is nowhere near that of Figure 14. From the reduced masses of the solvent-solute systems (in a.m.u.) and solvent molecular radii (calculated from density and molecular weight considerations, assuming a c.c.p. structure) given in Table 19, the microviscosity and mutual viscosity models were also examined. Plotting $\frac{\eta}{b}$ and $\frac{\eta}{\mu}$ against relaxation rate (Figures 16 and 17) gives a similar result to that of η versus T_q^{-1} ; the scatter of points is slightly less than that of Figure 15 but deviates markedly from the linearity expected on the basis of Equation (27).

As discussed more fully in Section G(ii)b, two behaviour patterns are discernible in Figures 15 - 17, one for low and one for high dielectric constant media. A plot of T_q^{-1} against viscosity/dielectric constant merely serves to accentuate the differences in the two types of behaviour, (Figure 18).

TABLE 18

^{14}N Relaxation Rates for methyl nitrate in various solvents at ambient temperature together with some physical properties of the solvents.

Solvent	T_q (sec)	T_q^{-1} (sec $^{-1}$)	*Viscosity (cP at 20°C)	$\frac{\text{Viscosity}}{\text{Dielectric Const.}}$ (cP at 20°C)
CH_3CN	0.0750	13.33	0.325	0.0084
CH_3COCH_3	0.0800	12.50	0.326	0.0152
CS_2	0.0850	11.76	0.367	0.1412
CDCl_3	0.0650	15.38	0.563	0.0670
$\text{C}_6\text{H}_5\text{CH}_3$	0.0800	12.50	0.590	0.2458
C_6D_6	0.0750	13.33	0.647	0.2813
DMF	0.0550	18.18	0.924	0.0246
CCl_4	0.0700	14.29	0.952	0.4327
C_6H_{12}	0.0925	10.81	0.960	0.4571
C_8H_{16}	0.0850	11.76	2.23	-
CH_3SOCH_3	0.0325	30.77	2.47	0.0505
neat	0.0625	16.00	-	-

*Data taken from International Critical Tables

(McGraw-Hill Book Company, Inc., New York, 1933)

FIGURE 15

^{14}N relaxation rate as a function of viscosity
in several solvents at ambient temperature.

ϵ = dielectric constant

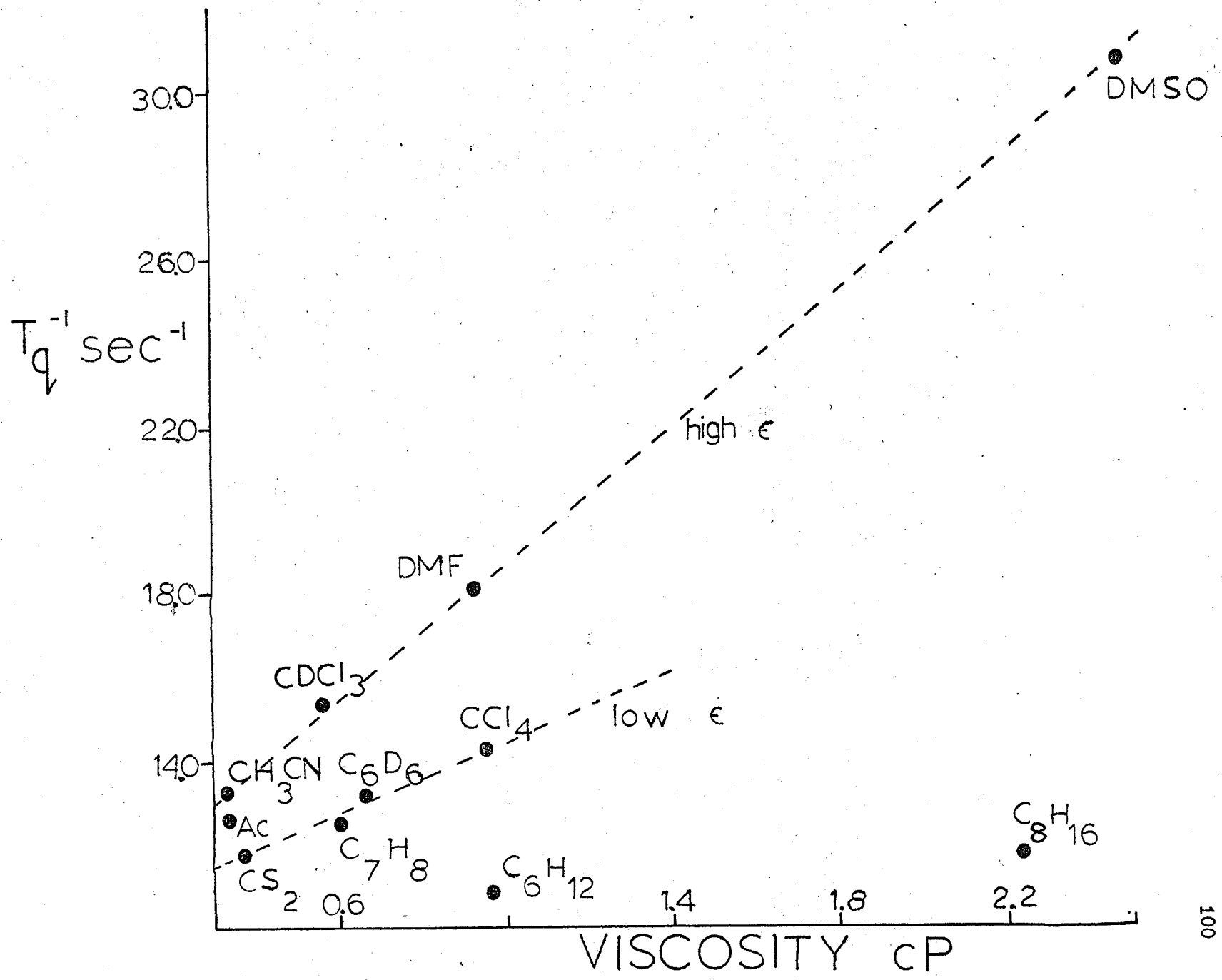


TABLE 19

Reduced Masses and "Molecular Radii" of the Solvents listed
in Table 18 together with the parameters used in Figures
16 and 17.

Solvent	Density (20°C) d gm. cc ⁻¹	Molecular Weight (a.m.u.)	* Reduced Mass μ	Viscosity Reduced Mass $\frac{\eta}{\mu} \times 10^2$	$\left(\frac{\text{Mol. Wt.}}{\text{Density}}\right)^{1/3}$ $\left(\frac{M}{d}\right)^{1/3}$	Viscosity $(M/d)^{1/3}$
CH ₃ CN	0.786	41.05	26.78	1.214	3.73	0.871
CH ₃ COCH ₃	0.791	58.08	33.12	0.984	4.19	0.778
CS ₂	1.263	76.14	38.29	0.958	3.92	0.936
CDCl ₃	1.492	120.38	46.97	1.199	4.32	1.303
C ₆ H ₅ CH ₃	0.867	92.13	41.96	1.406	4.73	1.247
C ₆ D ₆	0.879	84.11	40.21	1.609	4.57	1.416
DMF	0.944	73.10	37.51	2.463	4.26	2.169
CCl ₄	1.594	153.82	51.33	1.855	4.58	2.079
C ₆ H ₁₂	0.779	84.16	40.22	2.387	4.76	2.017
C ₈ H ₁₆	1.157	112.21	45.68	4.882	4.59	4.858
CH ₃ SOCH ₃	1.100	78.08	38.78	6.369	4.14	5.966

* Reduced mass, $\mu = \frac{M_1 M_2}{M_1 + M_2}$ where M_1 is the solvent molecular weight
and M_2 is the molecular weight of the
solute (= 77.04)

† The molecular radius is given by $r = \left(\frac{3 \times 0.74 M_1}{4\pi d N_0}\right)^{1/3}$ N_0 is the Avogadro
Number.
Only the term $\left(\frac{M}{d}\right)^{1/3}$ changes with solvent and this was therefore used.

FIGURE 16

^{14}N Relaxation Rate as a Function of Viscosity divided
by the "molecular radius" of the solvent.

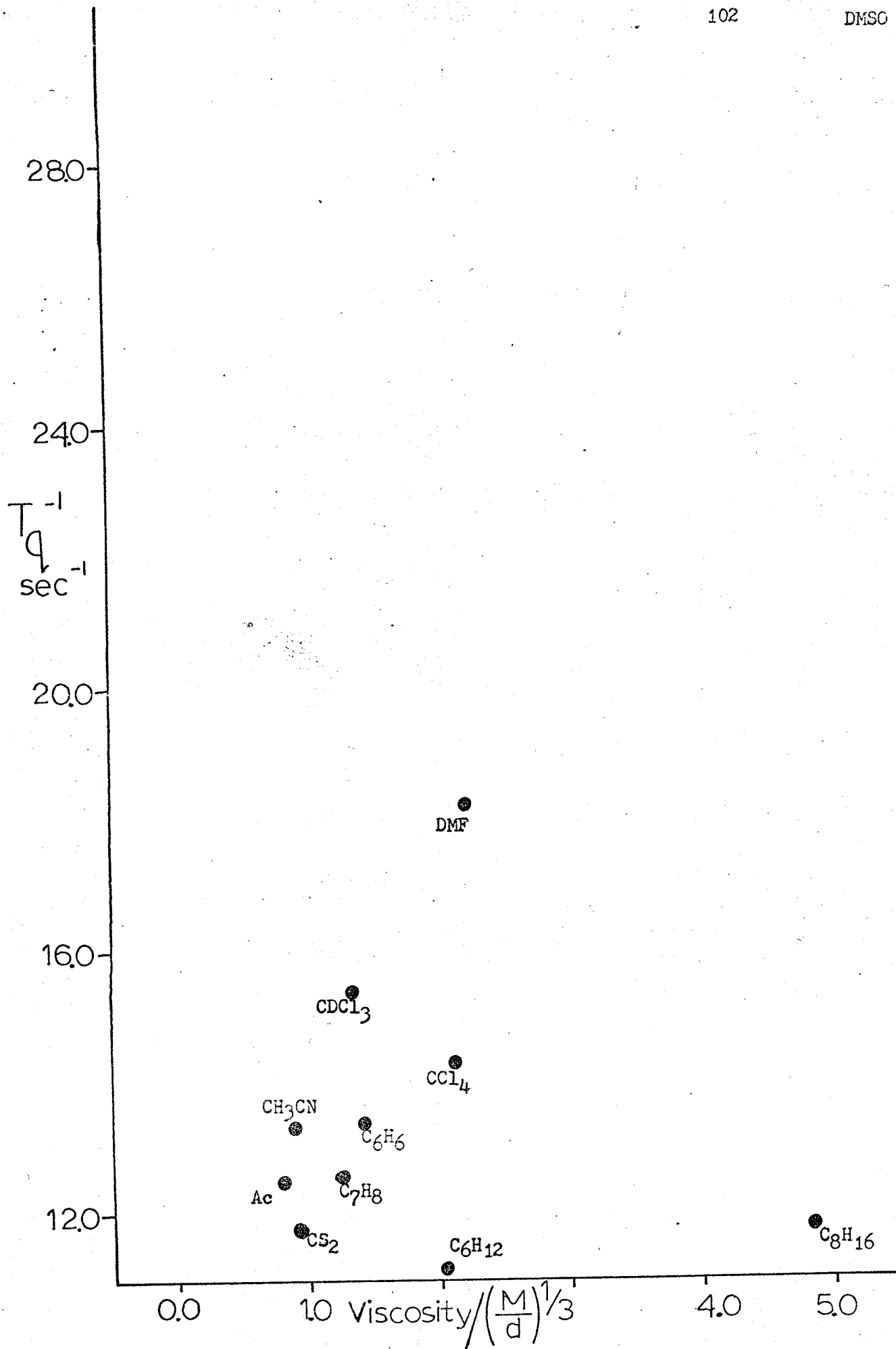


FIGURE 17

^{14}N Relaxation Rate as a Function of Viscosity
divided by the reduced mass of the solute-
solvent system.

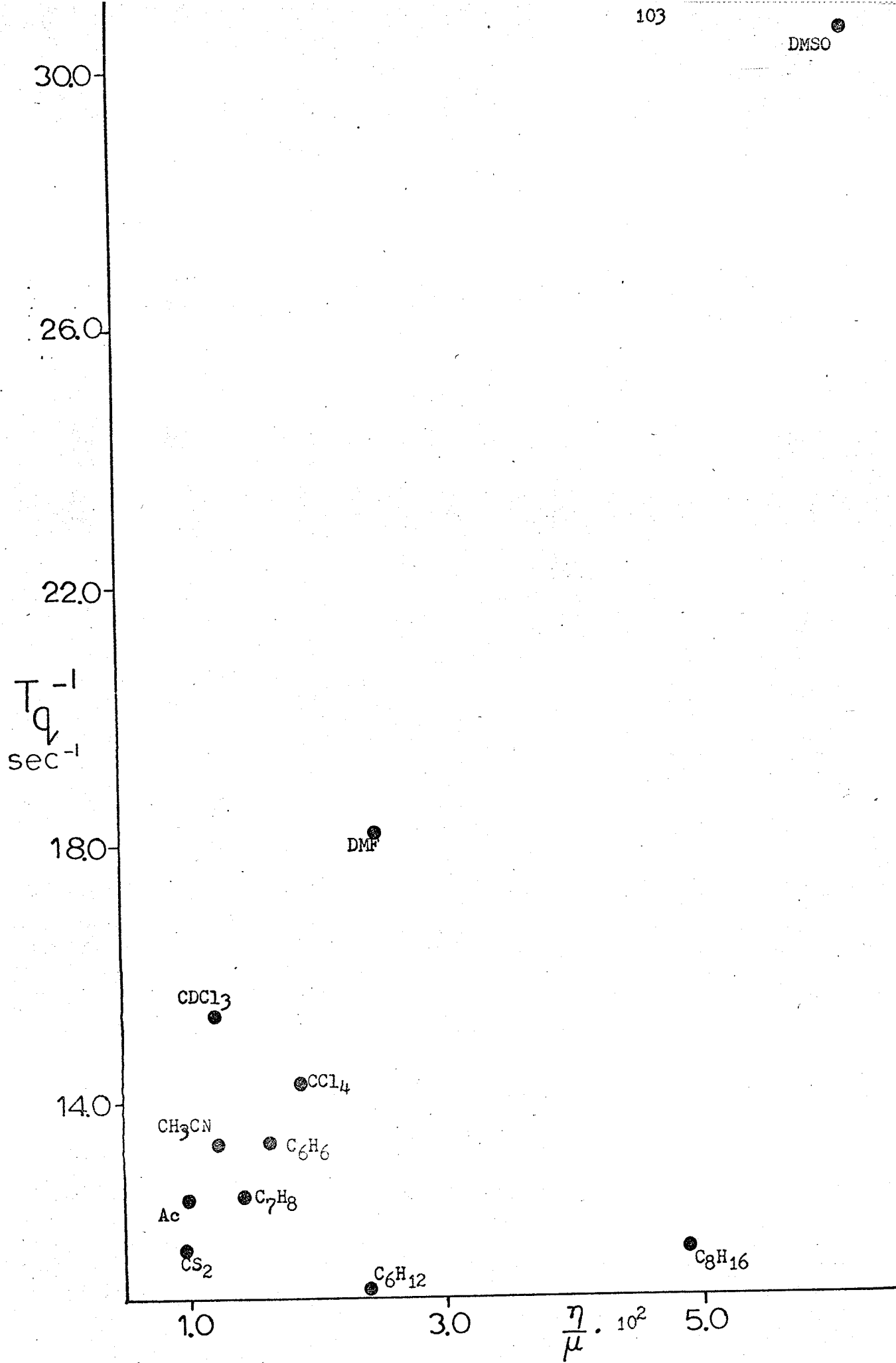
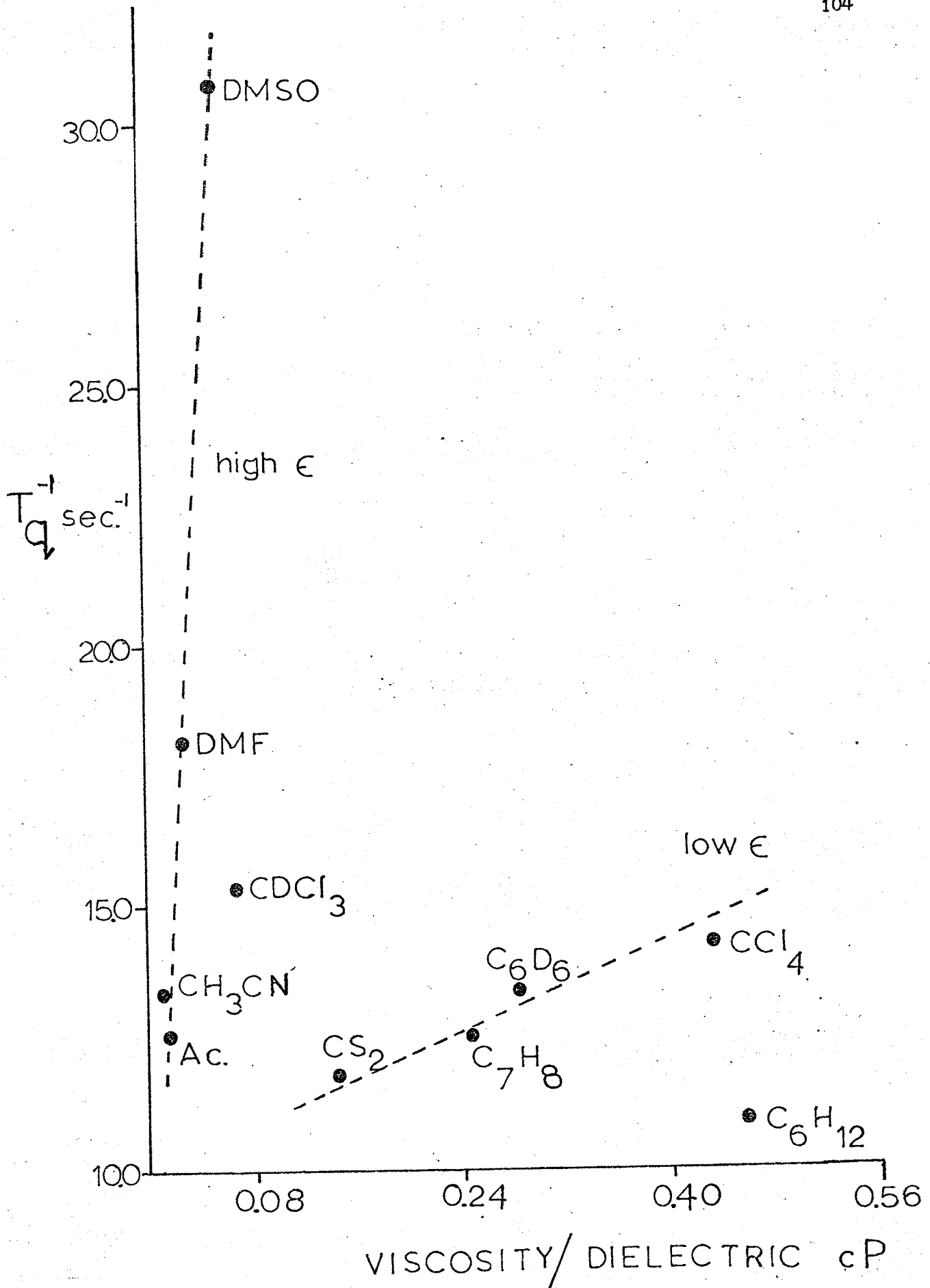


FIGURE 18

^{14}N relaxation rate as a function of viscosity
divided by dielectric constant, at ambient
temperature in several solvents.

ϵ = dielectric constant



(ii) Interpretation of Data(a) Thermodynamic ParametersMagnitude

Comparison of the results in Table 15 with those of Table 1 shows that the activation energies measured for methyl nitrate are of the same order of magnitude as those found for the reorientation of numerous other molecules; the differences are entirely compatible with the relative molecular shapes and sizes. A previously reported E_a value of $1.8 \text{ kcal.mole}^{-1}$ for the reorientation of methyl nitrate in tetrachloroethylene solution⁽²⁹⁾ lies between that found for DMF solution ($2.38 \text{ kcal.mole}^{-1}$) and cyclohexane solution ($1.36 \text{ kcal.mole}^{-1}$), indicating the importance of solvent in this respect; see page 108.

The parameters ΔS^\ddagger and τ_q^0 are less frequently quoted (but see^{(48), (103)}) due mainly to a lack of data on quadrupole coupling constants. However, as described in Appendix III, an approximate value for $\frac{e^2qQ}{h}$ may be derived, and hence ΔS^\ddagger and τ_q^0 (Table 15). The latter are therefore subject to considerable uncertainty, in view of which the agreement between τ_q^0 and the values found by Moniz and Gutowsky⁽⁴⁸⁾ is encouraging. For both solvents ΔS^\ddagger is negative, that for the cyclohexane solution being more so than for DMF. Confirmation of this result may be taken from the ΔS^\ddagger values for viscous flow and dielectric relaxation. These are also found to be small and negative⁽¹⁰⁴⁾. Thus it is reasonable to conclude that the activated state for rotational and translational motions is one of greater order than the normal state i.e. suggesting the existence of co-operative reorientation of the molecules.

Comparison with activation parameters of some physical phenomena.

In the introductory discussion it was shown that all intramolecular nuclear spin - relaxation processes are related to the way in which molecules reorient in the liquid phase. Obviously there are other physical processes which depend on such molecular motions; measurement and comparison of these should therefore provide a sensitive probe for molecular dynamics.

Viscosity is perhaps the property most extensively investigated in this way, data being readily available and the theory relatively simple (31). Section C(iii)b summarized the failings of this approach; the results for methyl nitrate (Table 19) concur with current opinion and give only qualitative agreement between the temperature dependences of relaxation rate (reorientational rate) and viscosity.

TABLE 20

Activation energies for reorientation and viscous flow
of methyl nitrate in DMF and C₆H₁₂ solutions

Solvent	E _a (NMR) kcal.mole ⁻¹	E _a (viscosity) kcal.mole ⁻¹
DMF	2.38	2.03
C ₆ H ₁₂	1.36	1.68

Other work ⁽⁴⁷⁾ showed that E_a for chlorine nuclear relaxation was consistently less than that for viscosity. Cyclohexane solution follows this pattern and it is therefore tempting to ascribe the opposite behaviour of

methyl nitrate in DMF to some specific MeNO_3 / DMF interaction. This, however, cannot be done with any justification since the differences in E_a values are quite small, and furthermore, microdynamical considerations reveal the basic fallacy of any such correlation. Viscosity depends on momentum transfer between liquid layers moving with different translational velocities (i.e. mainly a solvent - solvent interaction), whereas rotation is expressed in terms of the correlation function of the angular rotational velocity. For completely spherically symmetric frictionless molecules there would be no energy transfer between molecular linear and rotational angular momentum (rotation occurring without simultaneous translation of neighbouring molecules) and thus no relation between the viscosity and the rotational motion. In the "inertial limit" therefore⁽⁶⁰⁾, macroscopic viscosity is obviously a poor measure of the viscous drag actually encountered by the rotating molecule. As the molecule becomes increasingly nonspherical there is greater energy transfer between rotational and translational motions, so that the molecular rotation is more closely determined by the viscosity. The latter situation applies for methyl nitrate, where in addition to a lack of spherical symmetry, its highly dipolar character makes the "viscous medium" approximation quite realistic; rotation very likely requires simultaneous translation of neighbouring molecules. A similarity between E_a for viscous flow and for reorientation would then be predicted (Table 19).

For spin - relaxation mechanisms dependent entirely upon translational processes (i.e. those arising intermolecularly) there is good agreement between activation energies for viscous flow and for relaxation. An example is the quadrupolar relaxation of halide ions in electrolyte

solutions, where the fluctuating electric field gradients causing relaxation arise from molecular collisions. A close dependence on viscosity is thus expected and confirmed⁽⁶⁹⁾. In addition, Powles and Figgins found agreement between activation energies for intermolecular dipole - dipole relaxation and viscosity in their work on proton relaxation in liquid benzene⁽⁴¹⁾.

Analogously, phenomena dependent principally on rotation might be expected to have similar activation energies. Thus the temperature dependence of T_1 for quadrupole and intramolecular dipole - dipole relaxation should parallel that of Rayleigh light scattering (the latter following molecular reorientation via the associated reorientation of the anisotropic optical polarisability tensor). Agreement has been found for benzene⁽⁴¹⁾ and other systems⁽⁴⁶⁾ though unfortunately no comparison can be made for methyl nitrate as data on light scattering is unavailable.


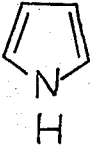
To summarize, then, the results in Table 20 give support to B.P.P. theory in the limit of a strongly interacting non-spherical solute molecule. However, comparison with macroscopic properties dependent on rotation would be more satisfactory.

Solvent Dependence

A more revealing aspect of the results in Table 20 is the difference of 1 kcal.mole^{-1} in the activation energies between the two solvents. Until recently, most measurements of E_a for molecular reorientation were for the pure liquid; little was known of the solvent dependence of E_a , though the present results show this to be significant. Examples of similar behaviour are given below in Table 21 together with some physical constants of the liquids.

TABLE 21

Activation Energies for molecular reorientation illustrating the dependence on solvent.

SOLUTE	SOLVENT	SOLUTE CONCENTRATION	ϵ^* (solvent) 20°C	η^* (solvent) cP 20°C	E_a kcal.mole ⁻¹	REF.
(CH ₃) ₂ N.NO ₂	tetrachloro- ethylene	1M	2.4	0.87	2.7	29
	pyridine	1M	13.1	0.97	2.4	
	2-fluoro- pyridine	100 mole %	16.1	0.82	1.6	72
	formamide	60 mole %	109	3.3	2.7	
	pyrrole	100 mole %	7.5	1.35	3.2	
	pyridine (d ₅)	15 mole %	12.3	0.97	2.2	105
	acetone	10-20 mole %	21.4	0.32	1.4	
CH ₃ ONO ₂	cyclohexane	15 mole %	2.0	0.96	1.4	this work
	DMF	15 mole %	37.6	0.92	2.4	

* Values taken from International Critical Tables (McGraw-Hill Book Company, Inc., New York, 1933)

From this table it is clear that changes in E_a well outside experimental error are associated with a change in solvent; a dependence on viscosity and dielectric constant is apparent. The work of Alger and Gutowsky⁽⁷²⁾, designed to test the van der Waals molecular association model, shows that a larger energy of activation is found with an increase in dielectric constant and viscosity of the medium. They ascribed the increase in E_a to greater association in a liquid of higher polarity (of which ϵ and η are a measure) although the nature of this "association" is not defined. The substantial decrease in E_a for pyrrole as the dielectric constant of the medium is increased⁽¹⁰⁵⁾ would therefore appear surprising were it not for the fact that viscosity changes are in the opposite direction (i.e. parallel to the changes in E_a). The dependence of relaxation rate on viscosity is well known and appears to be dominant over an approximately three-fold change in dielectric constant (from 7.5 to 21.4). This leads one to question the conclusions of Alger and Gutowsky re. 2-fluoropyridine, surely an increase in viscosity from 0.82 to 1.49 cP rather than the small increase in dielectric constant (from 16.1 to 19.7 for the 60 mole % solution) would cause the change of activation energy.

In the present work two systems were chosen with similar viscosity, but with vastly different dielectric constant in an attempt to separate the two factors. The results show clearly that media of high dielectric constant present a larger barrier to molecular reorientation than those with a lower value. The reason for this is a matter of much conjecture, but taken together with the evidence presented in Section G (ii)b certainly does imply a higher degree of structure in the CH_3ONO_2 - DMF solution than in CH_3ONO_2 - C_6H_{12} . This is entirely reasonable for the highly dipolar DMF and methyl nitrate molecules ($\mu = 3.8\text{D}$ and 2.9D

respectively⁽¹⁰⁶⁾) where some form of dipole - dipole complex in solution is to be expected. However, to go further and postulate the lifetime of such a complex (do, for instance, the two molecules rotate as a single entity or exchange partners several times during the course of a rotation?), requires additional measurements. Any form of association will serve to increase the rotational correlation time of the solute (and thus give a larger E_a) regardless of the lifetime of the interaction. The results presented here do not give a conclusive answer to questions of complex formation, as activation energy differences have many contributing factors. The following is also a plausible explanation of the data:

Ample evidence now demonstrates the dependence of T_q^{-1} (quadrupolar relaxation rate) on solution viscosity and dielectric constant. Specifically, an increase in the two latter properties causes an increase in the reorientational correlation time. Now, for DMF the temperature dependences of ϵ and η are both larger than for C_6H_{12} *. Hence a greater variation of τ_q with temperature in the former solvent would be predicted and confirmed from the E_a 's in Table 19. Of course, such an interpretation does not exclude the idea of complex formation (for what is the source of the large $\frac{d\eta}{dT}$, $\frac{d\epsilon}{dT}$ for DMF?) but only underlines the inadequacy of this type of experiment in distinguishing true complex formation from mere preferential molecular arrangements which have no time correlation. The concentration studies of Anderson⁽¹⁰⁷⁾ are more informative in this respect -- see Suggestions for Future Research.

* $\frac{d\epsilon}{dT} = 0.169$ and $0.0016 \text{ deg}^{-1}C$ for DMF and C_6H_{12} respectively.

For $\frac{d\eta}{dT}$ see Table 19.

(b) Factors Determining the Rate of Quadrupolar Relaxation

Figures 14 - 17 contain a wealth of information on the sensitivity of nuclear quadrupole relaxation rates to the surrounding medium. The more significant aspects are recognized and discussed in terms of current theories on molecular correlation times.

Figure 14

There are two points of significance attached to Figure 14, one is the linearity, the other the difference in slope for the two solutions.

The linearity implies (Equation 27) that the quadrupole coupling constant does not alter over the viscosity range obtained by the temperature variation, and neither do the shape/size parameters of the rotating molecule. As discussed in the Introduction, such behaviour is well known^(41,67-70) and demonstrates that molecular rotational rates follow directly changes in viscosity where such changes are not accompanied by a drastic alteration of the medium in any other respect.

The difference in slope between the two solutions (that for DMF being more than twice that of C_6H_{12}) cannot be explained by considering either the reduced masses (Hill theory) or solvent radii (microviscosity model) since these parameters are almost identical for the two solvents, Table 19. From the Hill model, Equations (26) and (27c), the gradient of T_q^{-1} versus η/T is proportional to the term $\frac{e^2qQ}{h} \frac{I_a}{\mu}$. Assuming that the quadrupolar coupling constant arises entirely intramolecularly (Appendix III) and is therefore constant the results imply that

$$\left(\frac{I_a}{\mu}\right)_{\text{DMF solution}} \approx 2\left(\frac{I_a}{\mu}\right)_{\text{C}_6\text{H}_{12} \text{ solution}}$$

or

$$(I_a)_{\text{DMF}} \approx 2(I_a)_{\text{C}_6\text{H}_{12}}$$

since the reduced masses are very nearly equal. In other words the rotating unit in DMF solution is larger and/or of higher moment of inertia than that in C_6H_{12} for the same solute molecule, methyl nitrate. These results are compatible with some type of CH_3ONO_2 - DMF complex which will obviously rotate more slowly than methyl nitrate itself. Both molecules are highly polar ($\mu = 2.88$ and 3.86 D, respectively) so that dipolar association is very likely; however, these experiments yield no information on the lifetime of such species.

Figures 15 - 17

Figures 15 - 17 were designed to test the predictions of B.P.P. theory and the mutual viscosity and microviscosity models (Equations 27a - 27c); all are clearly shown to be inadequate. In these plots a change in viscosity is accompanied by a change in numerous other physical properties associated with the new solvent whereas changing the viscosity by temperature variation (as in Figure 14) does not alter the chemical and physical nature of the medium to such an extent. Obviously then, factors other than macroscopic viscosity are important in determining the rate of quadrupolar relaxation.

From Figure 15 two distinct behaviour patterns are discernible (as suggested by the broken lines); these are evident also in the more "refined" theories represented in Figures 16 and 17. The ^{14}N relaxation rates for methyl nitrate in DMSO, DMF, $CDCl_3$, CH_3CN and CH_3COCH_3 are all abnormally large for the solvent viscosity compared to those in CS_2 , CCl_4 , C_7H_8 and C_6H_6 where T_q^{-1} is a more slowly changing (though still a linear) function of viscosity. It may therefore be concluded that viscosity is not an adequate parameter in describing the frictional forces acting on a rotating solute molecule in solution. It is unfortunate that

data on mutual viscosities is unavailable for these systems so that the Hill model cannot be examined in its complete form. Thus in view of the unsatisfactory nature of current theories on molecular correlation times it was considered worthwhile to outline the observed dependence of relaxation rate on certain other physical parameters with a view to developing a more successful theory.

A dependence on the dielectric constant of the medium is immediately suggested by Figures 15 - 17. T_q^{-1} is a linear function of viscosity at constant dielectric constant ($\epsilon \approx 2$ for all solvents on the lower line, Table 22); for larger ϵ T_q^{-1} continues to increase with η , but at a greater rate. These features (viz. abnormally large relaxation rates for the viscosity) are also apparent in the data on 2 - fluoropyridine⁽⁷²⁾ and some nitriles⁽⁷¹⁾ for the more polar solvents. (These studies, however, show a greater linearity between T_q^{-1} and η than does Figure 15.) The dependence of relaxation rate on dielectric constant is not a simple one; Figure 18 where T_q^{-1} is plotted against η/ϵ (in the hope of compensating for a large ϵ) merely accentuates the difference in behaviour types. Thus dielectric constant must be regarded as a physical property capable of upsetting the $T_q^{-1} \sim \eta$ linearity in a dramatic if somewhat irregular fashion.

A closely related parameter, the dipole moment, appears to have a similar effect on the relaxation rate. Reference to Table 22 shows that for all the solvents (except CDCl_3) on the upper T_q^{-1} vs η line $\mu > 2.0\text{D}$ and for those on the lower line $\mu \approx 0$. Again there is no straightforward dependence of T_q^{-1} on μ . In the theory of liquids it is suggested (e.g. Linder 108) that the cohesive forces between molecules are mainly dispersive (van der Waals type) until the dipole moment is

greater than approximately 2.0 D whereupon dipolar association becomes significantly important. Hence it would be reasonable to imagine the rotation of methyl nitrate ($\mu = 2.9$ D) to be more constrained in a polar solvent, regardless of the macroscopic viscosity, simply because thermal motion now has to overcome the aggregation of dipoles in addition to steric factors. This means slower rotation and thus more efficient quadrupole relaxation. Invoking solvent radius or solute-solvent reduced mass will obviously not account for such polar effects and it is therefore not surprising that both these modifications to the theory of B.P.P. fail in the more polar solvents.

In conjunction with each other macroscopic viscosity and dielectric constant can rationalize the main trends in relaxation rates shown by Figures 15 - 17. However, there are some results which contradict this argument. Why, for instance, should the relaxation rates in cyclohexane and carbon tetrachloride be different when both their viscosities and dielectric constants are so similar? In this case it appears reasonable to invoke bond polarisability as the cause of the discrepancy. The permanent dipole moments of C_6H_{12} and CCl_4 are both zero, but as seen from Table 22 the polarisability of the C - Cl bond is far greater than that of either bond type in cyclohexane i.e. methyl nitrate could induce a transient dipole in CCl_4 more readily than in cyclohexane. Thus the rotational motion of methyl nitrate in the vicinity of CCl_4 will be restricted by the dipole - induced dipole attraction, leading to slower reorientation (and hence the more efficient relaxation found experimentally). Another example is the relaxation rate in CS_2 which is significantly greater than that in C_6H_{12} although the reverse would be predicted from viscosity considerations. (The dielectric constants

are similar.) Following the argument above, this may arise from the relatively high polarisability of the C = S bond. Again, however, as with dielectric constant and dipole moment, there exists no simple relation between relaxation rate and bond polarisability. It is certainly a minor influence, significant only for solvents with no permanent electric dipole moment.

Finally it might be mentioned, though without any rigorous theoretical justification, that for some of the solvents there appears to be a connection between T_q^{-1} and the latent heat of vaporization at the boiling point, Figure 19. In as much as this parameter is a measure of intermolecular forces between solvent molecules, such a correlation may not be unreasonable, but is probably fortuitous.

There is one remaining point to be clarified; relaxation rates in cyclohexane and cyclooctane do not follow any correlation and in fact show an independence of viscosity which is at first sight disturbing. However, in C_6H_{12} and C_8H_{16} the restrictions on solute rotation are similar, viz. C - C and C - H bonds of low polarizability. The ease of translation of one large C_8H_{16} (or C_6H_{12}) molecule past another, of which the macroscopic viscosity is a measure, would hardly be expected to bear a close relationship to the ease of rotation of a smaller molecule, like methyl nitrate, in that medium. In other words, viscosity is a poor measure of the actual microdynamics in such solutions. Obviously this is only a tentative explanation. It would be interesting to investigate other members of the series, cyclopentane, cycloheptane etc. to see whether they display the same behaviour.

TABLE 22

Some Physical Properties of the Solvents.

Solvent	Dielectric Constant (20°C)	^a Dipole Moment (D)	^b Bond	Polarisability $\propto \times 10^{24} \text{ cm}^3$	^c Latent Heat of Vaporisation (kcal.mole ⁻¹)
CH ₃ CN	38.8	3.18	C≡N	3.1	7.13
CH ₃ COCH ₃	21.4	2.75	C=O	1.9	6.57
CS ₂	2.6	0	C=S	7.6	6.35
*CDCl ₃	≠8.4	1.18	C-Cl	3.7	6.69
C ₇ H ₈	2.4	0.5	C _{Ar} -C _{Ar}	2.2	7.85
*C ₆ D ₆	2.3	0	"	"	7.12
DMF	37.6	3.86	C-N C=O	0.9 1.9	8.88
CCl ₄	2.2	0	C-Cl	3.7	7.05
C ₆ H ₁₂	2.1	0	C-H C-C	0.8 1.9	7.15
C ₈ H ₁₆	-	-	"	"	8.77
CH ₃ SOCH ₃	48.9	3.9	S=O	>2	9.78
CH ₃ NO ₃	23.9	2.9	C-O N-O	0.8 -	6.78

^a Values in benzene solution (106)^b Reference (109)

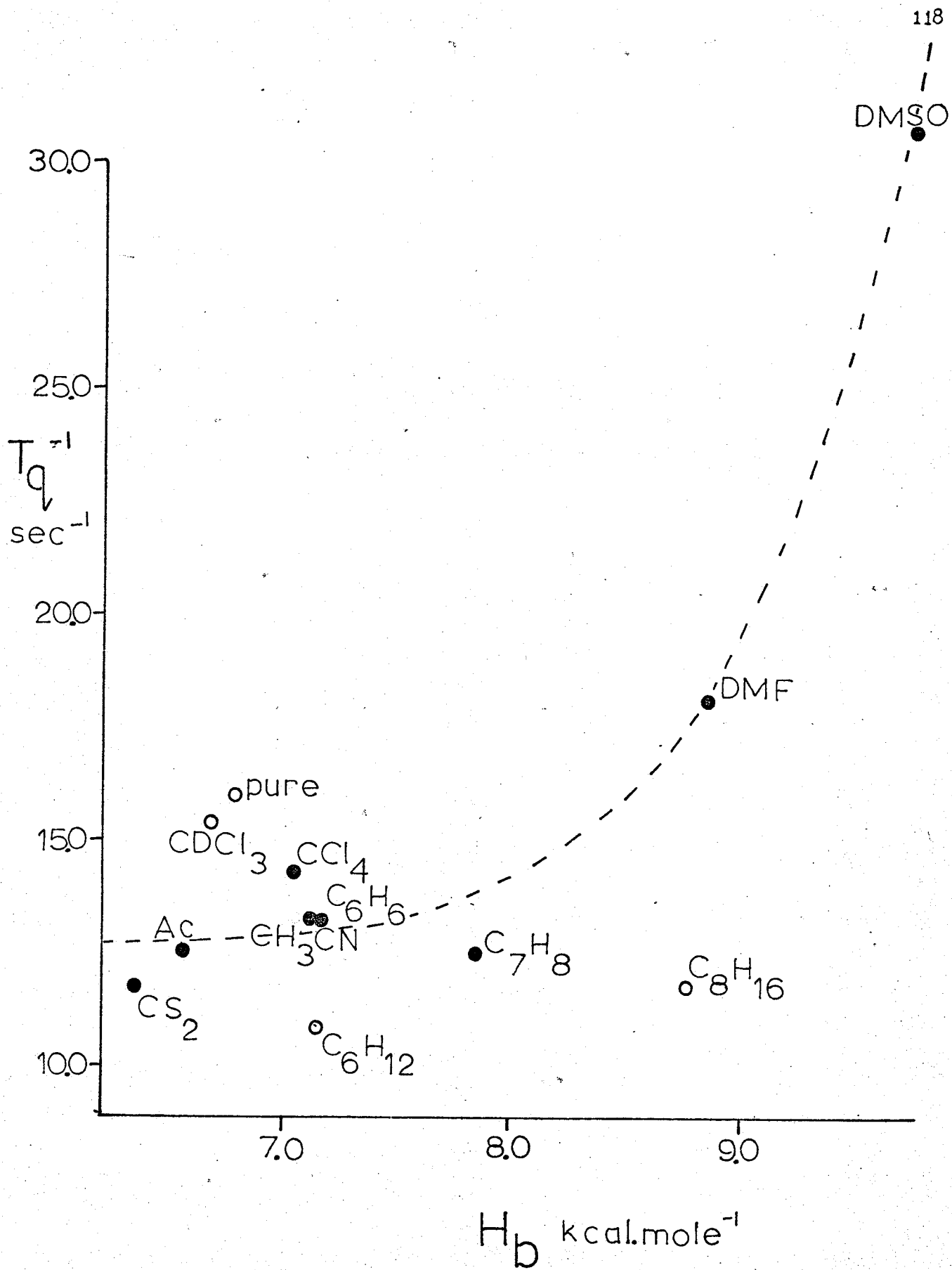
^c Values estimated from $H_v = 17.0T_b + 0.009T_b^2$
(J.H. Hildebrand and R.L. Scott, "The Solubility of nonelectrolytes." Dover Publications, Inc., New York, 3rd Edition, 1964, Page 427.)

* Physical properties taken to be those of the protonic species.

≠ Value calculated for 50 mole % solution (110) $\epsilon_{\text{CDCl}_3} = 5.05$

FIGURE 19

^{14}N relaxation rate at ambient temperature in several solvents plotted against the heat of vaporisation (H_b) of the solvent.



(c) Chemical Shift Variations

Table 6 shows that there is an appreciable solvent effect on the position of the methyl resonance, a difference of almost 100 Hz (at 100 MHz) between the toluene and DMF solutions. In addition a temperature dependence of 0.04 Hz per degree centigrade is shown by the DMF solution, whereas in cyclohexane the shift is constant. This clearly implies that there is no self-association of the solute molecules in the 15 mole % solution. The temperature variation of chemical shift in DMF solution is thus indicative of solute - solvent interaction.

Whilst the results of Table 6 are predictable by current theories on chemical shift⁽¹¹¹⁻¹¹³⁾ certain aspects are relevant to the idea of complex formation in the more polar solvents. The widely used (though little justified) Onsager model⁽¹¹⁴⁾ predicts a linear dependence of chemical shift on the function $\frac{\epsilon - 1}{2\epsilon + 2.5}$ for a polar solute molecule. The data in Table 23 when plotted (Figure 20) gives a scatter of points. However, ignoring benzene, toluene and the rod-shaped molecules carbon disulphide and acetonitrile where anisotropy effects are large^(111,115 and 116) thereby masking the polar term, and also carbon tetrachloride and chloroform (where the van der Waals term is abnormally large⁽¹¹⁵⁾) the remaining five solvents show a distinct curvature as is commonly found in Onsager plots at high dielectric constant⁽¹¹⁷⁾. Some authors e.g. reference⁽¹¹⁵⁾ attribute the non-linearity to specific intermolecular interactions in the more polar solvents; the added shift to low field over and above that predicted by the term $\frac{\epsilon - 1}{2\epsilon + 2.5}$ being due to the large electric fields associated with interactions such as hydrogen bonding or complex formation. This might be reasonable for the methyl nitrate results but for certain limitations in the Onsager model which

reduce the applicability of the equation to solvents of dielectric constant no greater than 9 at the most. It is therefore believed e.g. (118), that behaviour of the type shown in Figure 20 is probably due to inadequacy of the Onsager reaction field expression rather than specific interactions.

The dependence of chemical shift on some reaction field (though not that of the Onsager model) is demonstrated by the results of Laszlo and Musher⁽¹¹⁷⁾, but they make no suggestion as to the form of ϵ dependence. Interestingly, Schaefer and co-workers^(115,119) find a linear dependence of solvent shift on $\epsilon^{\frac{1}{2}}$ for much of the data which previously showed strong curvature. This function appears to give some improvement in the case of methyl nitrate (Figure 20) but with the limited number of points (and the 15 mole % samples used which will give significant dilution shifts) no definite conclusion can be drawn. There is no theoretical explanation of the empirical relationship. The theories of Goldstein⁽¹¹⁸⁾ and Johnston⁽¹²⁰⁾ which involve explicitly the dipole moment of solute and solvent appear to agree more closely with experimentally observed shifts. Their model involves the idea of a solute-solvent collision complex with well-defined thermodynamic properties K , ΔS , ΔH etc. It seems unlikely, however, that such a treatment would be relevant in the present case.

The sensitivity to temperature of the proton chemical shift in the $\text{CH}_3\text{NO}_3/\text{DMF}$ solution could, perhaps, be taken as evidence of an association between solute and solvent (following 121) which is temperature dependent. However, the dielectric constant of DMF itself has a large temperature coefficient; the resonance frequency of the

methyl protons follows the function $\frac{\epsilon - 1}{2\epsilon + 2.5}$ closely (Table 24 and Figure 21) though the changes are quite small. This suggests that in such a system the effect of temperature is primarily reflected through the variation of dielectric constant.

In summary then, chemical shift measurements do not imply anything definite on the question of complex formation. Lack of suitable data and a reliable theory make interpretation ambiguous and of little relevance in the present discussion.

TABLE 23

Proton Chemical Shift of Methyl Nitrate as a function
of solvent dielectric constant.

Solvent	Shift Hz	$\frac{\epsilon - 1}{2\epsilon + 2.5}$	$\epsilon^{\frac{1}{2}}$
CH ₃ CN	410.90	0.472	6.24
CH ₃ COCH ₃	415.31	0.471	4.63
CS ₂	403.62	0.211	1.62
CDCl ₃	410.63	*0.383	*2.89
C ₇ H ₈	322.29	0.190	1.54
C ₆ D ₆	361.97	0.181	1.51
DMF	419.49	0.471	6.13
CCl ₄	408.55	0.178	1.50
C ₆ H ₁₂	395.56	0.159	1.43
C ₈ H ₁₆	393.19	~ 0.15	~ 1.41
CH ₃ SOCH ₃	415.33	0.478	7.07
CH ₃ NO ₃	413.68	0.455	4.90

* Values calculated for 50 mole % solution.

FIGURE 20

Chemical shift of the methyl protons as a function
of the "reaction field" of the solvent

- o plotted against $\epsilon^{\frac{1}{2}}$.
- plotted against $\frac{\epsilon-1}{2\epsilon+2.5}$

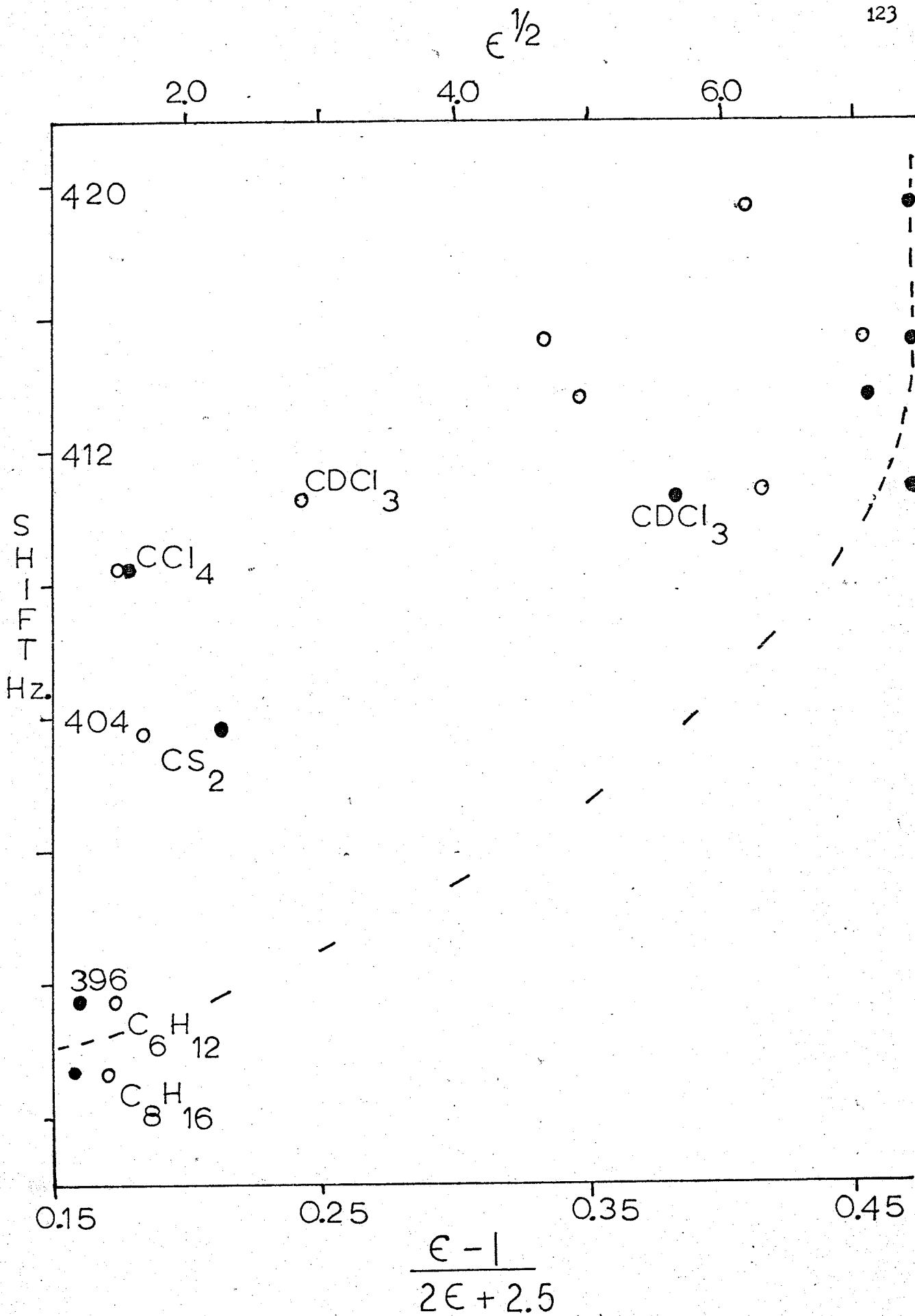


TABLE 24

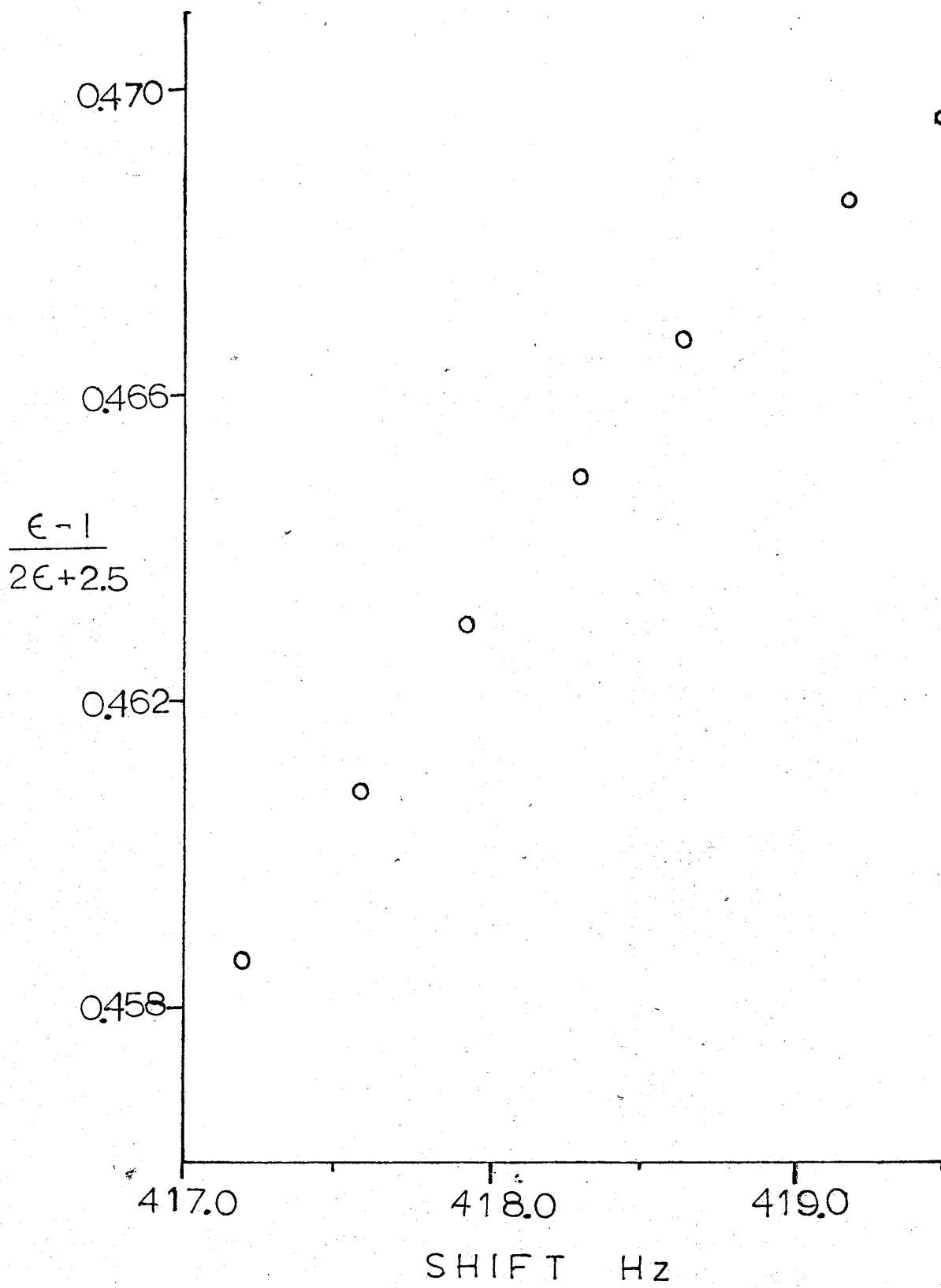
Proton Chemical Shift of Methyl Nitrate as a function
of the Dielectric Constant of the Solvent DMF at
different temperatures.

Temperature (°C)	Shift (Hz)	ϵ of DMF	$\frac{\epsilon - 1}{2\epsilon + 2.5}$
29.5	419.49	35.87	0.470
38.5	419.17	34.18	0.468
49	418.62	32.50	0.467
59	418.28	30.82	0.465
69.5	417.91	29.13	0.463
80	417.57	27.45	0.461
90	417.19	25.76	0.458

* Data taken from (121) assuming ϵ to be a linear function of temperature.

FIGURE 21

Chemical shift of the methyl protons as a function of the "reaction field" at different temperatures in DMF solution.



SECTION H

SUMMARY AND CONCLUSIONS.

A study of the ^{14}N relaxation process occurring in methyl nitrate was carried out by steady state proton magnetic resonance measurements. Temperature studies in the range 30° to 90°C were performed on the compound in two solvents, DMF and cyclohexane. Ambient temperature measurements were recorded for nine other solvents.

Quadrupole relaxation times, T_q , were determined by matching the experimental spectra with computer calculated ones using the line shape theory developed by Pople with a modification to include T_2 , the effective spin - spin relaxation time of the protons. The procedure was complicated by the difficulty in determining T_2 and J (the ^{14}N - H coupling constant); by measuring the solvent resonance in the first instance and by examining the ^{15}N satellite bands in the second, these problems were both overcome satisfactorily. The results show that for long quadrupolar relaxation times line shape analysis of the signals of protons spin - spin coupled to the nitrogen nucleus represents an accurate method for determining T_q and for studying the relevant molecular properties.

The various activation parameters for molecular reorientation were calculated from Arrhenius plots and from transition state theory. They are listed in Table 15. The activation energy for reorientation of methyl nitrate in DMF solution was found to be significantly larger than that for cyclohexane as the solvent. It is tempting to ascribe this difference to some type of complex formation in the more polar solvent; however, further considerations (including the results of chemical shift measurements) showed these experiments to be inconclusive.

Factors influencing the relaxation rate of a solute molecule were elucidated. First and foremost, as suggested by numerous models, there

is a strong dependence on macroscopic viscosity, although the linearity predicted by B.P.P. theory is not confirmed. Modifications of this simple theory which account for the size of the solvent molecule (the microviscosity model) and the mutual viscosity between solute and solvent (the Hill model) give only marginal improvement. They fail to predict the observed differences between reorientational rates in polar and non-polar solvents. Dielectric constant, dipole moment and even bond polarisability are all influential, though to a lesser extent than viscosity, in determining quadrupolar rates of relaxation. These three parameters modify T_Q^{-1} in an irregular way; attempts to find some function of η , ϵ , μ and α which bring all the points of Figure 15 onto the same straight line proved, not unpredictably, to be futile. The microdynamics of molecular rotation are apparently not reflected by these bulk properties in an obvious way.

SECTION I

SUGGESTIONS FOR FUTURE RESEARCH

"It is apparent that we are far removed from a fundamental understanding of the details of molecular reorientation in liquids", so write Burke and Chan in a recent paper (122) on nuclear spin relaxation. The same conclusion is markedly apparent from the work presented in this thesis. There is an obvious need for a new approach which would give closer agreement with experimentally observed correlation times for both polar and non-polar systems. Burke and Chan suggested (122) that the correlation time τ might be increased to τ' by a dipole-dipole interaction of energy ξ :

$$\tau' = \tau \exp \frac{-\xi}{kT}$$

$$\text{where } \xi = \frac{-2\mu_1^2 \mu_2^2}{3kTr^6}$$

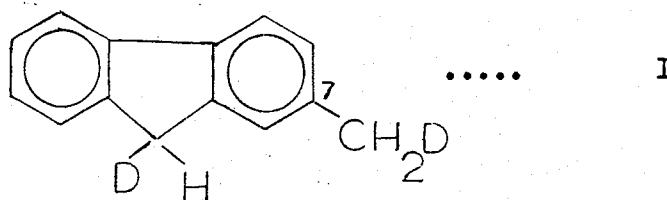
This represents the first attempt to account explicitly for the solvent dipole moment. The distance between dipoles, r , is difficult to estimate and the results are only partly successful. Clearly then, the theoretical aspects of molecular reorientation processes require further study.

Relaxation time measurements (of quadrupole nuclei in particular) are a powerful tool in the study of molecular motions; their scope has been widened by three recent publications:

- (1) Systems where the proton line shape is determined by scalar spin-spin coupling to other nuclei of spin $\frac{1}{2}$ as well as by the relaxation of a quadrupolar nucleus have been treated by Pyper (30). Hence previously unsuitable molecules may now be investigated.
- (2) Marshall (123) has discussed the relaxation times for quadrupolar nuclei in the presence of chemical exchange. The

overall relaxation rate is now determined by both exchange lifetimes and correlation times for rotation at each site. NMR measurements may thus be used to obtain information about any of these quantities. This is potentially useful in the "halide-probe" technique for determining macromolecular rotational correlation times (124).

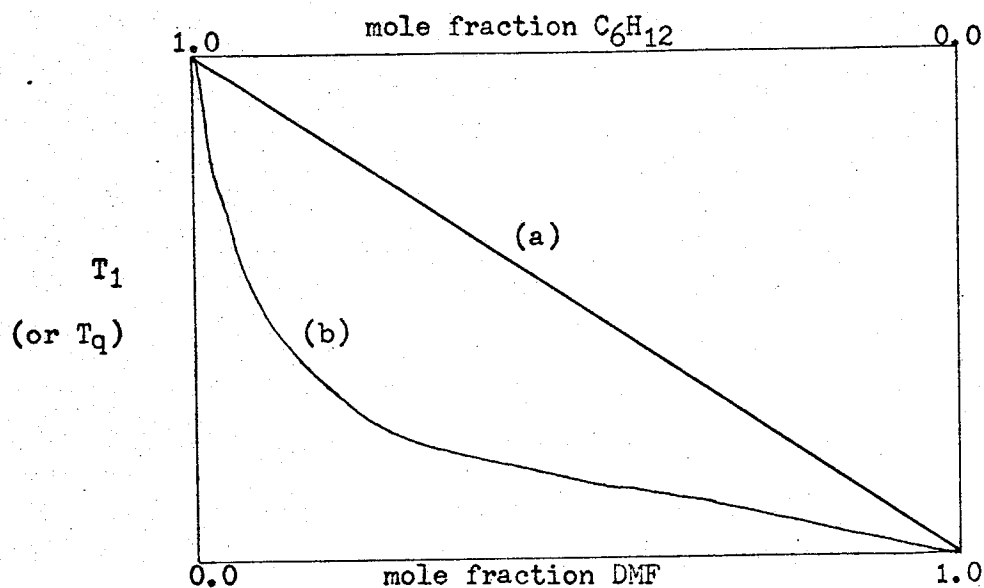
- (3) The effect of internal rotation on the overall molecular correlation time becomes important when the former have an energy barrier of a few kilocalories per mole. Kintzinger et al. (103) have successfully quadrupole "labelled" molecules such as I and obtained the barrier to internal rotation of the $-\text{CH}_2\text{D}$ group at C - 7.



Obviously this technique has wide applications.

Finally, a possible solution is offered to one aspect of the methyl nitrate problem which was not resolved in this thesis, viz. that of possible complex formation with polar solvents, and in particular, DMF. Anderson (107,125) has developed a technique which distinguishes between molecular association where the polymolecular complexes rotate as discrete units and association involving spatial correlations, but having molecules that rotate independently. Adapting this procedure to the problem at hand would involve measurement of the ^{14}N relaxation times in methyl nitrate for a series (5 or 6, say) of dilute (~ 10 mole %) solutions of methyl nitrate in a binary solvent of varying proportions C_6H_{12} (inert) and DMF (the suspected complexing agent). The T_q found for methyl nitrate in C_6H_{12} alone

gives the relaxation time for totally uncomplexed solute; the behaviour of T_q as the ratio DMF to C_6H_{12} is increased then permits distinction between the two situations described above. If T_q changes very rapidly when a little DMF is added and follows the curve designated (b) in Figure 22, Anderson has shown that the lifetime of the complex is long compared to the rate of molecular rotation. When no definite complex is produced the T_q values lie on line (a). Thus it should be possible to determine whether methyl nitrate forms a complex with solvents like DMF, DMSO etc. or whether there is simply a preferential spatial correlation of dipoles.



Hypothetical curves showing the dependence of T_1 (T_q) on the fraction of complexed molecules.

Figure 22

APPENDICES.

APPENDIX I

Contributions to the Spin-lattice Relaxation of ^{14}N .

Some approximate calculations readily show that the quadrupole interaction is by far the largest term in the relaxation rate of quadrupolar nuclei such as ^{14}N . The quadrupole rate,

$$\frac{1}{T_1} = \frac{3}{8} \left(\frac{e^2 q Q}{\hbar} \right)^2 \tau_q$$

becomes $\frac{1}{T_1} \approx 5 \times 10^{12} \tau_q \text{ sec}^{-1}$ - for a quadrupole coupling constant of the magnitude found in methyl nitrate ($\sim 0.7 \text{ MHz}$.) τ_q is a rotational correlation time, normally designated τ_c , since translational motions do not contribute to quadrupole interactions.

Relaxation mechanisms which are magnetic in origin (and important for spin- $\frac{1}{2}$ nuclei ^1H , ^{19}F etc.) are found to be negligible in the case of ^{14}N because the magnetogyric ratio is small. For instance, the fluctuating magnetic field generated by rotation of the methyl protons can relax the nitrogen nucleus by an intramolecular dipole-dipole mechanism, the rate of which is given by (126)

$$\left(\frac{1}{T_1} \right)_{\text{intra}} = \frac{\hbar^2 \gamma_N^2 \gamma_H^2}{r^6} \tau_c$$

γ_N and γ_H are the magnetogyric ratios of ^{14}N and ^1H , respectively, and r is the distance between ^{14}N and a neighbouring proton.

$$\gamma_N = 1.93 \times 10^3 \text{ radians sec}^{-1} \text{ gauss}^{-1}$$

$$\gamma_H = 2.67 \times 10^4 \text{ " " " " .}$$

$$\text{and } r = 2.5 \text{ \AA}, \text{ from structural data on methyl nitrate} \quad (127)$$

Hence,*

$$\left(\frac{1}{T_1} \right)_{\text{intra}} \approx 10^7 \tau_c \text{ sec}^{-1}$$

and is clearly dwarfed by the quadrupolar term.

Intermolecular dipole-dipole relaxation is also possible in principle. The relevant expression is (126)

$$\left(\frac{1}{T_1}\right)_{\text{inter}} = 4\pi^2 \gamma_N^2 \gamma_H^2 \frac{N}{a^2 r^0} \tau_t$$

where N is the number of spins per cc., here approximately 3×10^{22} ; a is the molecular radius and r^0 the distance of closest approach between spins on the different molecules. In the crudest approximation, r^0 may be replaced by $2a$. The small magnetogyric ratio of ^{14}N compared to that of ^1H and lower spin concentration per cc., means that dipole-dipole relaxation of ^{14}N by ^{14}N can safely be ignored; the above expression pertains only to relaxation by protons of solute or solvent molecules. A reasonable value of " a " bearing in mind that the ^{14}N nucleus is "buried" within the molecule would be $\sim 3\text{\AA}$ (128) so that

$$\left(\frac{1}{T_1}\right)_{\text{inter}} \approx 10^7 \tau_t$$

τ_t is the correlation time for translational motion. If this were very long compared to τ_c then the intermolecular contribution could become appreciable. However, there is no experimental evidence to this effect, so that intermolecular dipole-dipole relaxation is also negligible in comparison to the quadrupolar term.

Other mechanisms such as spin-rotational or anisotropic electronic shielding are difficult to estimate for ^{14}N . However, they are a factor $\left(\frac{\gamma_H}{\gamma_N}\right)^2 \approx 150$ times smaller than for protons (where they are of secondary importance), and thus may be neglected for ^{14}N nuclei.

APPENDIX II

Evaluation of the line shape expression, equation (15).

Equation (15) involves the multiplication of three matrices, one of which is to be inverted:

$$I(\omega) = \text{Re} \left\{ (1,1,1) (\vec{A}^{-1}) \begin{pmatrix} 1 \\ 1 \\ 1 \end{pmatrix} \right\} \dots\dots\dots(\text{II-a})$$

The inverse of a matrix is given by

$$A^{-1} = \frac{1}{|A|} \begin{bmatrix} a_{22}a_{33} - a_{23}a_{32} & -(a_{21}a_{33} - a_{23}a_{31}) & a_{21}a_{32} - a_{22}a_{31} \\ -(a_{12}a_{33} - a_{13}a_{32}) & a_{11}a_{33} - a_{13}a_{31} & -(a_{11}a_{32} - a_{12}a_{31}) \\ a_{12}a_{23} - a_{13}a_{22} & -(a_{11}a_{23} - a_{13}a_{21}) & a_{11}a_{22} - a_{12}a_{21} \end{bmatrix} \dots\dots\dots(\text{II-b})$$

where $a_{11} = i(\Delta\omega + J) - \frac{3}{5T_q} - \frac{1}{T_2}$ etc.

and $|A|$ is the determinant of \vec{A} , which evaluated from equation (15) is

$$|A| = \frac{8\Delta\omega^2}{5T_q} + \frac{3\Delta\omega^2}{T_2} - \frac{8\pi^2 J^2}{5T_q} - \frac{3}{5T_q^2 T_2} - \frac{4\pi^2 J^2}{T_2} - \frac{1}{T_2^3} - \frac{8}{5T_q^2 T_2} + i \left[-\Delta\omega^3 + 4\pi^2 \Delta\omega^2 + \frac{3\Delta\omega}{T_2} + \frac{3\Delta\omega}{5T_q^2} + \frac{16\Delta\omega}{5T_q T_2} \right] \dots\dots\dots(\text{II-c})$$

The symmetry properties of matrix \vec{A} (equation 15) give $a_{12} = a_{21} = a_{23} = a_{32}$ and $a_{13} = a_{31}$ so that equation (II-b) may be written

$$A^{-1} = \frac{1}{|A|} \begin{bmatrix} (a_{22}a_{33} - a_{12}^2) & (-a_{12}a_{33} + a_{12}a_{13}) & (a_{12}^2 - a_{22}a_{13}) \\ (-a_{12}a_{33} + a_{13}a_{12}) & (a_{11}a_{33} - a_{13}^2) & (-a_{11}a_{12} + a_{12}a_{13}) \\ (a_{12}^2 - a_{13}a_{22}) & (-a_{11}a_{12} + a_{13}a_{12}) & (a_{11}a_{22} - a_{12}^2) \end{bmatrix} \dots\dots(II-d)$$

The expanded form of equation (II-a), using the rules of matrix multiplication and labelling as shown above is

$$I(\omega) = \text{Re} \left\{ \frac{1}{|A|} \cdot (A' + B + C + D + E + F + G + H + I) \right\} \dots\dots(II-e)$$

which evaluated becomes

$$I(\omega) = \text{Re} \left\{ \frac{1}{|A|} \left[-3\Delta\omega^2 + 4\pi^2 J^2 + \frac{9}{5T_q^2} + \frac{24}{5T_q T_2} + \frac{3}{T_2^2} + i\Delta\omega \left(\frac{-24}{5T_q} - \frac{6}{T_2} \right) \right] \right\} \dots\dots(II-f)$$

To obtain a real denominator, equation (II-f) is multiplied through by $\frac{|A|}{|A|}^*$ where $|A|^*$ is the complex conjugate of equation (II-c). Hence

$$\text{Denominator} = |A| \cdot |A|^* = \left[\frac{8\Delta\omega^2}{5T_q} + \frac{3\Delta\omega^2}{T_2} - \frac{8\pi^2 J^2}{5T_q} - \frac{3}{5T_q T_2} - \frac{8}{5T_q T_2^2} - \frac{4\pi^2 J^2}{T_2} - \frac{1}{T_2^3} \right]^2 + \left[-\Delta\omega^3 + 4\pi^2 \Delta\omega J^2 + \frac{3\Delta\omega}{5T_q^2} + \frac{16\Delta\omega}{5T_q T_2} + \frac{3\Delta\omega}{T_2^2} \right]^2$$

Expanding and converting $\Delta\omega$ to $\Delta\nu$ (in Hertz), the denominator becomes

$$\begin{aligned} &\Delta\nu^6 + \Delta\nu^4 \left[-2J^2 + \frac{17}{50\pi^2 T_q^2} + \frac{4}{5\pi^2 T_q T_2} + \frac{3}{4\pi^2 T_2^2} \right] + \Delta\nu^2 \left[J^4 + \frac{9}{400\pi^4 T_q^4} + \frac{3}{25\pi^4 T_q^3 T_2} + \right. \\ &\left. \frac{128}{25\pi^2 T_q^2 T_2^2} + \frac{3}{T_2^4} - \frac{J^2}{50\pi^2 T_q^2} + \frac{J^2}{5\pi^2 T_q T_2} + \frac{2}{5\pi^4 T_q T_2^3} \right] + \frac{J^4}{25\pi^2 T_q^2} + \frac{J^4}{5\pi^2 T_q T_2} + \frac{J^4}{4\pi^2 T_2^2} \\ &+ \frac{3J^2}{100\pi^4 T_q^3 T_2} + \frac{31J^2}{200\pi^4 T_q^2 T_2^2} + \frac{J^2}{4\pi^4 T_q T_2^3} + \frac{J^2}{8\pi^4 T_2^4} + \frac{9}{1600\pi^6 T_q^4 T_2^2} + \frac{3}{100\pi^6 T_q^3 T_2^3} \\ &+ \frac{47}{800\pi^6 T_q^2 T_2^4} + \frac{1}{20\pi^6 T_q T_2^5} + \frac{1}{16\pi^6 T_2^6} \dots\dots(II-g) \end{aligned}$$

i.e. equation (II-g) is of the form $\Delta v^6 + C_4 \Delta v^4 + C_5 \Delta v^2 + C_6$.

From equation (II-f) the expression for the numerator is equal to

$$\text{Numerator} = \left[-3\Delta v^2 + 4\pi^2 J^2 + \frac{9}{5T_q^2} + \frac{24}{5T_q T_2} + \frac{3}{T_2^2} + i\Delta v \left(-\frac{24}{5T_q} - \frac{6}{T_2} \right) \right] |A|^* \dots\dots\dots(\text{II-h})$$

Substituting for $|A|^*$ from equation (II-c), expanding and keeping only the real part, equation (II-h), in Hertz, becomes

$$\begin{aligned} \text{Numerator} = & \frac{-3\Delta v^4}{T_2} + \Delta v^2 \left(-\frac{26}{25\pi^2 T_q^2 T_2} - \frac{12}{5\pi^2 T_q T_2^2} - \frac{3}{2\pi^2 T_2^3} - \frac{2J^2}{T_q} \right) - \frac{2J^4}{5T_q} \\ & - \frac{J^4}{T_2} - \frac{9J^2}{50\pi^2 T_q^3} - \frac{26J^2}{25\pi^2 T_q^2 T_2} - \frac{19J^2}{10\pi^2 T_q T_2^2} - \frac{J^2}{\pi^2 T_2^3} - \frac{27}{400\pi^4 T_q^4 T_2} - \frac{9}{25\pi^4 T_q^3 T_2^2} \\ & - \frac{143}{200\pi^4 T_q^2 T_2^3} - \frac{3}{5\pi^4 T_q T_2^4} - \frac{3}{16\pi^4 T_2^5} \dots\dots\dots(\text{II-i}) \end{aligned}$$

Equation (II-i) is of the form $C_1 \Delta v^4 + C_2 \Delta v^2 + C_3$.

The entire expression for the line shape I (v) is then given from equation (II-i) divided by equation (II-g), i.e.

$$I(v) = \frac{C_3 + \Delta v^2 (C_2 + \Delta v^2 C_1)}{C_6 + \Delta v^2 [C_5 + \Delta v^2 (C_4 + \Delta v^2)]} \dots\dots\dots(\text{II-j})$$

where C_1 and C_4 are the coefficients of Δv^4 in the expressions for numerator and denominator, respectively;

C_2 and C_5 are the corresponding coefficients for Δv^2 , and C_3 and C_6 are the numerical constants in equations (II-i) and (II-g), respectively. Inspection of equations (II-g) and (II-i) gives the precise form of the parameters. e.g.

$$C_1 = \frac{3}{T_2}, \quad C_2 = \frac{2J^2}{T_q} + \frac{1}{\pi^2 T_2} \left\{ \frac{1.04}{T_q^2} + \frac{2.4}{T_q T_2} + \frac{1.5}{T_2^2} \right\} \text{ etc. etc.}$$

APPENDIX III

Estimation of the Quadrupole Coupling Constant in Methyl Nitrate.

A value for the nuclear quadrupole coupling constant of ^{14}N in CH_3ONO_2 is required in the estimation of τ_q^0 and ΔS^\ddagger , (equations (30) and (33)). However, the term $\frac{e^2qQ}{h}$ is known only for a few ^{14}N -containing compounds, in the solid or gas phase. Normally coupling constants observed in solids are about 10% less than in the gaseous state; the "effective" coupling constant for the liquid no doubt lies between these two values, probably closer to that for the solid phase. Hence the solid state value is commonly used in liquid studies (48), an approximation supported by some recent measurements (130). Furthermore, $\frac{e^2qQ}{h}$ is assumed to arise entirely intramolecularly, and thus has no solvent dependence and shows negligible variation with temperature. (Note, however, the calculations of Packer (94) which indicate that highly polar solvent molecules may in fact contribute to the electric field gradient and hence to the coupling constant.)

To date there have been no values reported for the ^{14}N quadrupole coupling constant of methyl nitrate in any phase. Quantum mechanical calculations of τ_q (and thus of $\frac{e^2qQ}{h}$) are still in their infancy and provide only approximate values for simple systems (131,132,133). However, following the approach of Moniz and Gutowsky (48), $\frac{e^2qQ}{h}$ may be estimated from equation (8) by assuming a "reasonable" value for τ_q ; 2.0×10^{-12} sec. has been suggested (29). This gives

<u>Solvent</u>	T_q (30°C) (sec.)	$\frac{e^2qQ}{h}$ (MHz.)
C_6H_{12}	0.0925	0.60
DMF	0.0550	0.78
TCE	0.0600	0.73 (29)

The difference between solvents is unreasonable, the variation is really in τ_q , the correlation time for molecular reorientation, which from experimental values of T_q should be longer in DMF than in C_6H_{12} solution. Calculations based on

molecular models cannot estimate this difference.* Hence an average value of 0.7 MHz. was assumed for the quadrupole coupling constant of methyl nitrate in both solvents and used in the calculation of τ_q and ΔS^\ddagger . (c.f. values of 0.9⁽⁴⁸⁾ and 1.0⁽¹³⁴⁾ MHz. for ^{14}N in ethyl nitrate and nitric acid, respectively.)

* The approximate form of the Hill model (equation 26) requires the following data in order to estimate τ_q :

$$I = 95.9 \text{ a.m.u. } \text{\AA}^2 \quad (\text{averaging the three values quoted in (127)})$$

$$a = 2.6 \text{ \AA} \quad (\text{from density and molecular weight considerations, assuming a c.c.p. structure})$$

$$\mu_{\text{CH}_3\text{NO}_3/\text{DMF}} = 37.51 \text{ a.m.u.}$$

$$\mu_{\text{CH}_3\text{NO}_3/\text{C}_6\text{H}_{12}} = 40.22 \text{ a.m.u.}$$

$$\eta_{\text{DMF}} = 0.92 \text{ cp.}$$

$$\eta_{\text{C}_6\text{H}_{12}} = 0.96 \text{ cp.}$$

Substituting these values into $\tau_c = \frac{2Ia\eta}{\mu kT}$ gives

$$\text{For DMF solution, } \tau_c = 3.0 \times 10^{-12} \text{ sec.}$$

$$\text{For C}_6\text{H}_{12} \text{ solution } \tau_c = 2.9 \times 10^{-12} \text{ sec.}$$

BIBLIOGRAPHY

1. R.A. Ogg, *J. Chem. Phys.*, 22, 560 (1954).
2. J.N. Shoolery, Varian Associates, unpublished observations.
3. R.A. Ogg, *Disc. Faraday Soc.*, 17, 215 (1954).
4. E. Bullock, D.G. Tuck and E.J. Woodhouse, *J. Chem. Phys.*, 38, 2318 (1963).
5. J.M. Lehn and M. Franck-Neumann, *Mol. Phys.*, 7, 197 (1963).
6. J.M. Anderson, J.D. Baldeschwieler, D.C. Dittmer and W.D. Phillips, *J. Chem. Phys.*, 38, 1260 (1963).
7. I.D. Kuntz, P.R. Schleyer and A. Allerhand, *ibid.*, 35, 1553 (1961).
8. P. Hampson and A. Mathias, *Chem. Comm.*, 825 (1968).
9. A.H. Lambertson, I.O. Sutherland, J.E. Thorpe and Y.M. Yusuf, *J. Chem. Soc. (B)*, 6 (1968).
10. H.S. Gutowsky and A. Saika, *J. Chem. Phys.*, 21, 1688 (1953).
11. J.D. Roberts, *J. Amer. Chem. Soc.*, 78, 4495 (1956).
12. J.M. Lehn and M. Franck-Neumann, *J. Chem. Phys.*, 43, 1421 (1965).
13. L. Cavalli and P. Piccardi, *Chem. Comm.*, 825 (1968).
14. N.F. Ramsey, "Nuclear Moments", John Wiley and Sons, Inc., New York, (1953).
15. R.A. Ogg and J.D. Ray, *J. Chem. Phys.*, 26, 1339 (1957).
16. D. Wallach, *ibid.*, 47, 5258 (1967).
17. W.B. Dixon and E. Bright Wilson, Jr., *ibid.*, 35, 191 (1961).
18. D. Wallach and W.T. Huntress, Jr., *ibid.*, 50, 1219 (1969).
19. R.V. Pound, *Phys. Rev.*, 79, 685 (1950).
20. T.P. Das and E.L. Hahn, *Solid State Physics, Supplement 1*, 166 (1958).
21. J.A. Pople, *Mol. Phys.*, 1, 168 (1958).
22. J.A. Pople, W.G. Schneider and H.J. Bernstein, "High-Resolution Nuclear Magnetic Resonance", Mc.Graw-Hill, New York, 1959.
23. S. Libich, University of Manitoba, unpublished calculations.
24. P.W. Anderson, *J. Phys. Soc. Japan*, 2, 316 (1954).
25. R. Kubo and K. Tomita, *ibid.*, 2, 888 (1954).
26. R. Kubo, *ibid.*, 2, 935 (1954).
27. R.A. Sack, *Mol. Phys.*, 1, 163 (1958).

28. A. Abragam, "The principles of nuclear magnetism." Oxford University Press London, (1961).
29. J.P. Kintzinger, J.M. Lehn and R.L. Williams, Mol. Phys., 17, 135 (1969).
30. N.C. Pyper, *ibid.*, 19, 161 (1970).
31. N. Bloembergen, E.M. Purcell and R.V. Pound, Phys. Rev., 73, 679 (1948).
32. L.W. Reeves, Adv. in Phys. Org. Chem., 3, 187 (1965).
33. C.S. Johnson, Adv. Mag. Res., 1, 33 (1965).
34. H.G. Hertz, Prog. NMR Spect., 3, 159 (1967).
35. J.A. Pople, Disc. Faraday Soc., 43, 192 (1967).
36. R.A. Dwek and R.E. Richards, *ibid.*, 43, 196 (1967).
37. G. Bonera and A. Rigamonti, J. Chem. Phys., 42, 171 (1964).
38. D.K. Green and J.G. Powles, Proc. Phys. Soc., London, 85, 87 (1965).
39. K. Krynicki and J.G. Powles, *ibid.*, 86, 549 (1965).
40. P.S. Hubbard, Phys. Rev., 131, 1155 (1963).
41. J.G. Powles and R. Figgins, Mol. Phys., 10, 155 (1966).
42. D.W.G. Smith and J.G. Powles, *ibid.*, 10, 451 (1966).
43. J.G. Powles, M. Rhodes and J.H. Strange, *ibid.*, 11, 515 (1966).
44. K. Krynicki, Physica, 32, 167 (1966).
45. D.E. Woessner, J. Chem. Phys., 40, 2341 (1964).
46. G. Bonera and A. Rigamonti, *ibid.*, 42, 175 (1965).
47. D.E. O'Reilly and G.E. Schacher, *ibid.*, 39, 1768 (1963).
48. W.B. Moniz and H.S. Gutowsky, *ibid.*, 38, 1155 (1963).
49. J. Bacon, R.J. Gillespie and J.W. Quail, Can. J. Chem., 41, 3063 (1963).
50. J. Bacon, R.J. Gillespie, J.S. Hartman and U.R.K. Rao, Mol. Phys., 18, 561 (1970).
51. P.W. Atkins, A. Loewenstein and Y. Margalit, *ibid.*, 17, 329 (1969).
52. T.T. Bopp, J. Chem. Phys., 47, 3621 (1967).
53. D.E. Woessner, B.S. Snowden, Jr., and E. Thomas Strom, Mol. Phys., 14, 265 (1968).
54. D.L. Hogenboom, D.E. O'Reilly and E.M. Peterson, J. Chem. Phys., 52, 2793 (1970).

55. J.G. Powles and M.C. Gough, *Mol. Phys.*, 16, 349 (1969).
56. D.E. Woessner, *J. Chem. Phys.*, 36, 1 (1962).
57. W.T. Huntress, Jr., *ibid.*, 48, 3524 (1968).
58. D. Wallach and W.T. Huntress, Jr., *ibid.*, 50, 1219 (1969).
59. W.T. Huntress, Jr., *J. Phys. Chem.*, 73, 103 (1969).
60. W.T. Huntress, Jr., *Adv. Mag. Res.*, 4, 1 (1970).
61. P. Debye, "Polar Molecules", Dover Publications, New York, 1945. Chp. V
62. A. Spornol and K. Wirtz, *Z. Naturforsch.*, 89, 522 (1953).
63. A. Gierer and K. Wirtz, *ibid.*, 89, 532 (1953).
64. N.E. Hill, *Phys. Soc. Proc.*, 67, 149 (1954).
65. E.N. da C. Andrade, *Phil. Mag.*, 17, 497 (1934).
66. R.W. Mitchell and M. Eisner, *J. Chem. Phys.*, 33, 86 (1960).
67. G.M. Whitesides and H.L. Mitchell, *J. Am. Chem. Soc.*, 91, 2245 (1969).
68. C. Hall, R.E. Richards, G.N. Schulz and R.R. Sharp, *Mol. Phys.*, 16, 529 (1969).
69. C. Hall, G.L. Haller and R.E. Richards, *ibid.*, 16, 377 (1969).
70. G.T. Jones and J.G. Powles, *ibid.*, 8, 607 (1964).
71. D. Herbison-Evans and R.E. Richards, *ibid.*, 7, 515 (1964).
72. T.D. Alger and H.S. Gutowsky, *J. Chem. Phys.*, 48, 4625 (1968).
73. R.E. Richards and B.A. Yorke, *Mol. Phys.*, 6, 289 (1963).
74. L. Petrakis, *J. Phys. Chem.*, 72, 4182 (1968).
75. G. Benedek and E.M. Purcell, *J. Chem. Phys.*, 22, 2003 (1954).
76. A.W. Nolle and P.P. Mahendroo, *ibid.*, 33, 863 (1960).
77. A.A. Brocks, B.D. Boss, E.O. Stejskal and V.W. Weiss, *ibid.*, 3826 (1968).
78. T.E. Bull and J. Jonas, *ibid.*, 52, 2779 (1970).
79. D.E. Woessner and B.S. Snowden, Jr., *ibid.*, 52, 1621 (1970).
80. A.M. Pritchard and R.E. Richards, *Trans. Faraday Soc.*, 62, 1388 (1966).
81. G. Chiarotti, G. Cristianai and L. Guilotto, *Nuovo Cimento*, 1, 863 (1955).
82. W.A. Steele, *J. Chem. Phys.*, 38, 2404 (1963).

83. W.A. Steele, *ibid.*, 38, 2411 (1963).
84. W.B. Moniz, W.A. Steele and J.A. Dixon, *ibid.*, 38, 2418 (1963).
85. J.O. Hirschfelder, C.F. Curtiss and R.B. Bird, "Molecular Theory of Gases and Liquids", John Wiley and Sons, Inc., New York, (1954).
86. E.M^cLaughlin, *Trans. Faraday Soc.*, 55, 28 (1959).
87. D.E. O'Reilly, *J. Chem. Phys.*, 49, 5416 (1968).
88. J.R. Johnson (Ed.), *Organic Syntheses*, John Wiley and Sons, Inc., New York (1939), Vol. XIX P. 64.
89. B. Goodwin, M.Sc. Thesis, University of Manitoba, (1969).
90. G.M. Barrow, "Physical Chemistry", McGraw-Hill Book Company, 2nd. Edition, (1966), P. 543.
91. The Chemical Rubber Company, "Handbook of Physics and Chemistry", (46 th Edition, 1965).
92. M. Rabinovitz and A. Pines, *J. Am. Chem. Soc.*, 91, 1585 (1969).
93. A.V. Cunliffe and R.K. Harris, *Mol. Phys.*, 15, 413 (1968).
94. M. St. J. Arnold and K.J. Packer, *ibid.*, 10, 141 (1965).
95. R. Fields, J. Lee and D.J. Mowthorpe, *Trans. Faraday Soc.*, 65, 2278 (1969).
96. K.J. Laidler, "Chemical Kinetics", McGraw-Hill Book Co., Inc., (1950). P.94.
97. H. Labhart, *Chem. Phys. Lett.*, 1, 263 (1967).
98. M. Suzuki and R. Kubo, *Mol. Phys.*, 7, 201 (1963).
99. M. Broze and Z. Luz, *J. Phys. Chem.*, 73, 1600 (1969).
100. H.S. Gutowsky and F.M. Chen, *ibid.*, 69, 3216 (1965).
101. Z.M. Holubec and J. Jonas, *J. Am. Chem. Soc.*, 90, 5986 (1968).
102. J. Jonas, A. Allerhand and H.S. Gutowsky, *J. Chem. Phys.*, 42, 3396 (1963).
103. C. Brevard, J.P. Kintzinger and J.M. Lehn, *Chem. Comm.*, 1193 (1969).
104. E.J. Hennelly, W.M. Heston Jr. and C.P. Smyth, *J. Am. Chem. Soc.*, 70, 4102 (1948).
105. E. Rahkamaa, *J. Chem. Phys.*, 48, 531 (1968).
106. A.L. McClellan (Ed). *Tables of Experimental Dipole Moments*, W.H. Freeman and Co., San Francisco, (1963).
107. J.E. Anderson and P.A. Fryer, *J. Chem. Phys.*, 50, 3784 (1969).

108. B. Linder, *J. Chem. Phys.*, 33, 668 (1960).
109. K.G. Denbigh, *Trans. Faraday Soc.*, 36, 936 (1940).
110. R.J. Abraham, L. Cavalli and K.G. Pachler, *Mol. Phys.*, 11, 471 (1966).
111. A.D. Buckingham, T.P. Schaefer and W.G. Schneider, *J. Chem. Phys.*, 32, 1227 (1960).
112. P. Laszlo, "Prog. in NMR Spectr." 3, 231 (1967).
113. A.D. Buckingham, *Can. J. Chem.*, 38, 300 (1960).
114. L. Onsager, *J. Am. Chem. Soc.*, 58, 1486 (1936).
115. H.M. Hutton and T.P. Schaefer, *Can. J. Chem.*, 45, 1111 (1967).
116. F. Hruska, E. Bock and T.P. Schaefer, *ibid.*, 41, 3034 (1963).
117. P. Laszlo and J.I. Musher, *J. Chem. Phys.*, 41, 3906 (1964).
118. R.L. Schmidt, R.S. Butler and J.H. Goldstein, *J. Phys. Chem.*, 73, 1117 (1969).
119. G. Kotowycz and T.P. Schaefer, *Can. J. Chem.*, 45, 1093 (1967).
120. I.D. Kuntz Jr. and M.D. Johnston Jr., *J. Am. Chem. Soc.*, 89, 6008 (1967).
121. K.A. McLauchlan, L.W. Reeves and T.P. Schaefer, *Can. J. Chem.*, 44, 1473 (1966).
122. T.E. Burke and S.I. Chan, *J. Mag. Res.*, 3, 55 (1970).
123. A.G. Marshall, *J. Chem. Phys.*, 52, 2527 (1970).
124. A.G. Marshall, *Biochem.*, 7, 2450 (1968).
125. J.E. Anderson, *J. Chem. Phys.*, 51, 3578 (1969).
126. H.S. Gutowsky and D.E. Woessner, *Phys. Rev.*, 104, 843 (1956).
127. J.C. Brand and T.M. Cawthon, *J. Am. Chem. Soc.*, 77, 319 (1955).
128. V.A. Shlyapochnikov, I.M. Zamilovich and S.S. Novikov, *Zh. Prikl. Spektroskopii, Akad. Nauk Belorussk. SSR* 3 (3), 272 (1965).
129. E.A.C. Lucken, *Nuclear Quadrupole Coupling Constants*, (Academic Press London and New York) 1969.
130. K.T. Gillen and J.H. Noggle, *J. Chem. Phys.*, 52, 4905 (1970).
131. C.H. Townes and B.P. Dailey, *ibid.*, 17, 782 (1949).
132. C.S. Yannoni, *ibid.*, 52, 2005 (1970).
133. H. Betsuyaku, *ibid.*, 50, 3117 (1969).
134. D.J. Millen and J.R. Morton, *J. Chem. Soc.*, 1523 (1960).